ROTAVIRUS NSP1 IS AN INTERFERON SYSTEM ANTAGONIST

by

Joel Wallace Graff

A dissertation submitted in partial fulfillment
of the requirements for the degree

of

Doctor of Philosophy

in

Veterinary Molecular Biology

MONTANA STATE UNIVERSITY
Bozeman, Montana

July 2008

APPROVAL

of a dissertation submitted by

Joel Wallace Graff

This dissertation has been read by each member of the dissertation committee and has been found to be satisfactory regarding content, English usage, format, citation, bibliographic style, and consistency, and is ready for submission to the Division of Graduate Education.

Dr. Michele Hardy

Approved for the Department of Veterinary Molecular Biology

Dr. Mark Quinn

Approved for the Division of Graduate Education

Dr. Carl A. Fox

STATEMENT OF PERMISSION TO USE

In presenting this dissertation in partial fulfillment of the requirements for a doctoral degree at Montana State University, I agree that the Library shall make it available to borrowers under rules of the Library. I further agree that copying of this dissertation is allowable only for scholarly purposes, consistent with “fair use” as prescribed in the U.S. Copyright Law. Requests for extensive copying or reproduction of this dissertation should be referred to ProQuest Information and Learning, 300 North Zeeb Road, Ann Arbor, Michigan 48106, to whom I have granted “the exclusive right to reproduce and distribute my dissertation in and from microform along with the non-exclusive right to reproduce and distribute my abstract in any format in whole or in part.”

Joel Wallace Graff

July 2008

ACKNOWLEDGEMENTS

I would like to thank my “scientific mother”, Dr. Michele Hardy, for many years of guidance. The members of the Hardy Lab, past and present, have also been instrumental in the success of this project with helping tie up loose ends and brainstorming. My graduate committee of Dr. Mark Jutila, Dr. Ben Lei, and Dr. Jim Burritt have asked great questions and given important feedback during each step of the process. Last, but not least, I would like to thank my wife, Jill, for granting me an audience to practice my talks and editing nearly everything I have written.

TABLE OF CONTENTS

TABLE OF CONTENTS - CONTINUED

TABLE OF CONTENTS - CONTINUED

TABLE OF CONTENTS - CONTINUED

LIST OF TABLES

LIST OF FIGURES

LIST OF FIGURES - CONTINUED

ABSTRACT

Rotaviruses cause severe gastroenteritis in mammals, including humans and livestock. Most rotavirus proteins have known functions, either as a mediator of virus replication or as a component of the infectious virus particle. The function of nonstructural protein 1 (NSP1) was unknown. However, it has been suggested that the function of NSP1 involved interactions with cellular proteins. Using the NSP1 encoded by a bovine rotavirus as the bait protein of a yeast-two hybrid interaction trap, interferon regulatory factor 3 (IRF3) was identified as an NSP1-interacting protein. Due to the importance of IRF3 in initiating an interferon response, we hypothesized that NSP1 acts to antagonize the interferon system. A comprehensive set of experiments yielded the following observations. Interferon-β (IFNβ) induction was blocked in wild-type, but not NSP1 null, infected cells. Expression of NSP1 in the absence of infection resulted in proteasome-mediated degradation of IRF3. A cysteine-rich zinc-binding region near the amino-terminus of all known NSP1 sequences resembles a domain found in hundreds of E3 ubiquitin ligases. Mutational analysis of the zinc-binding domain was consistent with NSP1 acting as an E3 enzyme. The NSP1 of a murine strain of rotavirus also interacted with IRF3. The NSP1 proteins encoded by the bovine and murine rotavirus strains showed low sequence homology (37% identity), which indicated that directing degradation of IRF3 may be a common property of NSP1 proteins from many different rotavirus strains. Screening of simian, bovine, and porcine rotavirus strains indicated that the porcine strain OSU was the only wild-type strain that was unable to direct IRF3 degradation. Characterization of OSU showed that this strain was able to block IFNβ induction by antagonizing NFκB signaling, rather than IRF3 signaling. While analyzing NFκB signaling in rotavirus infected cells, we found that the F box protein, βTrCP, of the Skp1/Cul1/F box multi-subunit E3 enzyme was targeted for degradation by OSU NSP1 and the NSP1 of a bovine rotavirus strain. Together, the results presented in this dissertation have determined that rotavirus NSP1 functions as an interferon antagonist by directing the proteasome-mediated degradation of IFNβ induction signaling components, most likely by acting as an E3 ubiquitin ligase.

BACKGROUND

Rotaviruses

Genome, Proteome, and Structure

Rotaviruses belong to the family *Reoviridae* which cause disease in animals, plants, and insects (1). The nine genera within *Reoviridae* have dsRNA (dsRNA) genomes comprised of 10-12 segments. The members of *Reoviridae* that cause disease in animals target the gastrointestinal or respiratory systems and include the rotaviruses (1). Rotaviruses replicate efficiently in the mature enterocytes of the small intestine causing diarrhea via multiple mechanisms (2). Rotavirus genomes consist of 11 monocistronic segments with the exception of genome segment 11, which encodes for two proteins in most strains (3). Infectious rotavirus virions, also referred to as triple-layered particles (TLPs), encapsidate the dsRNA genome with three concentric icosahedral protein layers (4).

Rotavirus genome segments have several distinct features. The strands of RNA base pair end to end, with the exception that the plus strand contains a 5' cap (5, 6). Consensus sequences are found at the 5' and 3' termini of each genome segment (3). There are no polyadenylation signals in the 3' untranslated region (UTR) of the plus strand; instead the rotavirus genome segments have a conserved sequence of UGACC (7). Accordingly, the rotavirus mRNAs produced during an infection contain cap structures but are not polyadenylated (5, 6).

When cells are infected with two strains of rotavirus simultaneously, novel rotavirus reassortants can be generated that contain a full complement of 11 genome segments with both of the parent strains contributing to the gene constellation of the progeny strain (3). Rotavirus researchers have made use of virus reassortants to analyze the functions of the protein(s) encoded by each segment (8-17) due to the absence of an efficient reverse genetics system. More recently, RNA interference (RNAi) has been used as a method to investigate the functions of the rotavirus gene products (18-27).

During a rotavirus infection, 12 viral proteins are expressed. Six of the proteins are incorporated into the infectious virion and are aptly designated virion proteins (VP1-VP4, VP6, and VP7). The remaining six proteins are designated nonstructural proteins (NSP1-NSP6) due to their absence in the infectious virions (3). The function of each rotavirus protein will be discussed further in the rotavirus replication section.

The structure of rotavirus TLPs has been solved by electron cryomicroscopy (4, 28, 29). The inner protein layer of 120 VP2 dimers acts as a scaffold for proper incorporation of the 11 dsRNA segments, as well as 12 copies each of the polymerase (VP1) and the mRNA-capping enzyme VP3 (30). The intermediate protein layer consists of 260 trimers of the major structural protein VP6. One interesting structural features of rotavirus TLPs are the 60 spikes of VP4 dimers that are embedded within the outer protein layer consisting of 260 VP7 trimers. By electron microscopy, the morphological appearance of rotavirus

TLPs resemble wheels giving the virus its name as the prefix rota- is Latin for wheel (31).

Classification Systems

Rotavirus classification was originally based on serological analysis. The first level of distinction is based on cross-reactivity of antibodies to VP6, which identifies the serogroup (A-E) (3). An important characteristic of this level of classification is that rotaviruses can reassort with members from their own serogroup, but are unable to do so with strains belonging to other serogroups (32). The serogroup A rotavirus strains have been studied the most in depth because few strains belonging to other serogroups have been cultivated in tissue culture and the serogroup A strains are important in pediatric and animal pathogenesis (33, 34). All strains described in this report belong to serogroup A. Rotavirus strains can also be divided into serotypes that are defined by neutralizing antibodies to either of the two rotavirus surface proteins, the glycoprotein VP7 (G serotype) and the protease sensitive protein VP4 (P serotype) (3). VP4 neutralizing antibodies have been difficult to obtain, so VP4 is usually categorized by genotype (35-37). Furthermore, since sequencing partial and complete genomes of rotavirus strains is now common, an updated classification system based on genotyping each of the 11 dsRNA genome segments has been recently proposed (38).

Disease and Pathology

Villus enterocytes of the small intestinal epithelium secrete disaccharidases, peptidases, and other digestive enzymes through the apical surface into the lumen. Rotavirus replication in these mature, nonproliferative villus cells results in an increase in intracellular calcium from the endoplasmic reticulum and plasma membrane (39, 40). The increase in intracellular calcium causes disorganization in the cytoskeleton (41, 42) that has been suggested to impair the secretion of digestive enzymes (42). This results in inefficient digestion of disaccharides, fats, proteins, and carbohydrates (43). As the food bolus moves from the damaged small intestine into the colon, it is osmotically active causing diarrhea because the colon is unable to absorb excess water (43).

The pathology of rotavirus has been studied in a wide array of animal models. Damage in the small intestine from rotavirus infection can range from extensive villus blunting and crypt hyperplasia to no visible damage, depending on the animal model and the age of the animal (44-48). In addition to malabsorption, secretion of a virally encoded enterotoxin, stimulation of the enteric nervous system, and villus ischemia have also been cited as contributing factors in rotavirus-induced diarrhea (49-53). Many aspects of rotavirus-induced diarrhea are linked to intracellular expression of NSP4 (54) or secretion of an NSP4 fragment (amino acids 114-135) (49, 53)including increases in intracellular calcium and inhibition of ion transporters (54, 55), yet inactivated rotavirus particles induce diarrhea independently of NSP4 expression (56).

Extraintestinal spread of rotavirus in mice has been documented since the 1950s (57). Analysis of rotavirus reassortants revealed that the ability for extraintestinal spread mapped to genome segment 7, which encodes for NSP3, and that the route of extraintestinal spread occurs via the lymphatic system in a mouse model (58, 59). Detection of rotavirus in the serum or nonintestinal tissues of infected children has been reported, which suggests that rotavirus extraintestinal spread occurs in humans (60). Conclusive evidence for viremia in rotavirus infections came from a recent report where infectious rotavirus was isolated from the serum of rotavirus antigen positive children (61). Unlike the life-threatening consequences from rotavirus replication within the small intestine, the clinical importance of extraintestinal rotavirus spread is largely unknown.

Epidemiology

In humans, there are 111 million rotavirus episodes each year that result in 25 million clinical visits and about 500,000 deaths (62, 63). Rotaviruses also have a major economic impact in the livestock industry by causing disease in many animals including calves, lambs, foals, and piglets (64-67). Serogroups A-C cause disease in humans and animals while serogroups D and E only cause disease in animals (3). Rotavirus strains are severely attenuated in animals from which the strain did not originate (11, 68-76). This host-range restriction is the basis for current human vaccines which are reassortants of human and animal rotaviruses (77).

The epidemiology of human rotaviruses is complex and differs greatly geographically. For instance, in tropical climates, rotavirus infections occur throughout the year, whereas temperate climates tend to have infection rates peak in the winter (3). In agreement with the geographic theme, some rotavirus serotypes are common in North America, Europe, and Australia while other serotypes are common in South America, Asia, and Africa (78).

Rotavirus Replication

Attachment to Cells

Virus attachment to cells can often involve many interactions. The initial binding typically occurs through receptors common to many cell types. The post-binding interactions can function to increase tissue tropism, trigger fusion between the virus and the cell, or facilitate entry of the virus into the cell. Rotavirus attachment to cells is a multistep process and current models suggest as many as five receptor-ligand interactions, which are described below, are necessary (79).

Trypsin cleavage of the VP4 (88 kDa) spikes results in the formation of the cleavage products, VP5* (60 kDa) and VP8* (22 kDa) at the base and the tip of the spike, respectively (80, 81). This modification of the spike is necessary to convert the TLP to an infectious form (80, 81). Cell surface moieties, such as gangliosides, containing sialic acid (SA; also known as N-acetylneuraminic acid) are commonly described as the initial binding receptor for many rotavirus strains

(3). The SA-binding epitope of these strains has been mapped to VP8* (82, 83). However, some rotavirus strains are capable of infecting cells treated with neuraminidase (NA), suggesting that some strains do not initially bind receptors containing SA (84). This was countered by the observation that different SA-containing receptors have varying degrees of sensitivity to NA-treatment, therefore NA-resistant rotavirus strains may still bind SA (85).

The sequence of post-binding interactions has not been fully elucidated. Current models suggest an interaction between VP5* and either $\alpha 2\beta 1$ or $\alpha 4\beta 1$ integrins immediately follows the initial binding event (86, 87). In NA-sensitive rotavirus strains, the VP5*-$\alpha 2\beta 1$ interaction has been proposed as an alternative initial binding step to the VP8*-SA interaction (88). Three additional post-binding steps have been described, including a VP7 interaction with $\alpha v\beta 3$ integrin (88, 89), a VP5* interaction with heat-shock cognate 70 (hsc70) (90-92), and a VP7 interaction with $\alpha x\beta 2$ integrin (88, 93).

Several mechanisms of rotavirus entry have been proposed including general endocytosis, direct membrane penetration involving dynamin (94, 95), and calcium-dependent endocytosis in clathrin-coated vesicles (96, 97). Whatever the mechanism, lipid rafts are likely involved because rotavirus receptors (gangliosides, integrins, and hsc70) concentrate in rafts at the time of infection (98). Furthermore, cholesterol depletion and other methods of disrupting lipid rafts impair rotavirus infectivity (99).

Expression of Rotavirus Proteins

Upon entry into a cell, the rotavirus TLP loses its outer protein layer composed of VP4 and VP7, leaving a double-layered particle (DLP) that is transcriptionally active (100). Since VP7 contains calcium-binding sites (101, 102), the destabilization of the outer layer likely results from the drastic drop in calcium concentration in the cytoplasm relative to the extracellular space (103). In support of this model of outer layer destabilization, calcium chelators such as EDTA destabilize TLPs (104). VP1, an RNA-dependent RNA polymerase (105), and VP3, an mRNA capping enzyme (106, 107), form heterodimers and are anchored at each of the 12 five-fold vertices within the VP2 core (108). Each dsRNA genome segment is associated with a VP1:VP3 heterodimer and transcription of all 11 genes occurs simultaneously (109). The transcripts produced within the DLP are extruded through aqueous channels at the five-fold vertices (109).

For efficient translation, cellular mRNAs are circularized through the heterotrimer of eIF4E, which binds the cap structure at the 5' end, PABP, which binds the polyadenylated 3' end, and eIF4G, a scaffold protein (110-112). If rotavirus mRNAs are circularized, the mechanism has to be different than that for cellular mRNAs because the transcripts are capped but not polyadenlylated (5, 6). The 3' ends of rotavirus transcripts contain the conserved sequence, UGACC, that can be specifically bound by the amino terminus of NSP3 (7). Furthermore, the carboxy terminus of NSP3 binds to eIF4GI at the same site

used by PABP and with greater affinity (113). These observations led to the logical model whereby rotavirus transcripts are circularized through an eIF4E:eIF4GI:NSP3 heterotrimer (113, 114). Surprisingly, RNAi targeting of NSP3 does not antagonize rotavirus protein translation and may even enhance it (23).

Rather than playing a role in rotavirus gene expression, follow-up RNAi experiments that targeted NSP3 indicated that the inhibition of cellular translation normally seen during rotavirus infections was impaired (24). PABP, which would be utilized for translation of cellular mRNAs but not rotavirus mRNAs, accumulates in the nucleus in an NSP3-dependent manner (24). Earlier observations showed that NSP3 binds to eIF4GI with higher affinity than PABP (113). PABP is known to shuttle between the nucleus and the cytoplasm and is unable to bind eIF4GI in rotaviruse infected cells due to the presence of NSP3 (24). Therefore sequestration of eIF4GI would cause cytoplasmic PABP to immediately shuttle back to the nucleus (24).

The results from the NSP3 knockdown studies illustrate that the mechanisms of rotavirus protein translation regulation are not well defined. Rotavirus protein expression levels are regulated at both transcription and translation (115). For instance, transcriptional levels vary between rotavirus genes, and the protein levels do not always reflect the levels of their encoding transcripts (115). Mitzel *et al* found that discrepancies in VP6 and NSP1 abundance can be attributed to inefficient translation initiation for NSP1, not

differences in transcript levels (116). Further studies by our laboratory and others indicate that low NSP1 protein levels can be partially explained by NSP1 being degraded by the proteasome (117, 118). Proteasome-mediated degradation may also be a factor in regulating the abundance of other rotavirus proteins because several are ubiquitinated (119).

Viroplasms and the Formation of Double-Layered Particles

Rotavirus proteins and RNA accumulate in cytoplasmic foci, termed viroplasms, which are sites of genome replication and the formation of new DLPs (120-122). The nonstructural proteins, NSP2 and NSP5, coordinate the formation of viroplasms. In fact, co-expression of NSP2 and NSP5 in the absence of virus infection leads to the formation of viroplasm-like structures (123, 124). The importance of viroplasm formation in rotavirus replication was confirmed by RNAi experiments which showed a reduction in viral RNA, protein, and progeny when the expression of either NSP2 or NSP5 was reduced (21, 26).

The mechanisms of trafficking rotavirus structural proteins to viroplasms have not been determined. However, the cellular distribution of VP2, VP4, VP6, and VP7, which normally accumulate in or near viroplasms, is disrupted upon knock-down of NSP4 levels by RNAi, even though NSP2 and NSP5 formed viroplasm structures (21, 26). It has been shown that intracellular NSP4 (iNSP4) accumulates in several pools, with a fraction of iNSP4 colocalizing with LC3, a marker for autophagosomal membranes, to form cap-like structures on viroplasms (125). Many viruses use autophagosomal membranes as a physical

scaffold to concentrate viral proteins for efficient virus assembly (126). Taken together, a recruitment mechanism can be envisioned where the structural rotavirus proteins accumulate near viroplasm structures in a manner dependent on NSP4, but not on either NSP2 or NSP5, through the use of autophagy machinery.

Replication and packaging of rotavirus genomes into DLPs occurs within viroplasms in a stepwise fashion involving a number of distinct replication intermediates (RI) including the pre-core (VP1 and VP3), the core (the pre-core, VP2, NSP2, and NSP5), and the double-layered RI (the core and VP6) (127). Replication of dsRNA genome segments occurs simultaneously with the packaging of the segments into the cores, where the viral mRNAs serve as template for generating the minus strand (128, 129). The packaging is regulated so that the 11 genome segments are incorporated within cores at equivalent levels, though specific sequences within the genome segments have not been identified for this function (127, 130). Although *in vitro* replication systems have shown that the structural proteins of the cores (VP1, VP2, and VP3) are capable of synthesizing dsRNA (130-132), only replication systems that include NSP2 and NSP5 are able to package the dsRNA into cores (128). NSP6 may also be involved in genome packaging because it is located within viroplasms and interacts with NSP5 (133-135).

Morphogenesis

Rotavirus morphogenesis is the process whereby newly formed DLPs move from the cytoplasm to the lumen of the ER to form mature TLPs. Viroplasms generally form near the ER and once DLPs are generated, they accumulate in the cytoplasm around the viroplasm. VP7 and iNSP4, transmembrane proteins found within the ER, and VP4, a cytoplasmic protein, concentrate near the viroplasm-ER interface (136-139). The cytoplasmic domain of iNSP4 acts as an intracellular receptor to bind DLPs and helps translocate the DLPs into the ER (140, 141). DLPs are transiently enveloped during the process of translocation from the cytoplasm to the lumen of the ER (142). Since NSP4 forms a heterotrimer with VP7 and VP4, this complex has been suggested to be important for the budding of enveloped DLPs into the lumen of the ER (143). In an effort to determine whether NSP4 can act alone or whether the NSP4:VP4:VP7 complex is necessary for the translocation of DLPs from the cytoplasm to the ER, RNAi targeting each of these three gene products was performed. Only the knock-down of NSP4 led to DLPs being retained in the cytoplasm (21, 144) indicating that NSP4 is the critical receptor involved in translocation of DLPs into the ER lumen.

Rotavirus DLPs are transiently enveloped with a membrane contains the glycoproteins NSP4 and VP7 during the budding process into the ER lumen (136, 137, 139). The enveloped particles also contain VP4 that, like the VP6 on the surface of the DLPs, interacts with the cytoplasmic tail of NSP4 (143). RNAi

experiments targeting the ER-associated rotavirus proteins settled another longstanding debate about rotavirus morphogenesis by addressing which factors are involved in removal of the envelope. Several factors have been hypothesized to mediate the loss of the envelope such as NSP4, VP4, and the high calcium concentration in the ER (94, 145, 146). Surprisingly, experiments using RNAi to target VP7 resulted in the accumulation of enveloped DLPs within the ER lumen (20, 22). Reduction in the level of VP4 expression, on the other hand, allowed the formation of non-enveloped, poorly infectious TLPs that lacked spikes and knock-down of NSP4 prevented DLP translocation into the ER lumen (22, 27, 147). These experiments did not address the effect of high calcium concentration on the envelope, but it would be expected that the calcium would be important for stabilizing the outer protein coat of the TLP (104).

Release of Infectious Triple-Layered Particles

Details about the final assembly steps and the release of TLPs are cell-type specific. Notably, infection in MA104 cells, a non-polarized monkey kidney cell line, eventually causes cell lysis (148). In contrast, TLPs are released from the apical surface of Caco-2 cells, a human intestinal cell line that differentiates into polarized cells with several features similar to intestinal epithelia of live animals (149). The TLPs are shuttled through an unconventional export pathway from the ER to the plasma membrane in a manner that bypasses the Golgi apparatus in the Caco-2 cell (149).

Since the sorting of vesicles to the apical surface involves lipid rafts (150), several studies were aimed at identifying whether rotavirus proteins were associated with these membrane microdomains. Rotavirus proteins and dsRNA were found to associate with lipid rafts in Caco-2 cells and mouse enterocytes (147). Further analysis in Caco-2 cells indicated that VP4 associated with lipid rafts early in the infection, while other proteins of mature TLPs were found at lipid rafts later in the infection (151). These findings led to a proposed model of viral assembly whereby the addition of VP4 spikes to the TLP was an extra-reticular event, since ER membranes are thought to lack lipid rafts (151). This model was controversial because the incorporation of VP4 has historically been thought to occur during the budding process of DLPs entering the ER lumen (143) as described above. Two recent reports suggest that the discrepancy in VP4 assembly within the virus particle may be cell-type specific. VP4 association with particles in MA104 cells occurs in the ER lumen (20), whereas lipid rafts in Caco-2 cells probably serve as a scaffold for VP4 assembly onto particles in an extra-reticular event at the apical surface (148).

Nonstructural Protein 1 (NSP1)

Early attempts to identify the function of NSP1 (previously known as NS53) relied on analyzing sequences of NSP1 from a variety of rotavirus strains. The strains chosen for sequencing represented a wide range of animal origin. Phylogenetic analysis showed that NSP1 sequences segregate according to the species-specificity of the rotavirus strain (152, 153). For example, the NSP1

sequences from bovine strain RF and bovine strain UK share 92% sequence identity, whereas RF NSP1 shares only 38% identity with the NSP1 of simian strain SA11-Patton (153). An exception to this was that the NSP1 sequences of human and porcine rotavirus strains fell into a single group (152). From the phylogenetic analysis, Dunn et al speculated NSP1 is involved in host range restriction and further suggested that the function of NSP1 may be to act in conjunction with cellular proteins or that NSP1 modulates cellular proteins (152).

The sequence identity between NSP1 from different strains is low, but this characteristic allowed for highly conserved residues or regions of NSP1 to be identified. As an example of this, analysis of the first three NSP1 sequences (two bovine strains and one simian strain) showed that the first 150 amino acids have a higher sequence similarity than the carboxy terminus (154, 155). Even more striking is that from these three sequences, a cysteine-rich region within the amino terminus was identified (154, 155). The strict conservation of the seven cysteine residues and one histidine residue was maintained when the NSP1 sequence of additional rotavirus strains was determined (152, 153). Although the majority of the NSP1 sequences were from group A rotaviruses, the cysteine-rich domain was conserved in a group C rotavirus, but not a group B rotavirus (153, 156). The consensus sequence for the cysteine-rich domain is C-X2-C-X8-C-X2-C-X3-H-X-C-X2-C-X5-C (153-155). These structures were proposed to be a CCCC-HCCC two finger sequence based on comparisons to known zinc fingers (157, 158). However, the second finger is atypical since the histidine residue is

separated by a single amino acid from the first cysteine residue, instead of having the spacer be a major loop as is normal in zinc fingers (153). We perfomed an alignment of the 54 available full-length NSP1 sequences and found a highly conserved histidine separated by six amino acids downstream from the final cysteine of the second putative zinc finger. If the HCCC motif is not a functional finger, the histidine residue we identified may be involved in coordinating the binding of zinc. A putative zinc finger was also noted near the carboxy terminus of some bovine strains (159), but the first cysteine of this motif is not conserved in the majority of known NSP1 sequences (153). One or more of these zinc fingers are likely functional since NSP1 was shown to have affinity for zinc (159).

Besides the prominent cysteine-rich region(s), additional regions of conserved sequence were noted from the early NSP1 sequencing efforts. These include three short stretches (15-30 residues each) of basic amino acids near the amino terminus (153), a cluster of acidic amino acids in the last 15 residues of the NSP1 sequence from some strains (153, 155), and 11 isolated proline residues throughout the entire length of the sequence (153). The first eight amino acids of the NSP1 sequences were also strictly conserved, but the reason for this is likely for function at the nucleotide level rather than the amino acid level (153). The first 55 nucleotides from each of the known gene 5 sequences (which encode NSP1) were very highly conserved, including the entire 5' UTR and the nucleotides encoding the first eight amino acids (153). The use of gene-specific

primers used to clone the gene 5 segments that base pair with the 5' and 3' ends of the segments may have masked some differences in nucleotide sequence (153). RNA folding programs determined that a portion of this 55-nucleotide stretch formed an 11 base pair stem loop structure (153). It was proposed that this stem loop functions as a recognition site for genome packaging or for reducing the translation rate of NSP1 (153).

The ability of NSP1 to bind zinc, the cytoskeleton, and the 5' ends of all 11 rotavirus mRNA strands (160) were the only known properties of NSP1 prior to the studies described in this dissertation. The dsRNA-binding domain was mapped to the first 81 amino acids of NSP1 (160). This region of NSP1 contains the cysteine-rich region and one of the basic amino acid stretches. It is likely that both of these conserved elements are involved in binding dsRNA (160, 161). The binding of NSP1 to the 5' ends of rotavirus mRNA strands was shown to be specific because the interaction could be competitively inhibited by unlabeled rotavirus mRNA but not by control yeast RNA (160). The biological relevance of the RNA-binding by NSP1 is unknown. Immunofluorescence staining and cellular fractionation studies found that NSP1 localized to the cytoplasm and that NSP1 was found in soluble and cytoskeleton fractions in equivalent amounts (160). Deletion mapping suggested that a region of approximately 100 amino acids immediately downstream of the cysteine-rich region was responsible for this localization pattern (160).

Two rotavirus proteins, NSP1 and NSP3, are nonessential for replication. The lack of a need for NSP1 during replication was first seen when a rotavirus variant, brvA, was characterized that had a rearrangement in gene segment 5, which encodes NSP1 (162). The brvA variant did not express detectable levels of NSP1 and a follow-up study found that the coding region of this gene contained a point mutation resulting in a truncated NSP1 (163). A bovine rotavirus mutant, A5-16, was isolated that had a 500 base pair deletion within gene segment 5 causing a frame shift resulting in a truncated open reading frame upstream of the zinc-binding domain (164). RNAi targeting gene 5 to reduce NSP1 expression has confirmed the nonessential nature of this protein in replication (27). Recent insight into NSP1 and NSP3 proteins indicates that both proteins interfere with normal cellular function. Therefore, these proteins may be evolutionarily conserved due to selective advantage in natural, animal infection settings.

Interferon System

Type I Interferon System Overview

Interferons (IFN) are cytokines that were discovered over 50 years ago for their ability to interfere with viral replication (165). Based on the cognate receptor for each of the IFN gene products, three IFN families have been described (166). Here I will focus on the type I IFN family which includes IFNα, IFNβ, IFNω, IFNε, IFNκ, IFNτ, IFNδ, and IFNζ, although not all of these genes are found in the

human genome (166). Most cells can express type I IFN genes, but only T cells and NK cells can produce IFNγ, the only type II IFN gene product (167). Type III IFNs consist of IFNλ1, IFNλ2, and IFNλ3 which appear to function similarly to type I IFN (168).

The induction of type I IFN in response to viral infection consists of an early phase and a later, positive-feedback phase (169, 170). In the early phase, detection of viral pathogen-associated molecular patterns (PAMPs) is generally mediated by members of either the RIG-I-like receptor (RLR) or the Toll-like receptor (TLR) families of PAMP receptors and leads to the induction of type I IFN. Signaling from either of these receptor families can result in the activation of several transcription factor families. The binding of interferon regulatory factor (IRF3/7), nuclear factor κB (NFκB), and activator protein-1 (AP-1) transcription factors to the positive regulatory domain elements within the IFNβ promoter is required for efficient gene induction (Figure 1.1) (171). The positive-feedback phase is mostly a result of IFNβ binding the type I IFN receptor and signaling through the Janus-associated kinase/signal transducer and activator of transcription (JAK/STAT) pathway to induce IRF7, which is very efficient at inducing IFNβ and most of the IFNα genes (169, 170, 172, 173).

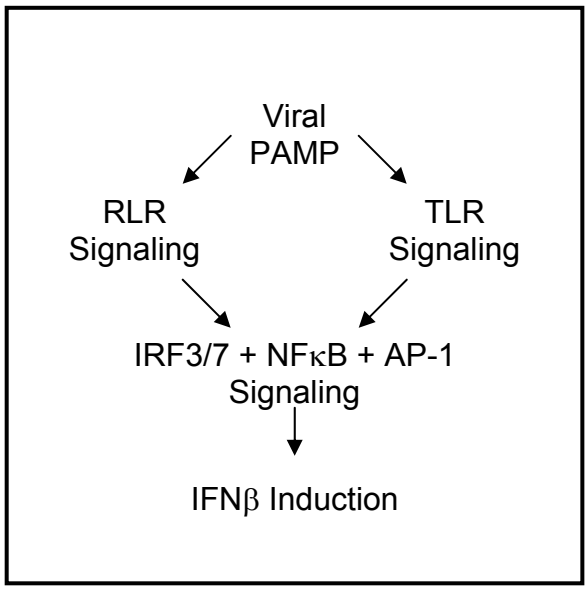

Figure 1.1: Overview of signaling pathways leading to IFNβ induction. Each signaling pathway is described below.

In addition to inducing IRF7, type I IFN signaling through the JAK/STAT pathway upregulates the expression of hundreds of genes (174). Many of these genes encode proteins or microRNAs that are effective at limiting the replication and spread of viruses (175, 176). As such, most viruses have developed mechanisms to antagonize the IFN system (177).

RIG-I-Like Receptor (RLR) Signaling

Several cytosolic receptors have been described that bind viral RNA and trigger the induction of type I IFN. The first RNA sensor identified that triggers type I IFN induction was retinoic acid inducible gene-I (RIG-I) (178). The protein structure of RIG-I is characterized by C-terminal helicase domains, important for binding viral RNA, and two N-terminal caspase activation and recruitment domains (CARDs), important for signaling downstream to activate NFκB and

IRF3 (178). Two additional viral RNA sensors in the RLR family, melanoma differentiation factor 5 (MDA5) and Lgp2, were soon discovered based on similarities between the helicases of these proteins (179, 180).

Unlike RIG-I and MDA5, Lgp2 lacks CARDs, which were known to be important for signaling downstream to activate NFκB and IRF3 (179, 180). Lgp2 was thought to be a dominant negative version of RIG-I and MDA5. Lgp2 overexpression reduced type I IFN induction in response to polyI:C and vesicular stomatitis virus (VSV) infection (179-181). However, this is not the case in response to all viral infections, since Lgp2$^{-/-}$ mice have a defective type I IFN response to encephalomyocarditis virus (EMCV) infections (179-181).

RIG-I$^{-/-}$ and MDA5$^{-/-}$ mice confirmed the importance of these RLRs in the induction of type I IFN responses (182, 183). The knockout mice also showed that RIG-I and MDA5 recognize different viral infections. For instance, RIG-I was shown to detect VSV, influenza, Sendai virus, and Japanese encephalitis virus (183), whereas MDA5 detects EMCV, Theiler's virus, Mengo virus, and polyI:C (183, 184). It was originally suggested that the helicases of RIG-I and MDA5 were sensors for dsRNA, but the receptor-specific responses to various viral infections indicate that the binding of dsRNA may be only a partial requirement for signal induction (185). Indeed, RIG-I has been shown to detect RNA with 5' triphosphate groups (186, 187) with the dsRNA feature playing a secondary role in discrimination between self and nonself RNA (185). An additional requirement for RIG-I activation is ubiquitination (lysine 63-linked polyubiquitin chains) via the

TRIM25 E3 ubiquitin ligase (188). Negative regulation of RIG-I and MDA5 in uninfected cells also differs. Overexpression of MDA5, but not RIG-I, leads to induction of type I IFN (185). This is likely due to the lack of an analogous inhibitory domain in MDA5, which was found in RIG-I (185). Since MDA5 lacks the autoinhibitory domain, negative regulation is provided by dihydroxyacetone kinase, DAK (189).

Although the ligands and regulation mechanisms for the RLR members RIG-I and MDA5 are unique, the downstream signaling pathway for both receptors appears to be shared (Figure 1.2). RIG-I and MDA5 both bind to a mitochondria-associated protein, MAVS (also known as IPS-1, VISA, and Cardif), via CARD-CARD interactions (190-193). The generation of $MAVS^{-/-}$ mice confirmed the necessity of this protein for RIG-I and MDA5 signaling to activate IRF3/7 and NFκB (194, 195). IRF3/7 are activated via phosphorylation by TANK-binding kinase 1 (TBK1) and the inducible IκB kinase (IKKi) (196-198). The TNF receptor-associated factor 3 (TRAF3) serves as a bridge to IRF3/7 activation by interacting with both MAVS and either TBK1 or IKKi (199, 200). MAVS also interacts with TRAF6, Fas-associated protein with the death domain (FADD), and receptor-interacting protein 1 (RIP1) (190, 193). The TRAF6/FADD/RIP1 complex mediates not only the activation of the IκB kinase (IKK) complex through an interaction between RIP1 and the IKK complex regulatory subunit IKKγ, but also the activation of mitogen-activated protein kinase (MAPK) pathways (201, 202).

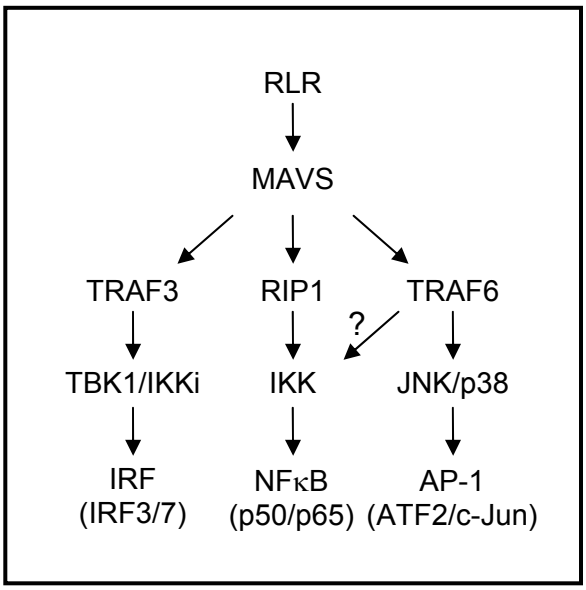

Figure 1.2: RIG-I-Like Receptor (RLR) Signaling. Key proteins involved in signal transduction initiated by the RLR, RIG-I or MDA5 leading to the activation IRF, NFκB, and AP-1 family members.

Toll-Like Receptor (TLR) Signaling

There are 10 Toll-like receptors (TLRs) in humans that recognize PAMPs from of a wide range of microorganisms including bacteria, viruses, fungi, and protozoa (203-209). TLRs are transmembrane proteins that are localized to either the plasma membrane (TLR1, TLR2, TLR4-6, and TLR10) or to the ER and endosomal vesicles (TLR7-9) (210-212). TLR3 is found at all three locations depending on the cell type (211-214). TLRs are generally expressed on hematopoietic cells although their expression levels differ from one cell type to another. In addition to expression on hematopoietic cells, TLR3 is also expressed by and signals properly in fibroblasts and epithelial cells (213-215).

TLRs are transmembrane proteins with extracellular/luminal domains containing leucine-rich regions that bind to specific PAMPs (216). The

cytoplasmic, Toll-IL-1 receptor domain serves as a scaffold for assembling signaling complexes in response to ligand binding to the extracellular domain (216). Each TLR recognizes a unique set of PAMPs. For instance, several TLRs recognize viral PAMPs, either nucleic acid (TLR3 and TLR7-9) or glycoproteins (TLR2 and TLR4) (217). Type I IFN is induced in response to viral recognition by all of these TLRs except for TLR2, which can activate NFκB and AP-1 signaling, but lacks the ability to signal for the activation of IRFs (218).

Downstream signaling to activate IRF3/7, NFκB, and AP-1 varies from one TLR to another and in some cases, the same TLR can signal differently depending on the cell in which it is expressed. The signaling by TLR3 (Figure 1.3) will be discussed here as it can respond to rotavirus genomic dsRNA (213, 215). Upon dsRNA stimulation, TLR3 moves into the endosomal compartment of the cell, either from the cell surface or from the ER (211, 212, 219, 220). Within the endosome, the TLR3 luminal domain forms a complex with CD14 to facilitate ligand binding (220). Like RLR signaling, TLR3 signals via TRAF3 complexes (198, 199, 221, 222) to activate IRFs and TRAF6:RIP1 complexes (223, 224) to activate both NFκB and AP-1 family members. Rather than signaling through the adaptor protein MAVS used in RLR signaling, TLR3 signals through the an adaptor protein called Toll/IL-1 receptor domain-containing adaptor inducing IFNβ (TRIF) (224). The cytoplasmic TIR domain of TLR3 interacts with c-Src, an event necessary for signaling, but the actual role of c-Src is unknown (219). TRIF interacts with the TRAF3, NAK-associated protein (NAP1), and either TBK1

or IKKi (198, 199, 221, 222) to signal downstream to IRF3. Just like in RLR signaling, TBK1 or IKKi mediate the activation of IRF3/7 via phosphorylation (196-198). However, the phosphorylation of IRF3/7 is incomplete without recruitment of phosphatidylinositol 3 kinase (PI3K) to the TIR of TLR3 and subsequent activation of the Akt kinase (225). TRIF also interacts with a complex composed of TRAF6 and RIP1, which signals through the MAPK pathway and the IKK complex to activate AP-1 and NFκB transcription factors, respectively (223, 224).

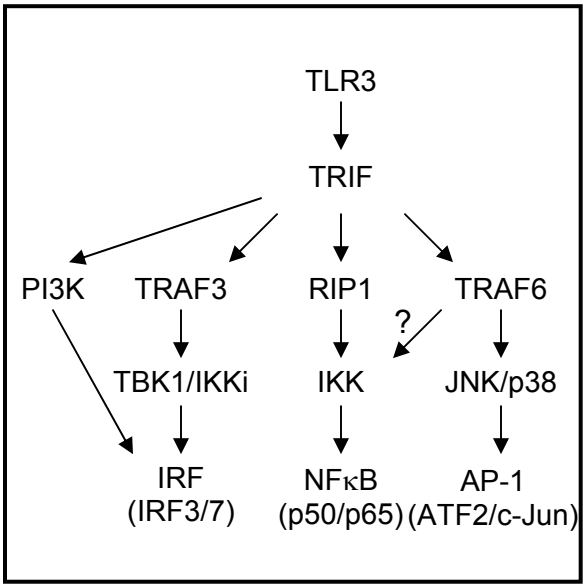

Figure 1.3: Toll-Like Receptor 3 (TLR3) Signaling. Key proteins involved in signal transduction initiated by TLR3 leading to the activation IRF, NFκB, and AP-1 family members.

RNAi targeting of RIG-I, but not TLR3, abrogated IFNβ induction in an intestinal epithelial cell line infected with an NSP1 defective rotavirus, showing that RIG-I is the main PAMP detector in rotavirus infections (226). However, numerous scenarios could lead to TLR3 signaling during a rotavirus infection.

Intestinal epithelial cells (IECs) die by lysis or apoptosis during rotavirus infection depending on the animal model (2, 44). If an infected IEC lyses, rotavirus genomic dsRNA would likely be released and detected by neighboring IECs, which would lead to intestinal epithelial injury in the small intestine (215). Conversely, if an infected IEC dies by apoptosis, the apoptotic body could be phagocytosed leading to dsRNA delivery to TLR3 containing vesicles (227). The RIG-I signaling in response to rotavirus infection was shown in epithelial cells, but rotavirus is also capable of replicating in dendritic cells and macrophages (228), both of which express TLRs at high levels (229). Rotavirus extraintestinal spread through the lymphatic system potentially occurs via the infection of these cell types (2). It remains to be seen whether rotavirus is detected by RIG-I in these cell types or if dsRNA is delivered to TLR3 containing vesicles in a mechanism involving autophagy machinery (218).

Interferon Regulatory Factor-3/7 Activation and Signaling

Nine interferon regulatory factor (IRF1-9) transcription factors have been described and are characterized by a conserved DNA-binding domain near the N-terminus (230, 231). IRF3-9 have an IRF-associated domain (IAD) within the carboxy terminus that is important for protein-protein interactions upon phosphorylation-mediated activation (230, 231). The IAD typically promotes either homodimer or heterodimer formation among IRF family members, but IADs can also interact with other protein families such as members of the STAT family (230, 231). Several IRFs have been implicated in type I IFN induction including

IRF1, IRF3, IRF5, and IRF7. However, $IRF1^{-/-}$ and $IRF5^{-/-}$ mice indicate that these transcription factors are dispensable for type I IFN induction (232, 233). The activation of IRF3 and IRF7 has therefore been studied in detail. Early studies identified that the main steps of IRF3 and IRF7 activation are similar (234). IRF3 is localized to the cytoplasm in a latent form in uninfected cells. Subsequent to viral infection, IRF3 becomes hyperphosphorylated and forms dimers (170, 171, 235, 236). The dimers accumulate in the nucleus, bind consensus DNA sequences, recruit histone acetyltransferases (HATs) to promote gene induction, and then are degraded in a proteasome-dependent manner (170, 171, 235, 236).

Hyperphosphorylation of serine and threonine residues near the carboxy terminus of IRF3 by TBK1 and IKKi is necessary for IRF3 activation (196-198). However, $IKKi^{-/-}$ mice have shown that this kinase is of minor importance (197). In all, there have been six serine residues and a single threonine residue near the carboxy terminus of IRF3 proposed to be important for IRF3 activation, but only two have been verified using phospho-specific antibodies (237, 238).

Two research groups independently determined the crystal structure for the carboxy-terminus of IRF3 (239, 240), from which two distinct mechanisms of IRF3 dimerization were proposed. Takahasi et al suggested that dimerization was facilitated by phosphorylated serine residues on two IRF3 molecules interacting with hydrophobic pockets on the opposing IRF3 molecule (240). Qin et al proposed that inhibitory domains, which conceal the IAD of each IRF3, are

displaced by repulsion forces upon IRF3 hyperphosphorylation to allow IAD-IAD interaction (239). Neither mechanism has been definitively proven.

IRF3 is known to shuttle between the cytoplasm and nucleus in uninfected cells. Cytoplasmic IRF3 is more prominent, presumably because IRF3 contains a weak nuclear localization signal (NLS) and a strong nuclear export signal (NES) (241). Hyperphosphorylated IRF3 dimers form a complex with histone acetyltransferases, CREB-binding protein (CBP) or p300 (170, 171, 235, 236). The holocomplex has high affinity for IRF consensus sequences (170, 171, 235, 236). Binding both DNA and CBP or p300 results in nuclear retention of IRF3 dimers (241, 242). The mechanism of gene induction will be described in the "Induction of IFNβ" section below. While in the nucleus, IRF3 is targeted for proteasome-mediated degradation that is dependent on a peptidyl-prolyl isomerase, PIN1 (243). The E3 ubiquitin ligase that directs IRF3 polyubiquitination is likely a Skp1-Cull1-F-box multiprotein complex, based on the requirement of cullin 1 for IRF3 degradation (244).

Sequence alignments show that IRF7 has serine and threonine residue spacing near its carboxy terminus similar to that found in IRF3 (234). IRF7 is also activated by hyperphosphorylation which, like with IRF3, is mediated by TBK1 and IKKi (198). IRF7 is expressed at low basal levels in most cell types and its expression is upregulated by IFN signaling (169, 170). It was originally thought that IRF3, but not IRF7, was essential for the early phase of type I IFN induction since $IRF3^{-/-}$ mice have an impaired type I IFN response (169, 170,

173, 173). However, IRF7$^{-/-}$ mice completely lack the ability to express type I IFN (245). A revised model suggests that IRF3/7 heterodimers or IRF7 homodimers are important for the initial induction of type I IFN (245). Following induced expression of IRF7 by IFN signaling, IRF7 is the major driver of a positive feedback mechanism that upregulates the expression of a wide range of the type I IFN genes (245).

NFκB Activation and Signaling

TRAF6 and RIP1 are involved in activation of NFκB and AP-1 in signal transduction cascades from both RLR and TLR signaling (190, 191, 193, 223, 246). TRAF6 and RIP1 act as adaptor proteins by interacting with either MAVS or TRIF and then signaling to downstream targets. TRAF6 is an E3 ubiquitin ligase capable of targeting several components of the NFκB signaling pathway for lysine 63-linked polyubiquitin chains (247, 248). However, the necessity for TRAF6 E3 activity in NFκB signaling is controversial. A negative feedback loop of NFκB signaling can be achieved through the activity of A20, a deubiquitinase whose expression is induced by NFκB (249). In contrast, results from various reports attempting to rescue NFκB signaling by ectopic expression of TRAF6 RING domain mutants in wild-type TRAF6 deficient cells are conflicting (250, 251). The necessity of the kinase domain of RIP1 for NFκB signaling has also been questioned (252). The ability of RIP1 to interact with the regulatory subunit

of the IKK complex, IKKγ, is important for NFκB signaling because it nucleates IKK complex oligomerization (253).

IKK activation is initiated with the phosphorylation of key serine residues in the kinase domains of the IKKα and IKKβ subunits of the IKK complex (254). It is unknown whether this event is a result of transautophosphorylation between IKKα and IKKβ or whether there is an IKK kinase that remains to be identified (253). As a negative feedback loop, activated IKK also phosphorylates the IKKγ regulatory subunit, which leads to dissociation of IKKγ and conformational changes in IKKα and IKKβ (255-257). This allows for the recognition and dephosphorylation of the kinase domain serine residues by phosphatases to inactivate the IKK complex (255-257).

Once activated, the IKK complex can phosphorylate three inhibitor of NFκB (IκB) proteins, IκBα, IκBβ, and IκBε (258). Phosphorylated IκB is recognized by the $SCF^{\beta\text{-}TRCP}$ E3 ubiquitin ligase complex leading to lysine 48-linked polyubiquitination of IκB, which is subsequently degraded by the proteasome (259). Differences in functional properties of the three IκB proteins are due to differences in the kinetics of their degradation and resynthesis (260). IκBα plays a central role in regulating NFκB signaling, as it is preferred over IκBβ by the IKK complex for phosphorylation, resulting in more rapid degradation of IκBα (261).

NFκB transcription factors are composed of homodimers and heterodimers of five NFκB subunits. The most common NFκB dimer is

composed of the p65 and p50 subunits (262) and is usually inhibited by association with IκBα (253). IκBα in complex with p65:p50 normally shuttles between the cytoplasm and the nucleus, but is predominantly found in the cytoplasm (263). The inhibitory activity of IκBα has been traditionally seen as a function of maintaining the cytoplasmic localization of p65:p50 since the return of nuclear p65:p50 to the cytoplasm correlates with the synthesis of new IκBα (264, 265). However, p65:p50 still remains mostly cytoplasmic in cells deficient in all three IκB proteins (266). Experiments with IκB deficient cells also showed that p65:p50 was capable of binding the NFκB consensus sites, albeit with low affinity (266). Therefore, the main inhibitory mechanism of IκBα appears to be antagonism of p65:p50 DNA binding.

Robust nuclear accumulation of p65:p50 free from IκB inhibition occurs when the DNA binding of this dimer is enhanced by phosphorylation of the p65 subunit on serine 276 (267, 268). This posttranslational modification is mediated by either the catalyticy subunit of protein kinase A (PKAc) in the cytoplasm or by mitogen- and stress-activated protein kinase-1 (MSK1) in the nucleus (267, 268). Serine 276 phosphorylation of p65 is essential for p65:p50 interaction with the histone acetyltransferases, CBP and p300 (269). CBP/p300 then acetylates p65 on lysine residue 310, a modification important to maximize transcriptional activity of this complex (269, 270).

AP-1 Activation and Signaling

The presence of a binding site within the enhanceosome region of the IFNβ promoter for an ATF-2 and c-Jun heterodimer has been known for many years (271). The importance of these AP-1 transcription factors is evident since the mutation of the AP-1 binding site within the enhanceosome inhibits the induction of IFNβ in response to viral infection (272). However, knowledge of the signaling mechanisms leading to the activation of ATF-2 and c-Jun during viral infection is limited. Unlike the IRF and NFκB transcription factor families, which are found in inactive forms in the cytoplasm and translocate to the nucleus following phosphorylation, AP-1 transcription factors can bind to DNA in the nonphosphorylated, inactive form (273, 274). Phosphorylation of ATF-2 and c-Jun increase the transactivating activity without changing the DNA-binding activity of these transcription factors (273, 274). MAPK family members such as JNK and p38 are responsible for phosphorylating c-Jun and ATF-2 (275-277). The contribution of p38 or JNK to IFNβ induction is variable and depends on the stimuli (264). Signaling from RLR through MAVS to activate MAPK pathways is likely bridged by TRAF6, since deficiency in TRAF6 E3 ubiquitin ligase activity has a detrimental effect on MAPK signaling (250, 278, 279).

Induction of IFNβ

Expression of IFNβ is tightly controlled at the level of transcription. The transcriptional start site is masked by nucleosomes in unstimulated cells (280). The promoter region of the IFNβ gene contains four positive regulatory domain

(PRD) elements, which are bound by IRFs (PRDI and PRDIII), NFκB (PRDII) and AP-1 (PRDIV) in response to viral detection (281, 282). The binding of these transcription factors to the promoter, as well as the high-mobility group protein HMG-1(Y), is referred to as the IFNβ enhanceosome (283). This complex is responsible for coordinated recruitment of histone acetyltransferases (280). The histones within the nucleosome that covers the transcriptional start site are subsequently acetylated (280). The modified histones recruit the Brahma-related gene (BRG)-associated factor (BAF) complex that acts to displace the nucleosome and thus uncover the transcriptional start site (280). TFIID binds to the start site and initiates IFNβ gene transcription by recruiting RNA polymerase II (280).

Type I Interferon Signaling

The type I IFN receptor (IFNAR) is composed of two chains, IFNAR1 and IFNAR2c, which coordinately bind to IFNβ or other type I IFN (284, 285). The transcription factor complex interferon-stimulated gene factor 3 (ISGF3) is formed by the heterotrimer of STAT1, STAT2, and IRF9 when type I IFN binds to the IFNAR (286-288). The signaling is a phosphorylation cascade mediated by members of the JAK family of kinases. Each chain of the receptor is associated with a JAK family member; Tyk2 interacts with IFNAR1 and JAK2 interacts with IFNAR2. Upon binding type I IFN, the IFNAR chains dimerize leading to Tyk2 phosphorylation by JAK1 and subsequent Tyk2 cross-phosphorylation of JAK1 (289-291). The activated JAK members first phosphorylate the IFNAR1 chain on

tyrosine at residue 466 (Y466) (292). Phosphorylated Y466 serves as a docking site for STAT2 (293), a transcription factor that is constitutively associated with IRF9 (294, 295). The activated JAK members phosphorylate tyrosine residues on both STAT2 and STAT1, the latter of which interact with each other via reciprocal Src-homology (SH2) domains (286, 287, 296, 297).

The ISGF3 complex accumulates in the nucleus and binds to interferon stimulated response element (ISRE) sites in the enhancer region of many interferon-stimulated genes (ISG) (298). Similar to the induction of IFNβ by the enhanceosome, ISGF3 induces transcription of target genes by recruiting the histone acetyltransferases CBP and p300 (299).

Although the activation of ISGF3 in response to type I IFN treatment has received much attention, many of the genes that are differentially regulated in response to type I IFN do not contain ISRE sites (298). This is because many additional transcription factors including STAT3-7, NFκB, and PU.1 are activated following type I IFN treatment as well (298, 300).

Effector Mechanisms

The importance of type I IFN signaling has been shown in type I IFN receptor (IFNAR) knock-out mice, which are unable to mount effective antiviral responses (301). The overall response to type I IFN treatment is complex since hundreds of genes are differentially regulated (174). These genes can be grouped according to the functional processes in which they participate to form a clearer picture of the general effects of type I IFN signaling (302). The

discussion below will focus on i) a positive feedback loop that enhances the IFN response, ii) antiviral effector molecules, and iii) development of an adaptive immune response due to the direct relevance of these processes in an immune response to virus infection.

Many of the proteins described in the induction of type I IFN are also upregulated in cells responding to type I IFN resulting in a positive feedback loop. These include TLRs, RLRs, IRFs, p65, and c-Jun (218, 302). Increased abundance of these proteins can lead to increased sensitivity by the host cells in responding to viral infections (218). Proteins involved in type I IFN signaling are also induced in cells responding to type I IFN, further propagating the positive feedback loop (218). These include both type I IFN receptor chains, as well as STAT1 and IRF9 (218, 302). These changes result in a more robust response to the presence of type I IFN. Of the IFN regulatory factor family members that are upregulated in response to type I IFN, IRF7 is arguably the most important. In the initial induction phase, IFNβ and IFNα4 are the only type I IFN genes upregulated. Induction of IRF7, which is normally expressed at low basal levels, leads to an increase in IRF7 homodimers which are efficient at inducing the expression of all type I IFN subtypes (169, 170, 172). Even though the different subtypes all bind to the type I IFN receptor, the downstream signaling differs for each subtype (303).

Of the many genes that are upregulated by type I IFN, only a small number encode proteins that have antiviral activity. These proteins tend to have

broad antiviral activity such as inhibiting translation (i.e. PKR, P54, P56) (304-306), or by cleaving RNAs, both cellular and viral, as is the case with the OAS/RNaseL system (307-309). An important aspect of the OAS/RNaseL system is that the RNA cleavage products are recognized by RIG-I; thus, activation of this system is part of the positive feedback loop in type I IFN production (310). Recently, it was shown that subsets of microRNAs (miRNAs) are induced in response to IFN. Some of these miRNAs targeted hepatitis C virus (HCV) sequences and were shown to effectively reduce HCV replication (175). Whether these miRNAs are complementary to sequences from additional viruses is unknown. Furthermore, it is surprising that the selective pressure exerted on HCV by the miRNAs does not result in the generation of HCV escape mutants immune to the effect of the miRNAs.

The IFN system arose during evolution at a similar time as the adaptive immune system (311, 312). Type I IFN is important for linking innate immunity with adaptive immunity (313-315). As an example, mice lacking the type I IFN receptor were unable to generate either effector T cells or memory T cells in response to LCMV infection (316). A suite of proteins involved in MHC class I presentation are upregulated in most cells in response to type I IFN, including MHC molecules, proteasome subunits, and transporter associated with antigen processing (TAP) (302). Type I IFN acts on many cells of the immune system. For instance, type I IFNs stimulate the proliferation of antigen-specific T cells, but not naïve T cells (195, 245, 316-319). These effects on T cell populations can be

partially explained by the ability of type I IFN to promote the maturation of dendritic cells (320).

Viral Modulation of the IFN System

In a recent review, Randall and Goodburn divided over a hundred of the known mechanisms that viruses use to antagonize the IFN system into five broad categories: i) interfering with host-cell gene expression, ii) blocking IFN induction by limiting PAMP exposure or by antagonizing IFN induction signaling pathways, iii) inhibiting IFN signaling, iv) blocking action of antiviral proteins, and (v) having a replication strategy that is resistant to the IFN system (321). The diversity of IFN antagonistic mechanisms is vast, so the mechanisms used by two viruses of high medical importance, hepatitis C virus (HCV) and influenza A virus (FLUAV), will be described here. Intense research of these viruses has shown that each uses multiple mechanisms spanning the five categories described above to modulate the IFN system (321). Additional mechanisms of IFN system modulation are described in the ubiquitin-proteasome system section of this chapter and in the discussion sections of each subsequent chapter.

HCV is resolved in only 15-25% of acute infections and the remaining cases lead to persistent infections (322). The infection will continue for the lifetime of the host unless IFN therapy can tip the balance to a resolved infection (322). The virally encoded NS3/4A protease complex, which functions in virus replication to cleave nonstructural proteins from the HCV polyprotein (323), is an important antagonist that blocks IFNβ induction (321). HCV PAMPs are

recognized by hepatocytes by both RIG-I and TLR3 (178, 324). The blockade of these two signaling pathways results from NS3/4A-mediated cleavage of the adaptor proteins, MAVS (191, 325-329) and TRIF (330), in RIG-I and TLR3 signaling, respectively. A peptidomimetic inhibitor of NS3/4A allowed IRF3 and NFκB to be activated in HCV infections (330-332).

Since HCV is sensitive to IFN treatment (333-335), it would be logical to conclude that an effective blockade of IFNβ induction would be sufficient for HCV to establish a persistent infection. However, IFN treatment does not always resolve HCV infections, which suggests that HCV has mechanisms to resist IFN signaling and/or IFN-induced antiviral effector proteins (336). Indeed, the HCV core protein interacts with STAT1, blocking STAT1 phosphorylation and interaction with STAT2 (337). The HCV core and NS5A proteins also induce the expression of cellular proteins, such as suppressor of cytokine signaling 3 (SOCS3) and protein phosphatase 2A, that function to negatively regulate IFN signaling (338, 339). The HCV core protein is multifunctional as it is also capable of interfering with IRF1, which is responsible for prolonged expression of ISGs (340). Acute cases of HCV infection that are resolved may be instances in which the HCV-encoded IFN system antagonists are unable to act before the host's IFN system responds (322).

Unlike HCV, which does not appear to use mechanisms of global cellular gene expression inhibition, FLUAV interferes with cellular mRNA stability and processing to prevent IFN system responses (341-346). FLUAV-encoded NS1

carries out this antagonism in a strain specific manner (347). It has recently been noted that strains inefficient at blocking cellular gene expression compensate by inhibiting RIG-I through a direct interaction between NS1 and RIG-I (187, 348-350). The ability of NS1 to bind dsRNA has been suggested to be important for preventing IFNβ induction (351-353). Others have argued that the NS1 sequesters dsRNA to prevent the dsRNA-mediated activation of the antiviral protein OAS (354, 355).

An interesting difference between HCV and FLUAV, which both use an impressive variety of mechanisms to block the IFN system, is that HCV encodes many IFN antagonists and FLUAV antagonism relies heavily on NS1-mediated activity. Host range restriction in FLUAV has been linked to the ability of a given FLUAV to block the IFN response of the inoculated species (356). IFN-sensitive FLUAV attenuated viral vaccines have been based on NS1 properties (357-360). At the other end of the spectrum, the extreme virulence exhibited by the 1918 influenza virus may be related to an NS1 with efficient IFN system antagonistic properties (361).

Ubiquitin-Proteasome System

Ubiquitin-Proteasome System Overview

The ubiquitin-proteasome system is responsible for the degradation of most short-lived proteins within a cell. This was shown by the characterization of a cell line with a temperature-sensitive defect in ubiquitination (362, 363).

Interestingly, the ubiquitin-proteasome system was originally studied to understand the requirement for ATP in protein degradation by this system because cleavage of a peptide bond is thermodynamically favorable. As such, most proteases do not require energy. However, the processes of ubiquitination and unfolding of a protein destined for degradation mediated by the proteasome require ATP. As expected, the process of cleaving the unfolded protein by the proteasome does not require energy.

Ubiquitination is a posttranslational modification in which ubiquitin, a small protein (8kDa), is covalently bound to a lysine side chain of the substrate. Proteins are ubiquitinated via an enzymatic cascade involving three enzymes (364). The enzymes, designated E1, E2, and E3, act in a hierachael manner, whereby the E1 can transfer ubiquitin to any E2. Then each E3 associates with an E2 to transfer the ubiquitin onto a substrate. Some E3s are able to use different E2s to catalyze the ubiquitination of a substrate (365). The E3 enzymes provide substrate specificity for the ubiquitin-proteasome system ultimately regulating which proteins are ubiquitinated (366). Although ubiquitination of a substrate can be used for many purposes, including signal transduction and endosome trafficking, a common result of ubiquitation is as a recognition signal for degradation of the substrate by the proteasome.

Ubiquitin

Ubiquitin is a polypeptide of 76 amino acids. Ubiquitin genes are translated as polyubiquitin chains that are cleaved by cysteine proteases called

deubiquitinating enzymes (discussed below) to release single ubiquitin molecules (367, 368). Substrates can be ubiquitinated in four ways. The first two involve monoubiquitination of either a single ε-amino group of a lysine side chain within the substrate or of the amino group located at the N terminus of the substrate. The third type of ubiquitination is multi-ubiquitination in which multiple lysine groups of the substrate are conjugated with ubiquitins. The final form of ubiquitination is polyubiquitination in which ubiquitins are polymerized through a series of ubiquitin-ubiquitin linkages. Among the conserved residues in the sequence of ubiquitin are seven lysines, each of which can be the target for the addition of another ubiquitin in the growing chain (369). The lysine residue used in the ubiquitin-ubiquitin linkages can result in different outcomes for the substrate. For instance, substrates with lysine-63 (K63) polyubiquitin chains are involved in signal transduction, whereas K11-, K29-, or K48-linked chains are recognition signals for degradation by the proteasome (368).

Enzymatic Cascade in Ubiquitination

Most organisms encode a single E1 ubiquitin activating enzyme (370, 371). Recently, a second E1 was characterized in humans (372). The activation of ubiquitin results in formation of a high energy thiolester bond between the active site cysteine of the E1 and the carboxy group of the C terminal glycine of ubiquitin (373). E1 is capable of binding an ubiquitin-adenlyate intermediate and a thiolester bound ubiquitin at the same time. After transferring the thiolester-bound ubiquitin to an E2, the ubiquitin-adenylate intermediate is transferred to

the active site cysteine, releasing the adenlylate in the form of AMP. The E1 then binds to both an ATP molecule and an ubiquitin to form a new ubiquitin-adenylate intermediate (374).

There are approximately 50 E2 ubiquitin conjugating enzymes encoded in a typical mammalian genome (375). Each E2 enzyme contains a conserved core of 150 amino acids that surrounds an active site cysteine (376-378). E2 enzymes function to transiently carry the activated ubiquitin via a thiolester bond. E3 enzymes act as a bridge between the E2 and the substrate. The E2 can either transfer the ubiquitin to an E3, which then transfers the ubiquitin to the substrate, or the E2 can transfer the ubiquitin directly to the substrate. All known E3 ubiquitin ligases have either a HECT domain or a RING domain (discussed below) (379-381). Transfer of the activated ubiquitin onto the substrate from the E2 is dependent upon the type of E3 (Figure 1.4).

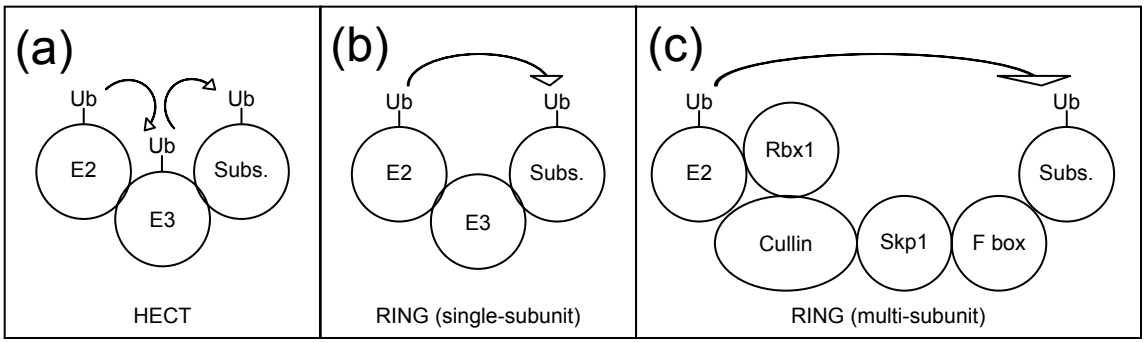

Figure 1.4: Methods of substrate ubiquitination mediated by different types of E3 ubiquitin ligases. (a) Ubiquitin is transferred onto HECT E3 enzymes prior to substrate ubiquitination. (b) Ubiquitin is transferred directly onto the substrate from the E2 enzyme in single-subunit RING E3 mediated reactions. (c) Ubiquitin is transferred directly onto the substrate from the E2 enzyme in multi-subunit RING E3 mediated reactions. The general organization of an SCF multi-subunit complex is also depicted. Other multi-subunit RING E3 enzyme complexes have similar organization. (Ub, ubiquitin; Subs., substrate)

There are hundreds of E3 ubiquitin ligase enzymes encoded in mammalian genomes (375), and all contain either a HECT domain or RING domain. The HECT E3 enzymes are named for domains with sequence homology to the E6-associated protein (E6-AP) C terminus (366). E6 is an oncogene encoded by human papillomavirus that targets the degradation of p53 by utilizing the cellular protein E6-AP (382). Within the HECT domain, there is a strictly conserved cysteine that forms a transient thiolester bond with ubiquitin prior to transfer of the ubiquitin to the substrate (Figure 1.4) (383). Most HECT E3 enzymes have not been well characterized (366).

All other known E3 ubiquitin ligases contain a RING (really interesting new gene) domain. RING domains consist of a series of cysteine and histidine residues that coordinate the binding of two zinc ions. Since these ions are not involved in catalysis, the RING domain is likely involved in molecular scaffolds important for protein-protein interactions (384). In support of this, a crystal structure of the RING E3, c-Cbl, in complex with its cognate E2 shows that the majority of the interaction surface between these proteins occurs along the RING domain of c-Cbl (385). The crystal structure analysis also suggested that RING E3 ubiquitin ligases catalyze the transfer of the activated ubiquitin from the active site cysteine of the E2 to a lysine side chain of the substrate by bringing the E2 and substrate into close proximity (Figure 1.4) (385). Point mutations of the cysteine or histidine residues of the RING domain prevent the E3 from targeting a substrate for degradation (386-389). For most E3 enzymes, the RING

mutations likely disrupt the E2-E3 interaction. However, these mutations have been shown to disrupt the E3-substrate interaction (390). An interesting property of RING E3 enzymes is that of autoregulation, whereby the RING E3 catalyzes its own ubiquitination (381, 386, 387). Mutations to the RING domain prevent this mechanism of autoregulation (386-389).

E3 ubiquitin ligases within the RING-domain family can be divided into single-subunit enzymes, in which a single protein is capable of coordinating the binding of the cognate E2 and the substrate, or multi-subunit enzymes, in which separate proteins carry out each of these tasks (Figure 1.4) (366). Single-subunit RING E3 ubiquitin ligases are capable of catalyzing polyubiquitin chains in the presence of ATP, ubiquitin, E1, and the cognate E2 in an *in vitro* ubiquitin conjugating assay (387).

Well-studied multi-subunit complexes include the Skp1-Cullin-F box (SCF) family, the anaphase-promoting complex (APC) and the Von Hippel Lindau-Elongin C-Elongin B complex (VCB) (366). The organization of the proteins within these complexes is similar (366). For example, Socs box proteins are functionally analogous to the F box proteins and the Elongin B/Elongin C proteins are functionally analogous to the Skp1 protein. Here I will discuss the organization of SCF complexes as an example because it is relevant to this study (see Figure 1.4(c)).

The RING domain-containing protein in SCF complexes, Rbx1 (also known as Roc1), coordinately binds to cullin family proteins and the cognate E2

enzymes (391-395). The cullin family member and Rbx1 display enzymatic activity by catalyzing the formation of polyubiquitin chains in the *in vitro* ubiquitin conjugating assay (392-396). F box proteins provide the SCF complexes with substrate specificity (366). These proteins are associated with the catalytically active cullin/Rbx1 core of the multi-subunit complex through the adaptor protein, Skp1 (379, 394, 397). SCF complexes are positively regulated by post-translational modification of the cullin protein through the conjugation of Nedd8, a ubiquitin-like protein, which leads to recruitment of the cognate E2 (379).

Proteasome

The protease responsible for degrading polyubiquitinated proteins is the proteasome, a 2.5 MDa complex comprised of at least 65 proteins (398). Two distinct subcomplexes known as the 20S proteasome and the 19S regulatory subunit combine to form an active 26S proteasome (399). The polyubiquitinated substrate is recruited to the proteasome through the action of subunits within the 19S regulatory particle (400-402). In an ATP-dependent manner, the 19S subunit unfolds and translocates the polyubiquitinated substrate into the proteolytically active chamber of the 20S proteasome for degradation (403-405). The polyubiquitin chain is spared from degradation by being cleaved from the substrate prior to proteolysis of the substrate (406).

The 20S proteasome structure consists of four rings containing seven subunits each stacked together to form a cylinder (404, 405). The rings on the ends of the cylinder are composed of alpha subunits (α1-α7), which interact with

the 19S regulatory particles that can be attached to one or both ends of the cylinder (407). The inner two rings of the cylinder are composed of beta subunits (β1-β7). The subunits β1, β2, and β5 have protease activity and cleave the substrate as it passes through the channel of the 20S proteasome (408, 409).

The IFN system can affect the proteolytic activity of proteasomes. Type I or type II IFN stimulation induces the expression of subunits called β1i, β2i, and β5i. These subunits replace the β1, β2, and β5 subunits of the constitutive proteasome to convert the 20S core to an immunoproteasome (410-412). The immunoproteasome processes proteins, including antigens, differently than the constitutive proteasome. The immunoproteasome is important since the modified activity of this proteasome produces peptide fragments that are readily loaded onto MHC class I molecules for antigen presentation (413). In support of this, transgenic mice lacking β1i or β5i genes have defects in displaying some antigens (414, 415).

Deubiquitinating Enzymes

Ubiquitination is a reversible process. Mammalian genomes encode around 70 deubiquitinating enzymes (DUBs) (398) that are proteases which cleave ubiquitin conjugates after the terminal carbonyl of ubiquitin (416). Two important activities mediated by DUBs were mentioned in the previous sections. The first is that some DUBs process ubiquitin precursors that are fused to some of the ribosomal subunits or are fused together as head-to-tail-linked ubiquitin multimers extending the entire length of the newly synthesized polypeptide (417).

The process of the releasing free ubiquitins from ubiquitin precursors is rapid, often occurring cotranslationally (418). The second activity is the rescue of polyubiquitin chains from substrates entering the proteasome. This activity is mediated by the only known essential DUB, Rpn11, a subunit of the proteasome 19S regulatory particle (419, 420).

There are two main classes of DUBs, ubiquitin processing enzymes (UBP) and ubiquitin carboxy-terminal hydrolases (UCH), and three minor classes of DUBs (416). The UBP enzymes remove entire polyubiquitin chains from proteins at the base of the chain and the UCH enzymes break down polyubiquitin chains or edit the ends of the polyubiquitin chains attached to substrates (407). The combined actions of the DUBs recycle polyubiquitin chains within a cell to a free ubiquitin pool, which is important for sustaining the normal rates of degrading ubiquitin-proteasome system substrates (421).

Additional processes mediated by DUBs include processing of unanchored polyubiquitin chains (422, 423) and editing anchored polyubiquitin chains as a quality control measure on mistakenly ubiquitinated proteins (424). A significant portion of the ubiquitin within a cell is found in the form of polyubiquitin chains, which are generated by E3 enzymes or are cleaved from polyubiquitinated proteins (425). The DUB with the highest activity for unanchored polyubiquitin chains is isopeptidase T (422, 423). Like with any cellular process, quality control systems are needed. Since K48-linked polyubiquitin chains of four or more are required for recognition by the

proteasome (400, 426), it has been proposed that DUBs can act as a proofreading mechanism, removing ubiquitin from proteins that should not be targeted for degradation (425).

Viral Modulation of the Ubiquitin-Proteasome System

There are many examples of viral modulation of the ubiquitin-proteasome system. Nearly all known mechanisms occur at the level of E3 ubiquitin ligase activity (427). Virus encoded proteins either have intrinsic E3 activity or reprogram cellular E3 enzymes (427). The outcome of ubiquitin-proteasome system modulation by viral proteins affects many aspects of normal cellular processes, including immune responses (428, 429).

The Kaposi sarcoma-associated herpes virus (KSHV) encodes three E3 ubiquitin ligases, MIR-1, MIR-2, and RTA (430, 431). The MIR-1 and MIR-2 proteins hinder adaptive immune responses by selectively targeting MHC class I molecules for degradation (430). It has been debated whether the cysteine-rich regions of these two proteins should be considered RING domains (432, 433). The third E3 encoded by KSHV, RTA, targets the degradation of IRF7 (431). Mutations to cysteine and histidine residues within the RING-like domain of RTA prevented both self-ubiquitination and IRF7 ubiquitination without affecting the RTA-IRF7 interaction (431). This data is consistent with the cysteine-rich region of this protein representing an atypical RING domain (431).

Another interesting example of a virally encoded RING E3 is the herpes simplex virus-1 protein, ICP0. Because it contains two herpes ubiquitin ligase

(HUL) domains, this protein has been described as a “two-headed ubiquitin ligase” (434). HUL-1 is located near the carboxy-terminus of ICP0 and is credited with targeting the degradation of Cdc34, an E2 ubiquitin ligase enzyme (435). Curiously, HUL-1 does not contain a RING domain or a HECT domain, yet deletion mapping showed this HUL domain to be responsible for the E3 activity (435). The second domain, HUL-2, is located near the amino-terminus of ICP0 and contains a standard RING sequence. HUL-2 is important for the degradation of a relatively large number of cellular proteins including p53 (436), two centromeric proteins (437, 438), promyelocytic leukemia antigen (439, 440), DNA protein kinase (441), and sp100 (440, 442).

The human papillomavirus oncogene, E6, was described above since the study of this protein revealed the first known HECT domain-containing protein, E6-AP (382). E6 reprograms E6-AP since this cellular protein is unable to target the degradation of p53 without the aid of E6 (443). However, not every protein that interacts with E6 is targeted for degradation. As an example, E6 interacts with IRF3 and prevents gene induction by blocking IRF3-mediated transcriptional activity (444).

There are many variations by which virus proteins modulate multi-subunit RING E3 enzymes (445). One example of this is the human immunodeficiency virus-1 (HIV-1) protein, Vpu, which reprograms an SCF complex by mimicking the recognition motif of the F box protein of this complex, βTrCP (446). $SCF^{\beta TrCP}$ recognizes a motif, DSGXXS (where X represents any residue), when the serine

residues are phosphorylated (447). Vpu contains this motif and is constitutively phosphorylated on residues 52 and 56 by casein kinase II (448). $SCF^{\beta TrCP}$ recognizes Vpu, but is unable to target this HIV-1 protein for degradation (446). Rather, Vpu redirects $SCF^{\beta TrCP}$ to degrade CD4 (446). In addition to blocking antigen presentation due to CD4 degradation, the reprogramming efforts of Vpu prevent $SCF^{\beta TrCP}$ from targeting the normal substrates of this complex, such as $I\kappa B\alpha$ (449).

Additional examples of virus proteins modulating multi-subunit RING E3 complexes include the V proteins encoded by members of the family Paramyxoviridae (450) and the HIV-1 protein, Vif (451, 452). The V proteins reprogram the DDB-1/Cul4A/Rbx1 complex to target STAT transcription factors (450). Interestingly, different V proteins target different STATs for degradation (450). Examples included simian virus 5 V protein targeting of STAT1 (453), human parainfluenza virus-1 V protein targeting of STAT2 (454), and mumps virus V protein targeting of STAT1 (455) and STAT3 (456). The modulation of multisubunit E3 enzymes by Vif is different than the Vpu- and V protein-mediated E3 modulation. Vif does not reprogram an intact cellular E3 but instead, Vif interacts with the cullin/Rbx1 core of the complex through the adaptors Elongin B and Elongin C (452, 457). Targets of the Elongin/Cullin/Vif complex include the RNA editing proteins APOBEC3G and APOBEC3F (451, 452), which have antiretroviral activity (458). These studies illustrate the commonality of viral

modulation of the host cell ubiquitin-proteasome system and the various methods different viruses have evolved for this function.

INTERFERON REGULATORY FACTOR 3 IS A CELLULAR PARTNER OF ROTAVIRUS NSP1

Purpose

This chapter describes experiments performed prior to the start of the dissertation project. Important observations in this chapter provide the foundation for the subsequent chapters. Together with observations from chapters 3 and 4, the conclusion can be drawn that rotavirus NSP1 is an IFN system antagonist with at least two mechanism of action. The data shown in Figures 2.1-2.3 was published previously (459).

Abstract

The function of rotavirus NSP1 has remained enigmatic. Since NSP1 null rotavirus strains are capable of replication, we hypothesized NSP1 confers a selective advantage to rotaviruses within natural infection settings by modulating cellular processes. A yeast two-hybrid interaction screen was used to detect protein-protein interactions between NSP1 from a bovine rotavirus strain and proteins from MA104 cells. An interaction between the bovine NSP1 and interferon regulatory factor 3 (IRF3) was detected repeatedly during the screening process. Mapping the domains of NSP1 important for this interaction showed that the C terminus of NSP1 was capable of interacting with IRF3. However, the ability of full-length NSP1 to bind IRF3 was dependent upon the integrity of a zinc-binding domain of NSP1 near the N terminus. The NSP1-

interacting domain was mapped to the C terminus of IRF3. Infection of cells with wild-type, but not NSP1-null, rotavirus strains prevented the induction of IRF3-regulated genes, including the type I interferon (IFN), IFNβ. The mechanism was determined to be the targeted proteasome-mediated degradation of IRF3 in cells infected with wild-type rotavirus strains. The results in this chapter indicate that rotavirus NSP1 to antagonize the induction of IFN.

Introduction

Rotaviruses are the most important cause of severe, often life-threatening gastroenteritis in infants and children under 2 years of age (460). These viruses are ubiquitous in nature and also are responsible for a significant proportion of neonatal gastrointestinal illness in domestic animals, particularly in bovine and porcine species (461, 462). Substantial research efforts have thus focused on understanding the correlates of a protective immune response to rotavirus infection and the molecular mechanisms of virus replication so that efficacious vaccines can be developed.

The rotavirus segmented double-stranded RNA genome encodes six structural proteins (VP) and six nonstructural proteins (NSP) (463). The structural proteins VP1, VP2, VP3, VP4, VP6, and VP7 are well characterized in terms of their antigenic, structural, and biochemical properties. The functions of the rotavirus nonstructural proteins NSP1 to NSP6 are less well defined and

have been proposed based predominately on biochemical properties and activities of recombinant proteins (463).

NSP1 displays several interesting properties that warrant investigation. NSP1 has a calculated molecular weight of approximately 54 kDa and is the least conserved protein encoded by the rotavirus genome when NSP1s of different strains are compared (153, 163). The N terminus contains a conserved zinc finger motif that binds zinc and viral mRNA in vitro (159, 160). Immunofluorescent staining showed NSP1 to be localized throughout the cytoplasm, in contrast to most other rotavirus proteins, which concentrate in viroplasms (163). NSP1 is also found associated with the cytoskeleton when analyzed by subcellular fractionation (163). NSP1 is not required for rotavirus replication because strains with rearrangements in gene 5 that result in the synthesis of truncated NSP1 have been isolated from animals and from both immune-deficient and immune-competent children (162, 164, 464-468). Each of the NSP1 defective strains replicates in cell culture to titers close to those of their wild-type counterparts, but they yield small- to minute-plaque phenotypes.

We addressed the possibility that NSP1 plays a role in modulating host cell responses. We first constructed an MA104 cell cDNA library into the activation domain vector of a yeast two-hybrid interaction screen and then screened the library with NSP1 as bait to identify candidate partners of NSP1 that would provide clues to its function in rotavirus infected cells. An important transcription factor for the induction of type I interferon (IFN), IFN regulatory

factor 3 (IRF3), was detected as an NSP1 binding partner in the two-hybrid analysis

IRF3-mediated gene induction is an important cellular response to infection and viruses have evolved a variety of mechanisms to interfere with such a defensive response (177). For instance, the adenovirus E1A protein down-regulates IRF3-induced transcription by competing with IRF3 for binding to CBP/p300 (469). A second mechanism of IRF3 inhibition is displayed by human papillomavirus type 16. The E6 protein of human papillomavirus type 16 binds IRF3 directly and downregulates induction of IFNβ (444). Finally, the NS1 protein of influenza virus inhibits nuclear translocation of IRF3 in infected cells (352). Analysis of the IRF3 signaling pathway revealed that NSP1 targets the degradation of IRF3 in a proteasome-mediated manner.

Methods

Cells and Viruses

MA104 cells (ATCC) were cultured in M199 medium (Cellgro) supplemented with 5% (v/v) fetal bovine serum (FBS) at 37^{o}C in 5% CO_2. Medium was changed to M199 media lacking FBS prior to all infections.

B641, NCDV, and A5-16 rotavirus were propagated in MA104 cells. Concentration of viral stocks was achieved by centrifugation, suspension in M199 medium lacking FBS, and storage at -80^{o}C. The titer of each stock was determined by plaque assay.

UV-psoralen inactivation of rotavirus (470) strains A5-16 and NCDV was achieved by first adding AMT-psoralen (Sigma) to a working concentration of 50 μg/mL to an aliquot of each virus and subsequently chilled on ice for 15 minutes. The virus stock was then positioned 8 cm from a 366 nm, 115V UV light source (UVP) for 1 hour with continuous incubation on ice. Plaque assays were performed to confirm complete inactivation.

Plasmids

Plasmids were constructed using standard cloning techniques. Table 2.1 describes the primers used for cloning genes into the yeast two-hybrid system plasmids. Table 2.2 describes the primers used to direct mutagenesis using the Quikchange XL Site-Directed Mutagenesis Kit (Stratagene). The plasmid

Table 2.1: Primers Used for Cloning into Yeast Two-Hybrid Vectors

Construct	Sense	Primer Sequence
pGBK-bNSP1	+	CGC GGA TCC CGA TGG CGA CTT TTA AGG AC
	-	CCG CTC GAG GGT TCA ACA TCT GAA AGT TC
pGBK-bNSP1 Δ62	+	CGC GGA TCC AGT GGT GCA GTC AGT ATA ACA GGT G
	-	CCG CTC GAG GGT TCA ACA TCT GAA AGT TC
pGBK-bNSP1 Δ326	+	CGC GGA TCC AGA TCA ATA ACC ATT ACA AAG TGT GG
	-	CCG CTC GAG GGT TCA ACA TCT GAA AGT TC
pGBK-bNSP1 Ω290	+	CGC GGA TCC TGA TGG CGA CTT TTA AGG AC
	-	CCG CTC GAG TAT TAC TGG TAA GTG TGA CAT
pGAD-IRF3 (ΔDBD)	+	CCG GAA TTC AAG ATC TAC GAG TTT GTG
	-	CCC CTC GAG CAC ACC ATG AGG AG
pGAD-IRF3 (PRO-AID)	+	CCC GAA TTC CCA CTG CCA GAT CC
	-	CCC CTC GAG CAC ACC ATG AGG AG
pGAD-IRF3 (IAD-AID)	+	CCG GAA TTC GGG GAA GAG TGG GAG
	-	CCC CTC GAG CAC ACC ATG AGG AG
pGAD-IRF3 (AID)	+	CCG GAA TTC ACG TGC CTC AGG GCC
	-	CCC CTC GAG CAC ACC ATG AGG AG

Note: Underlined sequence indicates restriction endonuclease recognition sites.

Table 2.2: Primers Used for Site-Directed Mutagenesis

Construct	Sense	Primer Sequence
pGBK-bNSP1 C54A	+	CAA ATT TGA CAT ATG CCA GAG GGT GCG CTC TAT ACC
	-	GGT ATA GAG CGC ACC CTC TGG CAT ATG TCA AAT TTG
pGBK-bNSP1 C54A/C57A	+	CAA ATT TGA CAT ATG CCA GAG GGG CCG CTC TAT ACC
	-	GGT ATA GAG CGG CCC CTC TGG CAT ATG TCA AAT TTG

encoding NSP1 from the EW murine rotavirus strain was a gift from Dr. H Greenberg, Stanford University School of Medicine, Stanford, CA. The cloning of pGBK-v15, also known as pGBK-VPg, was described previously (471). pGAD-T Ag is a control plasmid encoding SV40 T antigen available with the Matchmaker3 Yeast Two-Hybrid System (Clontech). pGEX-IRF3$_{24-422}$ was constructed by subcloning the longest IRF3 encoding region identified in the two-hybrid screen into the EcoRI and XhoI sites of pGEX-4T-1 (GE Healthcare).

cDNA Library Construction

A cDNA library cloned into the activation plasmid, pGADT7, was generated from MA104 cell mRNA. Briefly, total RNA was purified from MA104 cells using TRIzol Reagent (Invitrogen). Polyadenylated RNA was isolated using an mRNA isolation kit from GE Healthcare. After generation of oligo-d(T) primed, EcoRI- and XhoI-linker conjugated cDNA, the cDNA was purified using CHROMA-SPIN 400 Columns (Clontech) and ligated into EcoRI/XhoI digested pGADT7. By performing test transformations to determine the transformation efficiency of the library in ElectroMAX DH10B Cells (Invitrogen) and calculating the insert size of 50 EcoRI- and XhoI-digested clones, the library was estimated to contain 2.5 x 10^6 recombinants with an average insert size of 1.3 kilobases.

Yeast Two-Hybrid Interaction Screen

All yeast two-hybrid analyses were performed with AH109 yeast (Clontech) using the Matchmaker3 Two Hybrid System (Clontech) according to the manufacturer's recommendations. For nonselective conditions, yeast cultures were grown in YPAD media (1% yeast extract, 2% peptone, 100 mg/L adenine hemisulfate, 2% dextrose). For growing yeast in selective conditions, defined media was prepared by supplementing the Dropout Base (DOB) media (Q-BIOgene) with Complete Supplement Mixture (Q-BIOgene) lacking the appropriate combination of amino acids and/or nucleotides. Blue-white screening was carried out on media supplemented with 20 μg/mL X-α-Gal (α-5-bromo-4-chloro-3-indolyl-β-D-galactopyranoside: ICN).

GST Pull-Down Assays

BL21 bacteria transformed with either pGEX-4T-1 or pGEX-IRF3$_{24-422}$ were cultured at 37°C in LB broth to an OD_{600} of 0.6 and induced to express GST or GST-IRF3$_{24-422}$, respectively, by adding IPTG to 1 mM and continuing culture for 4 h. Bacteria were pelleted by centrifugation and suspended in buffer composed of 50 mM Tris pH 8.0, 2 mM EDTA and 1% Triton X-100. The bacteria were lysed by sonication with 10 s pulses. Soluble fusion proteins were collected from the supernatant following a 10 min centrifugation at 12 000 *g*. GST and GST-IRF3 were purified with glutathione-Sepharose 4B beads (GE Healthcare).

MA104 cells were infected with B641 at a multiplicity of infection (MOI) of 10 in the presence of 5 μg/mL of actinomycin D. At 2 hours post-infection (hpi),

50 μCi/mL of ^{35}S-trans label (ICN) was added and the infection was allowed to proceed for an additional 4 h. Cells were harvested in lysis buffer containing 50 mM Tris-Cl [pH 8.0], 15 mM NaCl, 140 mM KCl, and 2% NP-40. Radiolabeled lysates from infected or mock infected cells were then incubated with glutathione-Sepharose 4B beads (GE Healthcare) bound to either GST or GST-IRF3. Interacting proteins were eluted with 10 mM reduced glutathione, resolved by SDS-polyacrylamide gel electrophoresis (SDS-PAGE), and visualized by autoradiography.

Immunoblots

Whole cell extracts were harvested from MA104 cells in RIPA buffer (150 mM NaCl, 1% sodium deoxycholate, 1% Triton X-100, 0.1% SDS, 10 mM Tris–HCl pH 7.2) and proteins were resolved by SDS-PAGE. After transfer to nitrocellulose, membranes were blocked in 10% dry milk (w/v) in PBS (10% BLOTTO). Membranes were incubated overnight at room temperature with indicated primary antibody diluted in 0.5 % BLOTTO. Membranes were rinsed three times with 0.5% BLOTTO, and then incubated for 2 h at room temperature with peroxidase-conjugated secondary antibodies (Jackson ImmunoResearch). Proteins were detected with ECL Western Blotting Substrate (Pierce). Primary antibodies included anti-NSP1 monoclonal antibody (provided by Dr. J. Cohen, INRA, Jouy-en-Josas, France), anti-IRF3 (Active Motif, 1:3000), and anti-glyceraldehyde-3-phosphate dehydrogenase (GAPDH) (Ambion, 1:2000).

RT-PCR

Total RNA was harvested from MA104 cells using TRIzol reagent. After reverse-transcription with random hexamer-primed SuperScript II (Invitrogen), PCR was performed using HiFi Platinum Taq (Invitrogen) and gene-specific primers for IFNβ (forward 5' - CTC CTC CAA ATT GCT CTC CTG – 3'; reverse 5' – GCA AAC TGC TCA CGA ATT TTC C – 3'), ISG56 (forward 5' – AAC ACC TGA AAG GCC AGA ATG AGG-3'; reverse 5' – AAG ACA GAA GTG GGT GTT TCC TGC-3'), ISG54 (forward 5' – TAT GCC TGG GTC TAC TAT CAC ATG GGC – 3'; reverse 5' – AGC CAG GAG GAC TTT AAG GTA CTG G – 3'), and β-actin (forward 5' – CAT GTT TGA GAC CTT CAA CAC – 3'; reverse 5' – CAT CTC CTG CTC GAA GTC TAG – 3'). As a positive control for IRF3 activation, MA104 cells were transfected with polyI:C by a standard calcium phosphate technique.

Results

NSP1 Interacts with IRF3

We performed a yeast two-hybrid interaction screen with bovine NSP1 as bait to identify candidate cellular partners of NSP1 that would shed light on the function of this protein in rotavirus-infected cells. We identified several colonies that grew on defined media that selected for the presence of both transcription activation and DNA binding domain plasmids and for activation of reporter gene expression. Six library clones were isolated by transforming them into bacteria

and sequencing the activation domain plasmid inserts. A BLASTX search with the nucleotide sequence of each of these clones yielded matches with human interferon (IFN) regulatory factor 3 (IRF3). The cDNA clones ranged from 0.9 to 1.2 kb. The longest cDNA corresponded to a sequence from nucleotide 110 to the 3' polyadenylate tail, according to the published sequence for human IRF3 (472) (GenBank accession no. NM 001571). IRF3 is a transcription factor that responds to virus infection by inducing the expression of the genes for IFNα and IFNβ (469, 472-474). Subsequent IFN-stimulated gene products drive a cell to an antiviral state. Thus, identification of IRF3 as a partner of NSP1 was relevant and warranted further study.

We performed a number of control experiments to ensure that the defined interaction was not an artifact or a false positive interaction (Figure 2.1). We retransformed pGAD-IRF3 into yeast containing pGBK-bNSP1 and plated transformants on SC-L-W medium. Colonies capable of growth on this medium were then streaked onto SC-L-W-H-A medium containing X-α-Gal. Only yeast cells containing both plasmids were capable of growth on selective medium (Figure 2.1(a)). pGAD-IRF3 was negative for autoactivation, as was evidenced by its failure to activate reporter gene expression in the absence of pGBK-bNSP1. We also tested potential interactions between (i) bovine NSP1 and an irrelevant protein (simian virus 40 T antigen) in the activation domain plasmid, (ii) IRF-3 and an irrelevant protein in the binding domain plasmid (v15), and (iii) IRF-

3 with an empty bait plasmid (Figure 2.1(b) and data not shown). These tests were also negative.

To test whether this interaction was bovine NSP1-specific, we repeated the assay with the NSP1 of murine rotavirus strain EW (16) which shares 37% amino acid identity with B641 NSP1 over the full-length protein. The N-terminal 230 amino acids are 51% identical, and this conservation includes the zinc-finger domain. The ability of EW NSP1 to bind IRF-3 was tested to determine if the observed interaction was limited to the bovine NSP1 used in the initial screen. EW NSP1 also interacted with IRF-3 (Figure 2.1(a)). These data suggest that the NSP1-IRF3 interaction is not limited only to bovine rotavirus NSP1, even though the sequence divergence between bovine NSP1 and murine NSP1 is relatively high.

NSP1 Synthesized in Rotavirus-Infected Cells Binds IRF3

The ability of NSP1 synthesized in infected cells to interact with IRF3 was examined by a glutathione *S*-transferase (GST) pull-down assay as previously described (475). Figure 2.2(a) shows that NSP1 bound GST-IRF3, but not GST. The identity of the band migrating at the predicted molecular weight of NSP1 in the GST-IRF3 eluate was confirmed by immunoblotting with an anti-NSP1 monoclonal antibody (Figure 2.2(b)). Rotavirus proteins VP7 and NSP3 were also retained by GST-IRF3, but not GST. Whether these proteins are bound by IRF3 or by NSP1 complexed to IRF3 is not known. NSP1 binds the 5'

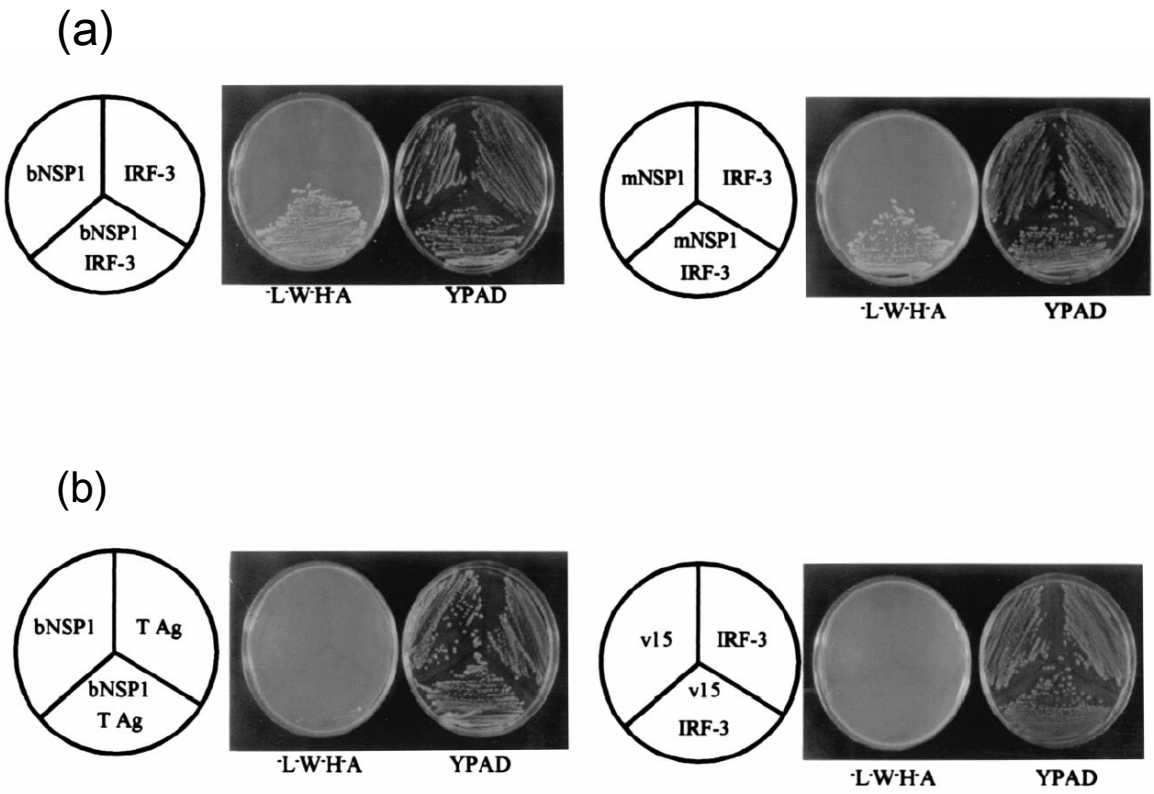

Figure 2.1: NSP1 interacts with IRF3. Bovine NSP1 (bNSP1) and murine NSP1 (mNSP1) in the yeast two-hybrid bait vector were tested for interaction with IRF-3 in the activation domain vector. Schematic diagrams indicate the regions of selection media where yeast containing the indicated plasmid(s) were streaked. (a) Interaction between bovine NSP1 and IRF3, or between murine NSP1 and IRF3, on nutrient selection medium; (b) interaction of bovine NSP1 with simian virus 40 T antigen in the activation domain plasmid (left panel), and IRF3 interaction with an irrelevant protein (v15) in the DNA binding domain plasmid (right panel). YPAD, yeast extract-peptone-adenine-dextrose media.

end of viral mRNA, and NSP3 binds the 3' end (7, 153). A direct interaction between NSP1 and NSP3 was shown in a yeast two-hybrid assay (133), but thus far has not been reported to occur in infected cells. It is possible that NSP3 is brought down in this assay through interaction with NSP1. Alternatively, NSP3 may be pulled down through a viral mRNA bound to NSP1. The detection of VP7 in the GST-IRF3 eluate is more difficult to interpret. It may be that this protein interacts with NSP1 in infected cells, but these interactions have not been

investigated or described. The data presented in Figure 2.2 show that NSP1 synthesized in a native rotavirus infection interacted with IRF3, and thus NSP1 and IRF3 are not binding partners unique to the yeast two-hybrid system.

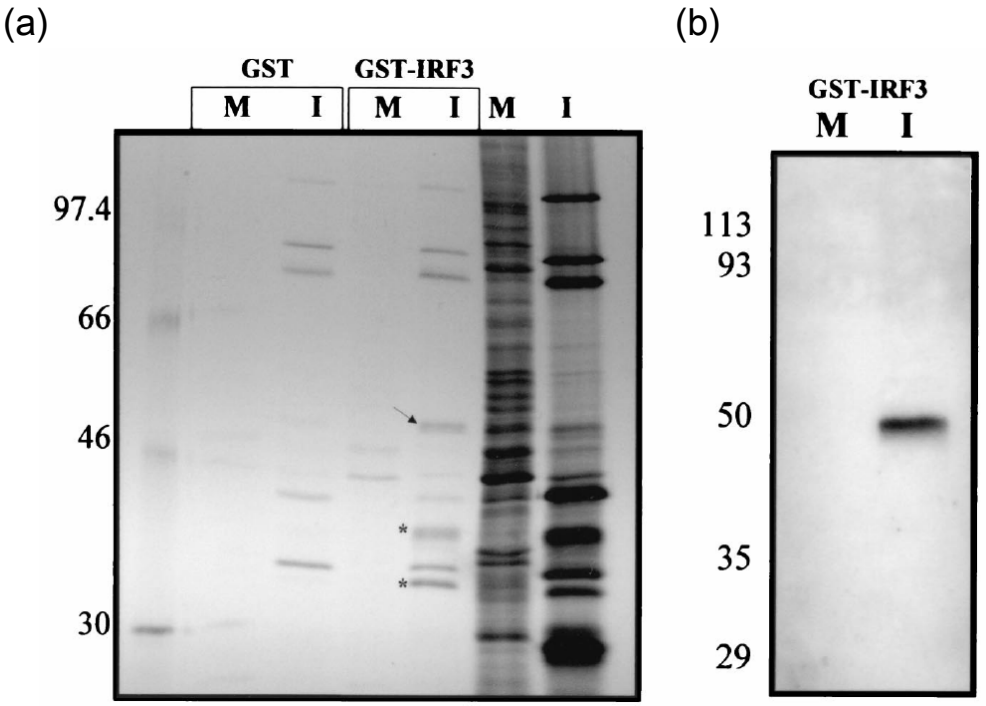

Figure 2.2: NSP1 interacts with IRF3 in a GST pull-down assay. IRF3 was expressed in bacteria as a GST fusion protein. GST-IRF3 or GST alone was bound to glutathione-Sepharose 4B, and radiolabeled mock-infected (M) or B641-infected (I) lysates were incubated with the beads. (a) The arrow indicates a 50-kDa NSP1 pulled down by GST-IRF3. Asterisks indicate VP7 (38 kDa) and NSP3 (34 kDa). M and I lanes contain lysates not subjected to the pull-down assay. (b) Immunoblot of GST-IRF3 eluates with an anti-NSP1 monoclonal antibody (provided by Dr. J. Cohen, INRA, Jouy-en-Josas, France). Molecular mass markers are noted at the left.

The NSP1 Zinc Finger is Important, but not Sufficient, to Mediate Binding to IRF3

NSP1 shows considerable divergence in amino acid sequence among different rotavirus strains (153). The N-terminal 230 amino acids are more conserved than the C-terminal residues, yet the C terminus does retain some predicted structural conservation. We made a series of mutations in NSP1 to

define the domain(s) that mediates the interaction with IRF3. Schematic diagrams of the bovine NSP1 mutants used in the following analyses are shown in Figure 2.3(a). Each mutant NSP1 bait construct was transformed into AH109 cells alone or into AH109 cells containing pGAD-IRF3. Transformants were then scored for interaction based on the ability to grow on nutrient-deficient medium. The zinc finger domain present between amino acids 42 and 79 (numbering according to that of B641 NSP1) in NSP1 is completely conserved among rotavirus strains. Mutant Δ62 was constructed to ascertain the contribution of the N-terminal zinc finger to the interaction between NSP1 and IRF3. Figure 2.3(c) shows that deletion of the N-terminal 62 amino acids abolished the interaction with IRF3, as evidenced by the inability of yeast cotransformed with Δ62 and IRF3 to grow on selective medium. A second construct (Δ326) contained only the C-terminal 164 amino acids. This mutant scored positive for interaction with IRF3, though the colonies consistently grew more slowly than those with full-length NSP1 (Figure 2.3(c)). A construct containing the analogous C-terminal residues of EW NSP1 (Δ327) also interacted with IRF3 (data not shown). A final deletion mutant, Ω290, consisted of the N-terminal 200 amino acids and contained the zinc finger. Surprisingly, this mutant failed to interact with IRF3.

The results of the NSP1 deletion analyses were not straightforward, and they suggested that structure played a significant role in the IRF3 interaction. Therefore, we performed site-directed mutagenesis to disrupt the N-terminal zinc finger so that the overall structure of the protein would be maintained as much as

possible. In one mutant, the cysteine at position 54 was replaced with alanine (C54A mutant). In a second mutant, the cysteines at position 54 and position 57 were replaced with alanines (C54A/57A mutant) (Figure 2.3(b)). Neither of these mutants interacted with IRF3 (Figure 2.3(d)). Taken together, the mutagenesis data suggest that proper folding and the structure of NSP1 are important for interaction with IRF3. The inability of mutant Δ62, the C54A mutant, and the C54A/57A mutant to interact with IRF3 and the reduced growth rate of Δ326 suggested that the zinc finger was important for binding. However, this domain was not sufficient for binding because the Ω290 mutant, which contained the entire zinc finger, did not interact with IRF3. The interaction of the C-terminal 164 amino acids of NSP1 with IRF3 (Δ326 and EW Δ327) and the lack of interaction between Ω290 and IRF3 suggest that the interaction is not an artifact mediated simply by a zinc finger domain that may be present in a wide variety of proteins.

NSP1 Interacts with the C Terminus of IRF3

IRF3 has a DNA-binding domain (DBD) near its N terminus and an IRF-associated domain (IAD) near its C terminus. These two domains are found in all interferon regulatory factors (234). The DBD and IAD are separated by a proline-rich region (PRR). The extreme C terminus of IRF3 has been studied in detail as it contains an autoinhibitory domain (AID). In the unphosphorylated form, this domain has been suggested to prevent IRF3 dimerization with other IRF3 molecules or with IRF7. Phosphorylation within this domain is thought

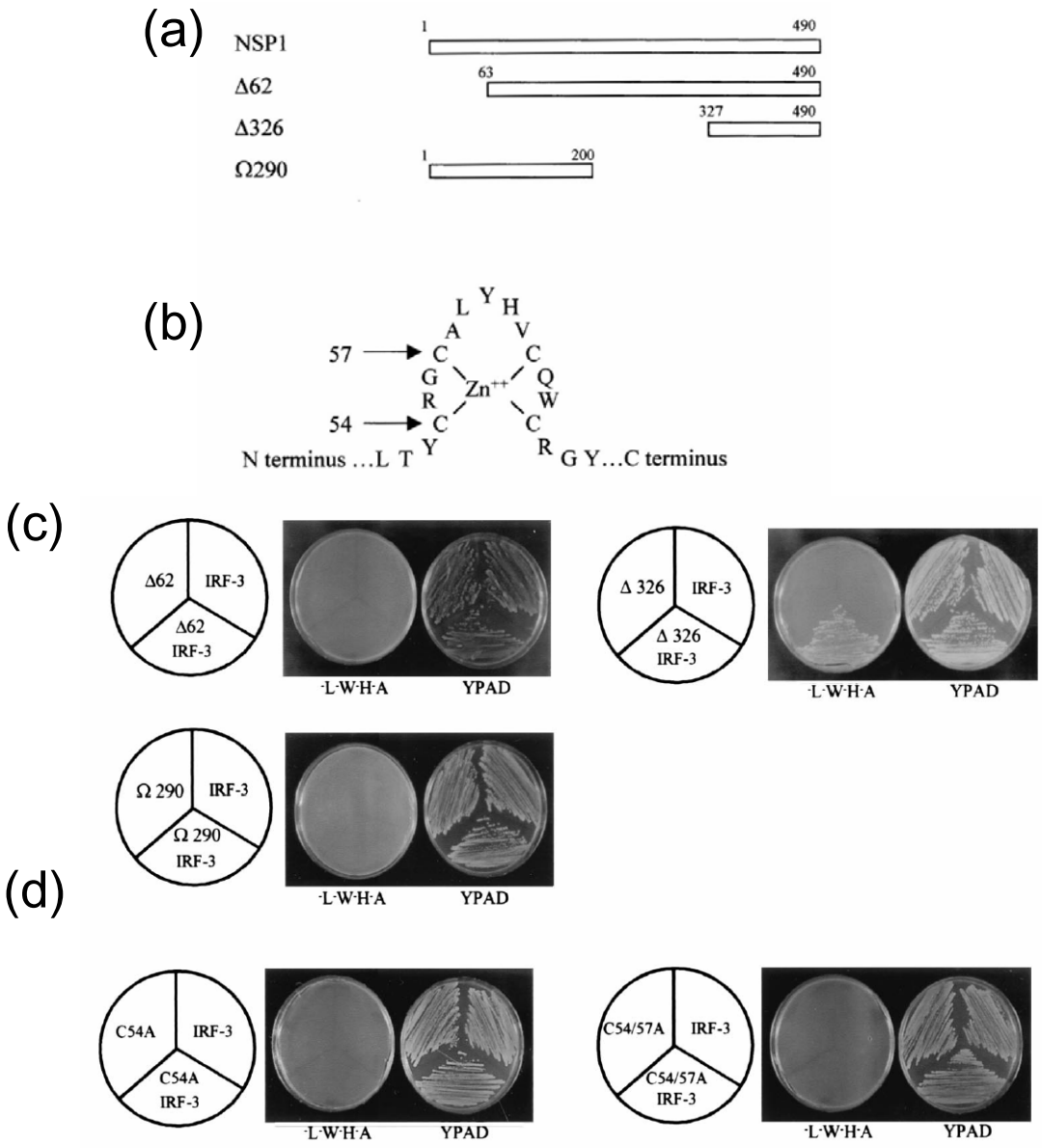

Figure 2.3: Mutational analysis of NSP1 and the interaction with IRF3. (a) Schematic diagram displaying deletion mutants constructed in the two-hybrid bait vector and analyzed for interaction in yeast. Amino acid numbers (relative to strain B641 numbering) are indicated. (b) Potential structure of the N-terminal conserved zinc finger with cysteine residues altered to alanines by site-directed mutagenesis as indicated. (c) Yeast two-hybrid interaction analysis of the deletion mutants depicted in panel a. (d) Yeast two-hybrid analysis of the cysteine mutants depicted in panel b.

to relieve the inhibition by electrostatic charges displacing the AID (169-171, 235, 236, 239, 476). Knowledge of these domains (see Figure 2.4(a)) was used to perform rational deletion analysis to map the NSP1-interacting region of IRF3.

A panel of deletion mutants was cloned into the prey plasmid and transformed into AH109 yeast for autoactivation tests and into AH109 yeast previously transformed with the bNSP1 bait plasmid to test for NSP1-IRF3 mutant interaction. Full-length IRF3, which contains an intact DNA-binding domain, caused autoactivation of the reporter genes; however, none of the IRF3 deletion mutants did so (data not shown). The DBD and PRR of IRF3 were shown to be dispensable for NSP1-IRF3 interaction, while the IRF3 deletion mutant containing the IAD and the AID interacted with NSP1 (Figure 2.4(b)). Efforts to further refine the NSP1-interacting region of IRF3 failed. The AID of IRF3 did not interact with NSP1 (Figure 2.4(b)). The IAD of IRF3 also did not interact with NSP1 (data not shown).

IRF3-Regulated Genes Are Induced Only in Cells Infected with Rotavirus Deficient in NSP1

IRF3 resides latently in the cytoplasm, and upon infection by a virus or exposure of cells to double-stranded RNA, IRF3 is phosphorylated, dimerizes, and translocates to the nucleus, where it complexes with transcription coactivators such as CBP/p300 (235, 477, 478). We predicted that the NSP1-IRF3 interaction in rotavirus-infected cells results in the functional inhibition of IRF3 and downregulation of the innate cellular IFN response.

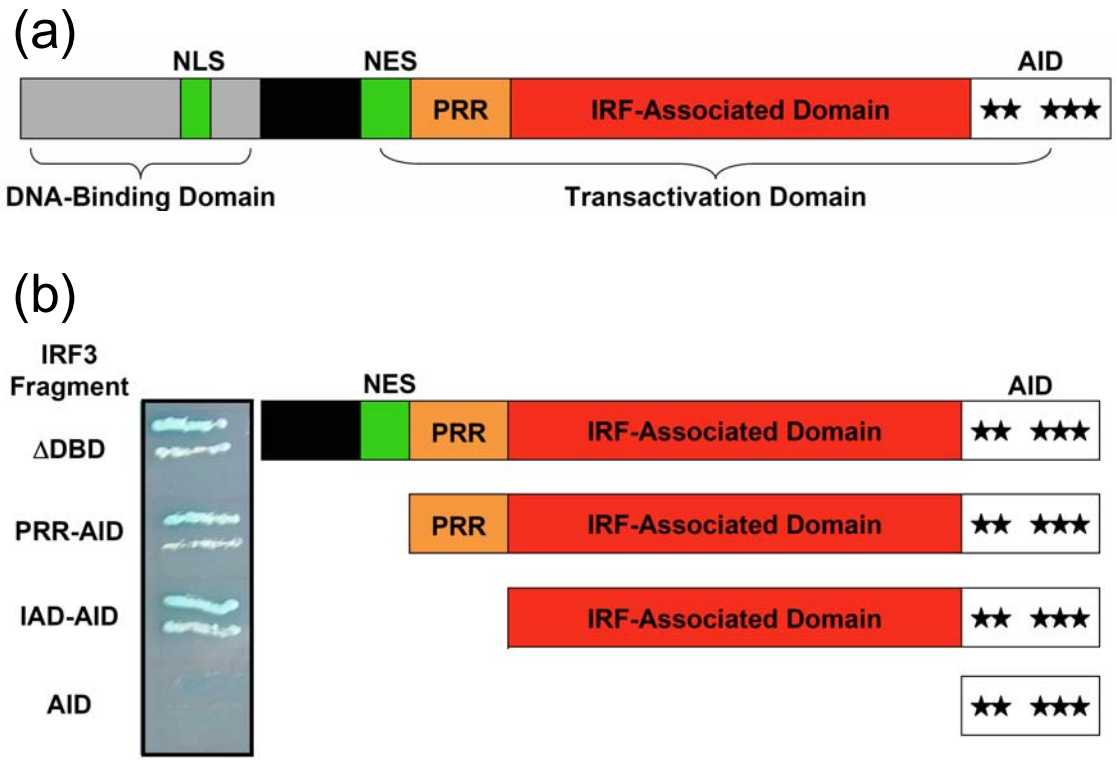

Figure 2.4: Mutational analysis of IRF3 and the interaction with NSP1. (a) Schematic diagram displaying the known functional domains of IRF3. (b) Yeast two-hybrid interaction analysis of IRF3 deletion mutants. bNSP1-IRF3 deletion mutant cotransformed yeast were tested for their ability to grow on nutrient deficient media (-L-W-H-A) supplemented with X-α-Gal. DBD, DNA-binding domain; NLS, nuclear localization signal; NES, nuclear export signal; PRR, proline-rich region; AID, autoinhibitory region; stars represent approximate location of phosphorylated serine and threonine residues.

Since IRF3 is an important transcription factor for the induction of IFNβ, as well as genes with antiviral activity, RT-PCR analysis was performed to detect the induction of IRF3-regulated genes in cells infected with a wild-type bovine rotavirus strain, NCDV, or an NSP1 null rotavirus strain, A5-16 (164). The basal level of the three representative IRF3-regulated genes (IFNβ, ISG56, and ISG54) was low or undetectable in mock-infected cells, whereas these genes were highly induced in cells transfected with the synthetic double-stranded RNA (polyI:C), as a condition which mimics viral infection (Figure 2.5(a) and (b)). The expression

levels of the IRF3-regulated genes increased throughout the course of infection with A5-16 (Figure 2.5(a)), but were not detected above basal levels at any time after infection with NCDV (Figure 2.5(b)).

IRF3 is Degraded in Cells Infected with Wild-Type Rotavirus

IRF3-mediated gene induction is an important cellular response to infection and viruses have evolved a variety of mechanisms to interfere with such a defensive response (177). For instance, the adenovirus E1A protein down-regulates IRF3-induced transcription by competing with IRF3 for binding to CBP/p300 (469). A second mechanism of IRF3 inhibition is displayed by human papillomavirus type 16. The E6 protein of human papillomavirus type 16 binds IRF3 directly and downregulates induction of IFNβ (444). Finally, the NS1 protein of influenza virus inhibits nuclear translocation of IRF3 in infected cells (352).

To determine the point of IRF3 antagonism in wild-type rotavirus infected cells, we first examined the phosphorylation status of IRF3. Hyperphosphorylated forms of IRF3 can be detected as higher molecular weight bands by immunoblot analysis. In mock-infected MA104 lysates, two forms of hypophosphorylated IRF3 were typically seen (Figure 2.5(c)). Over the course of an A5-16 infection, hyperphosphorylated forms were initially detected at 6 hours post-infection (h p.i.) and were the predominant form by 8 h p.i. Unexpectedly, infection with either B641 or NCDV resulted in a reduction in IRF3 abundance by 2-6 h p.i. (Figure 2.5(c)). Since IRF3 transcript levels remained constant in cells

infected with wild-type and NSP1-null rotaviruses (Figure 2.5(d)), the loss of IRF3 protein in NCDV infected cells is likely due to protein degradation, rather than inhibition of IRF3 gene transcription.

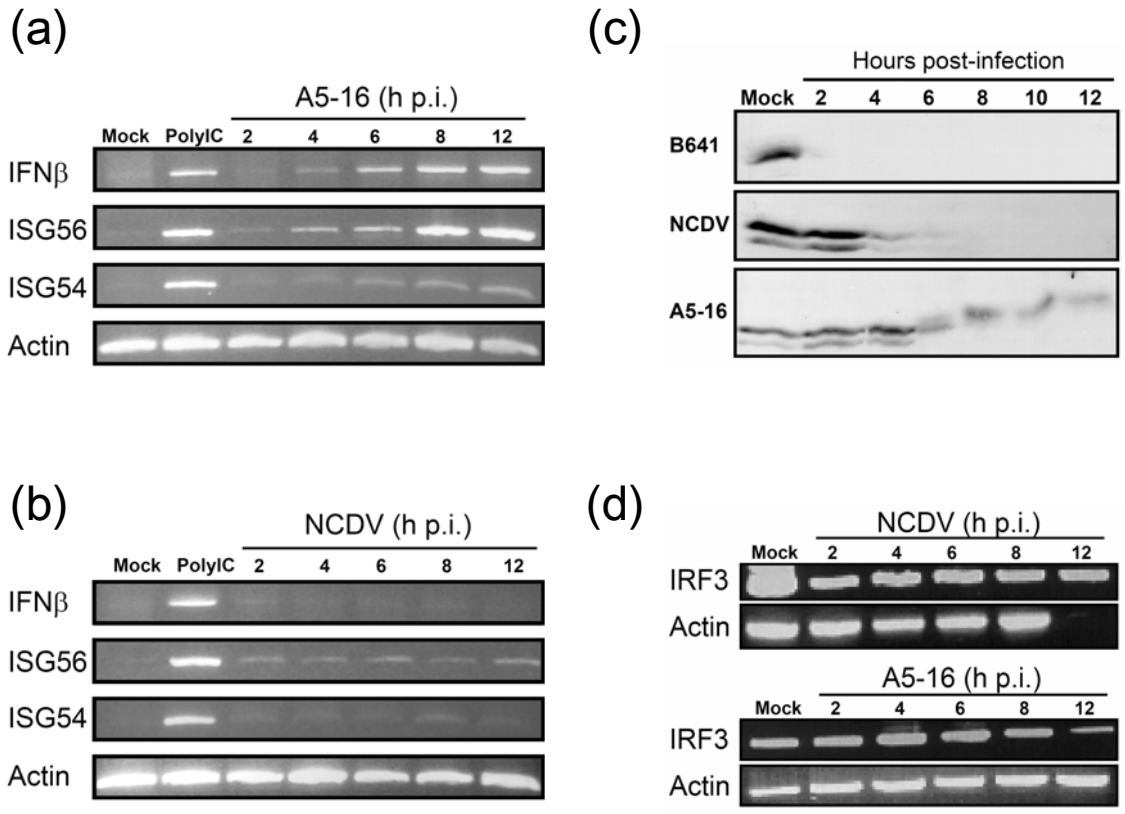

Figure 2.5: Degradation of IRF3 prevents the induction of IRF3-regulated genes in wild-type rotavirus infections. (a) RT-PCR analysis of IRF3-regulated genes. MA104 cells were mock infected, transfected with polyI:C, or infected with A5-16 at 1 pfu/cell. RNA was harvested at the indicated times post-infection. RT-PCR of actin was performed as a template control. (b) Same as in panel a, except cells were infected with NCDV. (c) Immunoblot analysis of IRF3. MA104 cells were mock infected or infected using the indicated rotavirus strain at 1 pfu/cell. Whole cell extracts (WCE) were harvested at the indicated times post-infection. (d) RT-PCR analysis of IRF3. RNA was harvested at the indicated times post-infection from MA104 cells infected with either NCDV or A5-16 at 1 pfu/cell. RT-PCR of actin was performed as a template control.

Replication is Required to Target IRF3 for Degradation in Wild-Type Rotavirus Infections

The data presented thus far suggest that IRF3 is degraded by an undefined mechanism in rotavirus-infected cells. This model relies on the comparison of IRF3 signaling between cells infected with the NSP1 null A5-16 strain and the wild-type strains. The NCDV, B641, and A5-16 strains have different genetic backgrounds, so there are differences in many of the gene segments, not just gene segment five, which encodes NSP1. In an effort to further correlate the degradation of IRF3 with expression of NSP1, MA104 cells were infected with virus that was inactivated by UV-psoralen treatment. These virus particles are capable of cell entry but are unable to transcribe viral mRNA (470). Since NSP1 is not part of the infectious virus particle, the cells infected with the inactivated virus particles would be exposed to rotavirus binding and entry, as well as structural proteins, however the cells would not be exposed to NSP1.

IRF3 abundance was examined in MA104 cells infected with UV-psoralen-treated NCDV and A5-16, which originated from the same stocks that were used in Figure 2.5. IRF3 levels remained constant over the course of the infection with the inactivated NCDV (Figure 2.6(a)).

Replication is Required to Activate IRF3 in NSP1 Null Rotavirus Infections

The IRF3 immunoblots were also informative for analyzing IRF3 phosphorylation status in the cells infected with the UV-psoralen-treated virus.

IRF3 does not display increased phosphorylation over the course of infection with either of the replication deficient rotavirus strains relative to mock-infected cells (Figure 2.6(a)). To confirm the lack of IRF3 activation in cells infected with the UV-psoralen-treated virus, RT-PCR was used to determine the level of IFNβ transcript levels over the course of infection. In the replication deficient rotavirus infected cells, IFNβ transcript levels were not upregulated until 12 h p.i. (Figure 2.6(b)). The kinetics of IFNβ induction lag behind those seen in cells infected with replication competent A5-16 in Figure 2.5(a). This indicates that the main mechanism used by the host cell to detect rotavirus infection does not occur upon viral attachment or entry.

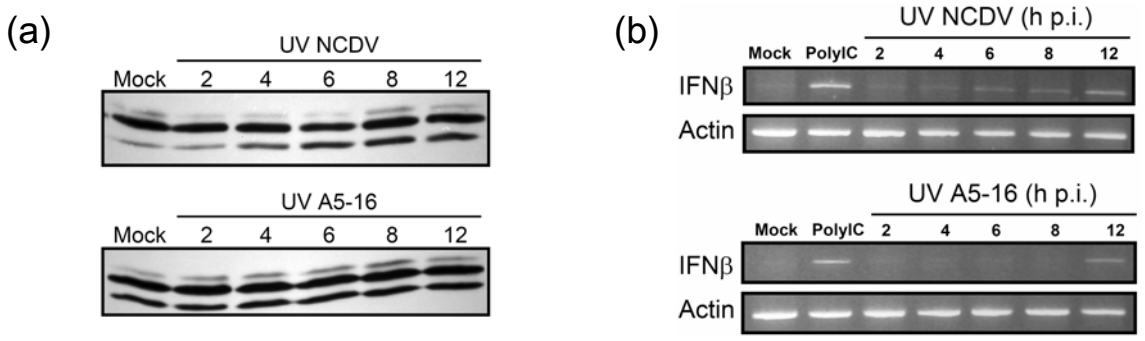

Figure 2.6: Replication is required for degradation of IRF3 in wild-type rotavirus infected cells and for activation of IRF3 in NSP1 null rotavirus infected cells. (a) Immunoblot analysis of IRF3. MA104 cells were mock infected or infected using UV-psoralen inactivated NCDV or A5-16. Whole cell extracts (WCE) were harvested at the indicated times post-infection. (b) RT-PCR analysis of IFNβ. MA104 cells were mock infected, transfected with polyI:C, or infected with UV-psoralen inactivated NCDV or A5-16. RNA was harvested at the indicated time post-infection. RT-PCR of actin was performed as a template control.

IRF3 Degradation is Mediated by the Proteasome in Wild-Type Rotavirus Infections

IRF3 is degraded in a proteasome-dependent manner following phosphorylation, dimerization, nuclear translocation, and transactivation activity in cells infected with Sendai virus (235). IRF3 signaling has also been linked to apoptosis (476, 479), a form of programmed cell death that is mediated in part by cysteine proteases, called caspases, which are inactive prior to proteolytic cleavage (480). To determine if either of these cellular processes were involved in the degradation of IRF3 seen in wild-type rotavirus infected cells, IRF3 immunoblots were performed using WCE from cells infected with NCDV in the presence of caspase or proteasome inhibitors. Figure 2.7 shows that the treatment of cells with the proteasome inhibitor, MG132, prevented the degradation of IRF3 in NCDV-infected cells.

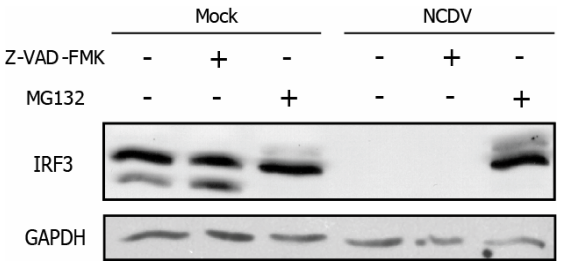

Figure 2.7: IRF3 is degraded via a proteasome-dependent process in wild-type rotavirus infected cells. MA104 cells were mock or NCDV infected at 1 pfu/cell. At the time of infection the cells were treated either with vehicle alone (DMSO), a pan-caspase inhibitor (Z-VAD-FMK; 20 μM), or a proteasome inhibitor (MG132; 20 μM). IRF3 immunoblot analysis was performed using WCE harvested at 8 h p.i.

Discussion

We sought to identify cellular binding partners of NSP1 with the rationale that by using an unbiased approach, such as the yeast two-hybrid interaction trap, the function of NSP1 may be inferred from the function of the cellular protein. Indeed, by analysis of cells infected with either wild-type or NSP1 null rotavirus strains, we show that NSP1 likely functions as an antagonist of the IFN system. These experiments were initiated as a follow-up to the detection of an interaction between NSP1 and a key transcription factor involved in the induction of an IFN response, IRF3.

The combined data from the deletion and mutagenesis studies of NSP1 lead us to propose that at least one point of contact with IRF3 resides in the C-terminal domain of NSP1. The inability of mutant Δ62 or the zinc finger point mutants to interact with IRF3 in yeast might be explained by a structural inhibition of C-terminal binding in the absence of the zinc finger. Alternatively, proper folding of full-length NSP1 may require formation of the zinc finger, and thus the authentic conformation may be disrupted even by the point mutations. Computer predictions of the secondary structures of the C terminal 164 amino acids of B641 and EW NSP1 show conserved regions of α-helices connected by random coils. Consistent with the mutagenesis data, it is likely that this structure is critical, and the interaction between IRF3 and NSP1 may be driven primarily by the α-helical content of the C terminus of NSP1. Secondary-structure analysis of three viral proteins known to interact with or modulate the function of IRF3,

influenza virus NS1 (352), adenovirus E1A (469), and human papillomavirus E6 (444) also predicts 40% α-helices and 40% random coils, suggesting that these structures may be important. Further mutational analyses that disrupt discrete structures in the C terminus are required to refine domains important in the interaction.

The region responsible for interacting with NSP1 was mapped to the C terminus of IRF3, which includes the IRF-associated domain (IAD) and the autoinhibitory domain (AID). NSP1 did not interact with IRF3 deletion mutants of either the IAD or the AID alone. These results suggest that NSP1 may interact with a portion of IRF3 that spans both domains or that the smaller IRF3 deletion mutants do not fold properly when expressed in yeast. A recent study, which presented data mapping the domain of IRF9 that interacts with STAT2, generated IRF9 deletion mutants based on secondary structure prediction within the C terminus (481), rather than functional domains as we have reported here. Since the C termini of IRF3 and IRF9 have a very similar arrangement of secondary structural units (481), it may be possible to refine the region of IRF3 that interacts with NSP1 by generating deletion mutants based on secondary structure.

Upon entry into cells, infectious rotavirus triple-layered particles (TLPs) lose the outer layer of protein consisting of VP4 and VP7. The resulting double-layered particles (DLPs) are transcriptionally active and begin releasing rotavirus mRNA through channels of the DLPs (100). Also, packaging of the dsRNA

genome during morphogenesis is thought to occur simultaneously with the formation of new DLPs (129). Together, these two processes are thought to prevent the host cell from sensing the dsRNA genome of rotavirus. The discrepancy in induction kinetics of IFNβ between cells infected with UV-psoralen-treated and untreated A5-16 (compare Figure 2.5(a) and Figure 2.6(b)) hints that dsRNA is likely being detected within the infected cell. The source of the dsRNA may be attributed to secondary structure within the viral mRNA or defective replication in which the dsRNA genome segments are not confined within NSP2 cores.

In addition to analyzing the IRF3-NSP1 interaction, we also showed that IRF3 is degraded in cells infected with viruses that encode NSP1 and that IRF3 is not degraded in cells infected with replication-deficient wild-type virus which are unable to express nonstructural proteins. Additional experiments could provide direct evidence that NSP1 mediates the degradation of IRF3. Unfortunately, transient expression of NSP1 is either toxic to cells or is below the level of detection. An alternate approach to demonstrate NSP1-mediated IRF3 degradation could be shown by the targeted knockdown of NSP1 expression in infected cells using RNA interference technology. This approach has been hampered by the limited availability of NSP1-specific antibodies.

The role of type I IFN in rotavirus infection is unclear, as the data are conflicting and dependent on the species studied. Both humans and animals infected with rotavirus have serum IFNα and excrete IFNα in stool (482-484).

Calves treated with recombinant human IFNα2 were protected from diarrhea induced by tissue culture-adapted bovine rotavirus (485), whereas piglets were not (486). The colon adenocarcinoma cell line HT-29 shows weak or no IFNβ response following rotavirus infection, although evidence for IFN-induced gene expression was apparent (487). HT-29 and CaCo-2 cells become resistant to rotavirus infection when they are pretreated with IFNα (488). Despite evidence for a protective effect of IFN, studies in mice which were administered exogenous IFNα/β or mice lacking the IFN receptor (IFNα/β receptor$^{-/-}$) showed no differences in disease severity or duration compared to controls (489). These data suggested that the IFN response was not an important nonimmune mediator of protection from rotavirus disease in mice. Collective interpretation of these data is difficult because of the wide range of rotavirus strains, cell lines, species of virus, means of cell isolation, methods of virus adaptation, and animal models used.

Prior to this investigation, there were no reports of mechanisms that rotaviruses may have evolved to ameliorate the IFN response to promote infection and spread. The data presented here suggest that NSP1 may fulfill such a function in the rotavirus replication cycle by directing proteasome-mediated degradation of IRF3. Since the NSP1 of both bovine and murine rotavirus strains are capable of interacting with IRF3, we are currently testing whether IFN antagonism is correlated with the expression of NSP1 encoded by rotavirus strains isolated from infections of a wide variety of species.

ZINC-BINDING DOMAIN OF ROTAVIRUS NSP1 IS REQUIRED FOR PROTEASOME-DEPENDENT DEGRADATION OF IRF3 AND AUTO-REGULATORY NSP1 STABILITY

The data in this chapter was published previously (117).

Abstract

Interferon regulatory factor 3 (IRF3) is a key transcription factor involved in the induction of interferon (IFN) in response to viral infection. Rotavirus non-structural protein NSP1 binds to and targets IRF3 for proteasome degradation early post-infection. Mutational analysis of cysteine and histidine residues within the conserved N-terminal zinc-binding domain in NSP1 of bovine rotavirus strain B641 abolished IRF3 degradation in transfected cells. Thus, the integrity of the zinc-binding domain in NSP1 is important for degradation of IRF3. In contrast to bovine strain B641, IRF3 was stable in cells infected with porcine rotavirus strain OSU and OSU NSP1 bound only weakly to IRF3. Both B641 NSP1 and OSU NSP1 were stabilized in cells or cell-free extracts in the presence of the proteasome inhibitor MG132 and when the zinc-binding domain was disrupted by site-directed mutagenesis. Data from the B641 analyses that show IRF3 degradation is dependent on the presence of NSP1 and the integrity of the N-terminal zinc-binding domain, coupled with the regulated stability of IRF3 and NSP1 by the proteasome, collectively support the hypothesis that NSP1 is an E3 ubiquitin ligase.

Introduction

Recent data have assigned one role for non-structural protein NSP1 in evasion of the innate immune response to rotavirus infection. NSP1 binds the cellular transcription factor interferon regulatory factor 3 (IRF3) (459) and targets it for degradation by the proteasome early post-infection (490). IRF3 resides latent in the cytoplasm and is activated in response to virus infection (472). IRF3 is phosphorylated by kinases TBK1/IKKi and it then dimerizes and translocates to the nucleus, where it assembles in coordination with additional transcription co-factors on interferon (IFN) and IFN-stimulated gene (ISG) promoters (171, 196, 491). IRF3 is required for induction of IFNβ; thus interference with its function effectively downregulates antiviral gene expression. Downregulation of IFN expression through inhibition of IRF3 function has been reported for viruses within several families. The mechanisms of IRF3 antagonism vary and include inhibition of phosphorylation (331, 492, 493), nuclear translocation (352) and inhibition of transcription complex assembly (469, 494). Rotavirus NSP1 is the only viral protein shown thus far to inhibit IRF3 activation by a mechanism involving early proteasome targeting.

Modification of eukaryotic proteins with ubiquitin (Ub) prior to proteasome degradation requires an E1 activating enzyme, E2 conjugating enzyme, and an E3 ligase that interacts with both the E2 and the target substrate to mediate the transfer of Ub from the E2 to the target substrate (366). E3 ligases fall into two

major classes of proteins that contain either a catalytic HECT domain or a RING domain (495). HECT domains have homology to E6-AP, with strict conservation of a cysteine residue approximately 35 amino acids from the C terminus that transiently interacts with Ub. RING-finger domains, in contrast, are cysteine–histidine-rich adaptor domains that facilitate transfer of Ub from E2 to the substrate protein. Typical RING domains in cellular proteins consist of cysteine and histidine residues spaced in a C3HC4 pattern that coordinates two zinc ions in a cross-brace motif (496). However, evidence continues to accumulate that variations of the C3HC4 pattern exist in the RING superfamily and are present in both viral and cellular proteins with E3 ligase activity (432).

Several viral proteins with cysteine-histidine-rich zinc-binding domains have demonstrated E3 ligase activity, and many of the cellular targets of viral E3s are associated with regulation of immune responses to infection. For example, V proteins of viruses in the family *Paramyxoviridae* target the signal transducers and activators of transcription (STATs) for proteasome degradation and consequently downregulate type I IFN responses (450). The Kaposi's sarcoma herpesvirus (KSHV) RTA protein targets IRF7 to the proteasome (431) and the KSHV K3 proteins MIR-1 and MIR-2 downregulate major histocompatibility complex class I expression (430). Herpes simplex virus (HSV) ICP0 is known to induce, either directly or indirectly, proteasome-dependent degradation of the stress-related kinase DNA-PK and promyelocytic leukemia protein PML, among

others (434). Each of these proteins has intrinsic E3 ligase activity, but only ICP0 has a typical RING-domain signature.

NSP1 is the least conserved protein encoded by the rotavirus genome, but an N-terminal zinc-binding motif is completely conserved (155). This domain is not necessary for virus replication because rotavirus strains that encode a truncated NSP1 that lacks the zinc-finger motif replicate in cell culture, although plaque sizes are smaller than those of wild-type counterparts (164). We have shown that the zinc-binding domain is important, but not sufficient, for interaction with IRF3 (459). The presence of this domain and the finding that NSP1 targets IRF3 for proteasome degradation suggest that NSP1 may have E3 Ub ligase activity.

To increase understanding of the mechanisms by which NSP1 modulates the function of IRF3, we investigated the role of the zinc-binding domain in NSP1-mediated IRF3 binding and degradation. Expression of NSP1 of bovine rotavirus strain B641 in transfected cells resulted in IRF3 degradation, and mutation of conserved cysteine and histidine residues abolished this activity. In addition, two residues in the zinc-binding domain, as well as another highly conserved histidine residue outside the zinc-binding domain, were associated with differential stability of NSP1. Together, the data illustrate the importance of the zinc-binding domain of NSP1 in interference with the function of IRF3 and suggest that NSP1 may have E3 ligase activity associated with an atypical RING domain. We further discovered that IRF3 was activated and stable in cells infected with porcine

rotavirus strain OSU. OSU NSP1 has an intact zinc-binding domain and showed a weak interaction with IRF3. Disruption of the zinc-binding domain of OSU NSP1 resulted in increased stability, similar to B641 NSP1. The data derived from experiments with OSU NSP1 suggest the existence of rotavirus strains with the inability to downregulate IFN responses by targeting IRF3 and raise the possibility of alternative targets of NSP1 in antiviral signaling pathways.

Methods

Cells and Viruses

MA104 African green monkey kidney cells were maintained in M199 medium (Mediatech) supplemented with 5% fetal bovine serum (FBS; Atlanta Biologicals), 25 IU/mL penicillin, and 25 µg/mL streptomycin. HEK293 (293) human embryonic kidney cells were maintained in RPMI 1640 (Mediatech) supplemented with 10% FBS, penicillin-streptomycin, 10 mM HEPES, 2 mM L-glutamine and 1 mM sodium pyruvate. Isolation, characterization and propagation of rotavirus strains B641 (bovine), A5-16 (bovine), OSU (porcine) and SA11-4F (simian) have been described (164, 497-499). Rotavirus TLPs were concentrated by centrifugation for 2 h at 26 000 r.p.m. in an SW28 rotor at 4°C, and then banded on a 3.09 M CsCl gradient prepared in TNC buffer (10 mM Tris pH 7.5, 100 mM NaCl, 5 mM $CaCl_2$). Infectious TLPs were collected and concentrated by centrifugation for 2 h at 35 000 r.p.m. in an SW55 rotor. The

TLPs were suspended in M199 lacking FBS and stored at –80°C. Virus titers were determined by plaque assay.

Immunoblotting

Protein samples were separated on SDS-polyacrylamide gels. After transfer to nitrocellulose, membranes were blocked in 10% milk (w/v) in PBS (10% BLOTTO). Membranes were incubated overnight at room temperature with indicated primary antibody diluted in 0.5 % BLOTTO. Membranes were rinsed three times with 0.5% BLOTTO, and then incubated for 2 h at room temperature with peroxidase-conjugated secondary antibodies (Jackson ImmunoResearch). Proteins were detected with ECL (Pierce). Primary antibodies include anti-GFP (BD, 1:500), anti-IRF3 (Active Motif, 1:3000), anti-glyceraldehyde-3-phosphate dehydrogenase (GAPDH) (Ambion, 1:2000) and anti-*c*-myc (BD, 1:2000).

IRF3 Analysis in Virus-Infected Cells

MA104 cells were infected at the indicated m.o.i. with rotavirus strains that were activated with 10 µg/mL trypsin for 30 min at 37°C. Whole-cell extracts were prepared by scraping the cells into radioimmunoprecipitation (RIPA) buffer containing 150 mM NaCl, 1% sodium deoxycholate, 1% Triton X-100, 0.1% SDS, 10 mM Tris–HCl pH 7.2. IRF3 levels were determined by immunoblot as described above.

Plasmids

Plasmid construction was performed using standard cloning techniques. Site-directed mutagenesis reactions were carried out using a QuikChange XL kit (Stratagene). Table 3.1 lists the primers used in these experiments. B641 NSP1 (primers 1 and 2) and OSU NSP1 (primers 3 and 4) were cloned into pGBKT7 (BD Clontech). To generate a bicistronic construct encoding EYFP and NSP1, the poliovirus internal ribosome entry sequence (IRES) was amplified (primers 5 and 6) from pNLink (kindly provided by Dr. R. Lloyd, Baylor College of Medicine, Houston, TX, USA) and cloned into pEYFP-C1 (BD Clontech) to generate pEYFP-IRES. pB-NSP1 and pO-NSP1 were constructed by amplifying myc-tagged B641 NSP1 (primers 7 and 8) and myc-tagged OSU NSP1 (primers 7 and 9) from the pGBKT7 constructs described above followed by insertion into pEYFP-IRES downstream of the IRES motif.

Table 3.1: Primers Used in Plasmid Construction and Site-Directed Mutagenesis

1	CGC**GGATCC**CGATGGCGACTTTTAAGGAC
2	CCG**CTCGAG**GGTTCAACATCTGAAAGTTC
3	CGC**GGATCC**GCATGGCTACTTTTAAGGATGC
4	CGC**GGATCC**TTATTCAACATCAGATATACCGG
5	CAC**AAGCTT**GATCCCTCGACTGG
6	CAC**GAATTC**CACACTCAATGGAGCG
7	CACA**CCGCGG**GTAATACGACTCACTAT
8	GCGC**AGATCT**TTCAACATCTGAAAGTTC
9	GTCC**CCGCGG**TTATTCAACATCAGATATACC
10*	CAAATTTGACATAT**GCC**AGAGGGTGCGCTCTATACC
11*	GTTTCTTAGATGAAGAACCC**CTT**TTGCTGAGAATGCGAAC
12*	GTATTTGTTAGAATGGTATAAC**CTC**TTACTAATGCCAATAACATTGC
13*	CAGCATACTGATCTAACATAC**GCT**CGAGGCTGTACCATGTATCAT

Primers 1-9 were used in plasmid construction – bases in bold type indicate the restriction enzyme site used for cloning.
Primers 10-13 (denoted with an asterisk) were used in site-directed mutagenesis – the bold type indicates the mutated codon.

For site-directed mutagenesis, the primers listed in Table 3.1 and their corresponding reverse complement sequences were utilized. A panel of single amino acid substitutions in B641 NSP1 was generated with primers 10–12 for changing residues C54, H79, and H136, respectively. Primer 13 was used to construct a mutation at residue C54 in OSU NSP1.

Transfections

293 cells were cultured to approximately 90% confluence in 12-well plates or 60 mm dishes and transfected with indicated plasmids using *Trans*IT 293 transfection reagent (Mirus) according to the manufacturer's specifications. Whole-cell extracts were harvested at 48 h post-transfection by scraping into RIPA buffer. Transfection efficiencies were determined by fluorescence microscopy or by GFP immunoblots. Proteasome inhibitor MG132 (Calbiochem) was included in the medium at a concentration of 100 μM where indicated.

GST Pull-Down Assay

GST pull-down assays were performed as described previously (471). GST and GST-IRF3$_{24–422}$ (459) were induced with 1 mM IPTG for 4 h at 37°C. Bacteria were pelleted by centrifugation and suspended in buffer composed of 50 mM Tris pH 8.0, 2 mM EDTA and 1% Triton X-100. The bacteria were lysed by sonication with 10 s pulses. Soluble fusion proteins were collected from the supernatant following a 10 min centrifugation at 12 000 *g*. GST and GST–IRF3 were purified with glutathione–Sepharose 4B beads (GE Healthcare).

Transfected 293 cells were rinsed once with PBS and detached from the plastic by treatment with 0.5x trypsin–EDTA. The cells were transferred to 1.5 mL microcentrifuge tubes and pelleted for 5 min at 500 *g*. Cells were lysed in 200 µL lysis buffer composed of 50 mM Tris pH 7.5, 15 mM NaCl, 140 mM KCl, 2% NP-40, and the volume was increased by addition of 500 µL wash buffer (20 mM Tris, pH 7.5, 15 mM NaCl, 140 mM KCl, 0.1% NP-40).

For pull-down assays, 300 µL transfected cell lysate was incubated with 200 µL GST or GST-IRF3 bound to glutathione-Sepharose 4B beads and this mixture was incubated for 2 h at 4°C with end-over-end rotation. The beads were pelleted for 5 min at 500 *g* and then washed three times with 500 µL wash buffer. Proteins were eluted with 10 mM reduced glutathione and analysed by SDS-PAGE, followed by Coomassie staining or immunoblot. Images of the immunoblots were obtained on an Image Station 2000MM (Kodak). The ratio of NSP1 bound by GST–IRF3 to the input level of NSP1 was calculated by densitometric analysis using 1D Image Analysis software v3.6 (Kodak).

In Vitro Transcription-Translation

OSU NSP1 wild-type and OSU NSP1 C54A RNA were transcribed from pGBKT7-OSU NSP1 and pGBKT7-OSU NSP1 C54A plasmids and then translated for 90 min at 30°C in the presence of 0.4 µCi/µL (14.8 kBq) Trans ^{35}S label (MP Biomedicals) in the TNT T7 Coupled Reticulocyte Lysate system (Promega). Reactions included 100 µM MG132 or an equivalent amount of DMSO as a vehicle control.

Pulse-Chase Analysis

Wild-type and mutant B641 NSP1 proteins were translated in cell-free extracts for 90 min at 30°C in 25 µL reactions in the presence of 0.4 µCi/µL (14.8 kBq) Trans ^{35}S label. Reactions were chased by adding unlabeled methionine and cysteine to a final concentration of 1 mM each. Samples (5 µL) were collected from the reactions at 0, 30, 60 and 120 min post-chase and mixed with SDS-PAGE loading buffer. NSP1 was visualized by SDS-PAGE and autoradiography, and expression levels were quantified by densitometry.

Results

IRF3 is Degraded in B641-Infected Cells, but not in A5-16- or OSU-Infected Cells

We characterized the status of IRF3 in cells infected with several rotavirus strains to establish a system where mechanisms by which NSP1 targets IRF3 for proteasome degradation could be studied. In MA104 cells infected with bovine rotavirus B641 or simian strain SA11-4F, IRF3 was degraded completely by 6 h post-infection (Figure 3.1). These data are consistent with those reported for cells infected with simian strain SA11-4F (490). A5-16 is a bovine rotavirus variant with a rearrangement in gene segment 5 that encodes an NSP1 truncated at 40 aa (164). In contrast to B641-infected cells, IRF3 was activated and stable when cells were infected with A5-16. These results were expected given the lack of a full-length NSP1 encoded in the A5-16 genome. An unexpected result was

the observation that IRF3 was activated and stable over the course of infection with porcine strain OSU. Gene 5 of OSU was cloned and sequenced and there is 100% amino acid identity between NSP1 of our laboratory strain and that in the published database (GenBank accession no. U08432). These data demonstrate the existence of NSP1 variants that have contrasting phenotypes with respect to targeting IRF3 for proteasome degradation.

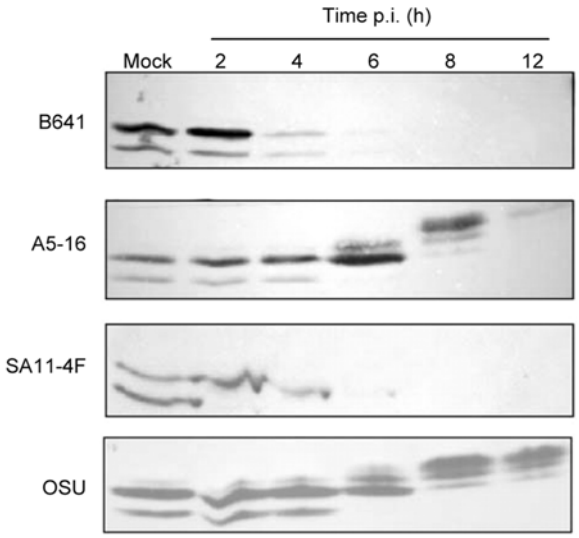

Fig. 3.1: IRF3 activation in cells infected with different rotavirus strains. Cell extracts were prepared at 2, 4, 6, 8 and 12 h post-infection (h p.i.) from MA104 cells infected at an m.o.i. of 3 with the indicated rotavirus strain. Mock-infected cell lysates were collected at the 12 h time point. Lysates were electrophoresed on SDS-polyacrylamide gels and immunoblots were probed with anti-IRF3 mAb. Bands were detected with chemiluminescent substrate.

IRF3 is Stable in OSU-Infected Cells and in OSU NSP1-Transfected Cells

One explanation for IRF3 stability in OSU-infected cells is that NSP1 was not expressed at a sufficiently high level to have an effect on IRF3. We addressed this possibility first by increasing the m.o.i. of OSU to 20. Infected cell lysates were prepared 6 h post-infection and the levels and activation status of

IRF3 were determined by immunoblot. Infections with Nebraska calf diarrhea virus (NCDV, a B641-like strain) and SA11-4F caused IRF3 degradation under these conditions, whereas IRF3 was phosphorylated and stable in OSU infections (Figure 3.2(a)). We evaluated OSU NSP1 expression by metabolic labeling of cells infected at an m.o.i. of 20 and, although B641 NSP1 and SA11-4F NSP1 were detectable, OSU NSP1 could not be unequivocally discerned from the background of cell proteins (data not shown). These results suggested that the level of OSU NSP1 could be a limiting factor in effects on IRF3.

We constructed a vector that directs transcription of a bicistronic mRNA that expresses EYFP by cap-mediated translation and the protein of interest under the control of the poliovirus IRES. Both OSU NSP1 and B641 NSP1 were cloned into the pEYFP-IRES vector (pO-NSP1 and pB-NSP1, respectively) to investigate functions of NSP1 in the absence of virus infection. Transient transfections were carried out in 293 cells because the transfection efficiency of MA104 cells was poor. We confirmed the IRF3 degradation phenotypes in 293 cells infected with each of these viruses (data not shown). OSU NSP1 was consistently present at higher levels than B641 NSP1 (Figure 3.2(b)). The status of IRF3 was measured in transfected cells by immunoblot and, as observed in OSU-infected cells, IRF3 was stable, whereas IRF3 was degraded in the presence of B641 NSP1 (Figure 3.2(c)). Together these data show that OSU NSP1 is not able to direct proteasome-dependent degradation of IRF3 in human or monkey cell lines.

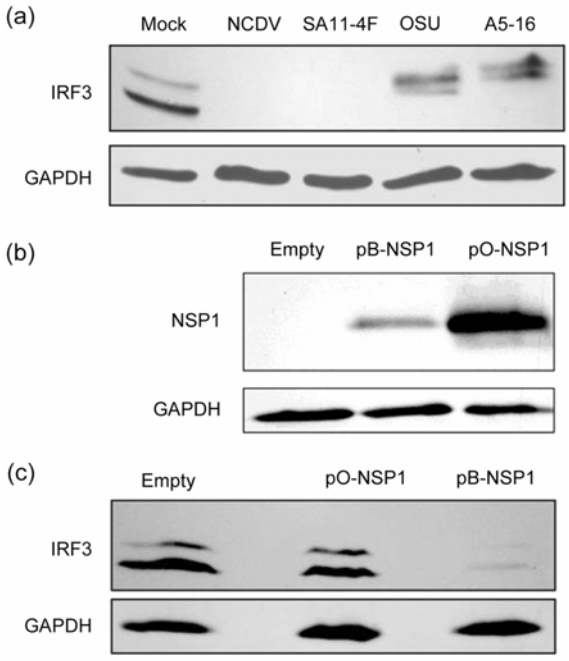

Figure 3.2: IRF3 is stable in the presence of OSU NSP1. (a) MA104 cells were mock-infected or infected at an m.o.i. of 20 with the indicated virus. Cell lysates were prepared at 6 h p.i. and electrophoresed on SDS-polyacrylamide gels. Immunoblots were probed with anti-IRF3 mAb (top panel) or anti-GAPDH mAb (bottom panel). (b) 293 cells were transfected with pEYFP-IRES (Empty), pB-NSP1 or pO-NSP1 plasmids and cell extracts were prepared 48 h post-transfection. Immunoblots were probed with anti-myc mAb to detect myc-tagged NSP1 (top panel) or anti-GAPDH mAb as a loading control (bottom panel). (c) Cell lysates described in (b) were probed with anti-IRF3 mAb (top panel) or anti-GAPDH (bottom panel).

Comparative Analysis of B641 NSP1 and OSU NSP1 Interactions with IRF3

The observation that OSU NSP1 expression could not induce degradation of IRF3 suggested that these two proteins may not interact. The interaction between B641 NSP1 and IRF3 was discovered in a yeast two-hybrid screen. We first tested for a potential interaction between OSU NSP1 and IRF3 in yeast, and no interaction was observed (data not shown). To test for possible interaction in an alternative system, GST pull-down assays were performed with GST-IRF3$_{23–422}$ and pB-NSP1- or pO-NSP1-transfected cell lysates. Despite the difference in

NSP1 levels (Figure 3.3(a)), significantly more B641 NSP1 bound GST-IRF3 than did OSU NSP1 (Figure 3.3(b)). The same amount of GST-IRF3 was eluted from each reaction (Figure 3.3(b)). Binding was quantified by determining the ratio of NSP1 bound to GST–IRF3 to the input levels of NSP1. OSU NSP1 bound IRF3

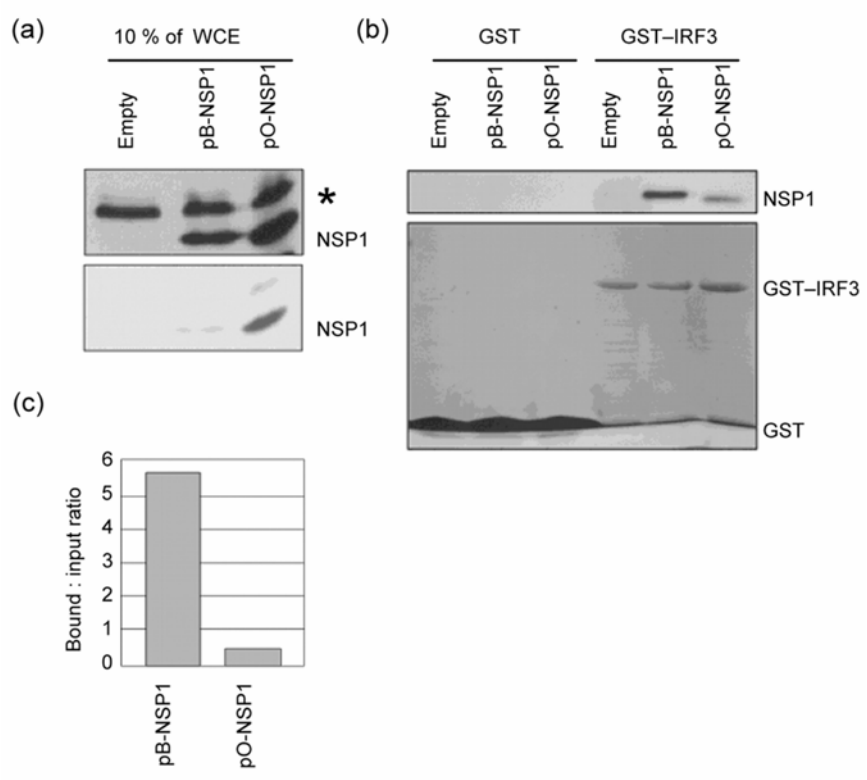

Figure 3.3: OSU NSP1 interacts weakly with IRF3 by GST pull-down assay. Cell extracts were prepared from 293 cells transfected with pEYFP-IRES (Empty), pBNSP1 or pO-NSP1 at 48 h post-transfection. Ten percent of the lysates was saved for an input control and the remaining lysates were divided evenly between GST and GST–IRF3 adsorbed to glutathione-Sepharose 4B beads. (a) Myc-tagged B641 NSP1 or myc-tagged OSU NSP1 used in the pull-down assay. The top panel is overnight exposure and the bottom panel is a 15 min exposure. The asterisk indicates a non-specific protein typically present in the blots probed with the anti-myc antibody. (b) Top panel: immunoblot of pull-down eluates from GST or GST-IRF3 and indicated transfected cell lysates, probed with anti-myc mAb to detect myc-tagged NSP1. Bottom panel: Coomassie-stained gel of purified GST and GST-IRF3 eluted in the pull-down reactions. (c) Relative binding was determined with densitometry by calculating the ratio of GST-IRF3-bound NSP1 to input NSP1 and is expressed in arbitrary units.

at a detectable level, but the binding was <10% of that observed for B641 NSP1 (Figure 3.3(c)). These data suggest that the stability of IRF3 in OSU-infected cells and in OSU NSP1-transfected cells is due to the lack of a stable interaction with IRF3 in human or monkey cell lines.

B641 NSP1 Mutants with Substitutions in the C/H-Rich Zinc-Binding Domain Have Reduced IRF3-Binding and -Degradation Activity

To begin to dissect the role of the zinc-binding domain in IRF3 degradation, NSP1 sequences from several rotavirus strains were compared and mutations were made to conserved histidine and cysteine residues within and downstream of the zinc-binding domain of B641 NSP1. Each mutant was tested for the ability to bind IRF3 by pull-down assay and to cause IRF3 degradation in transfected cells. 293 cells were transfected with pEYFP-IRES, pB-NSP1 (wild-type) or pB-NSP1 mutants containing single amino acid substitutions C54A, H79L or H136L. Each mutation reduced the B641 NSP1-IRF3 interaction compared to the wild-type protein (Figures 3.4(a) and 3.4(b)). The H136L mutant retained the highest level of IRF3 binding at approximately 30%.

Analysis of transfected cell lysates showed that each NSP1 mutant accumulated to significantly higher levels than wild-type NSP1 (Figure 3.4(c)). Also, the C54A and H79L mutants were unable to direct degradation of IRF3 (Figure 3.4(c)). The significant increase in the amount of mutant protein

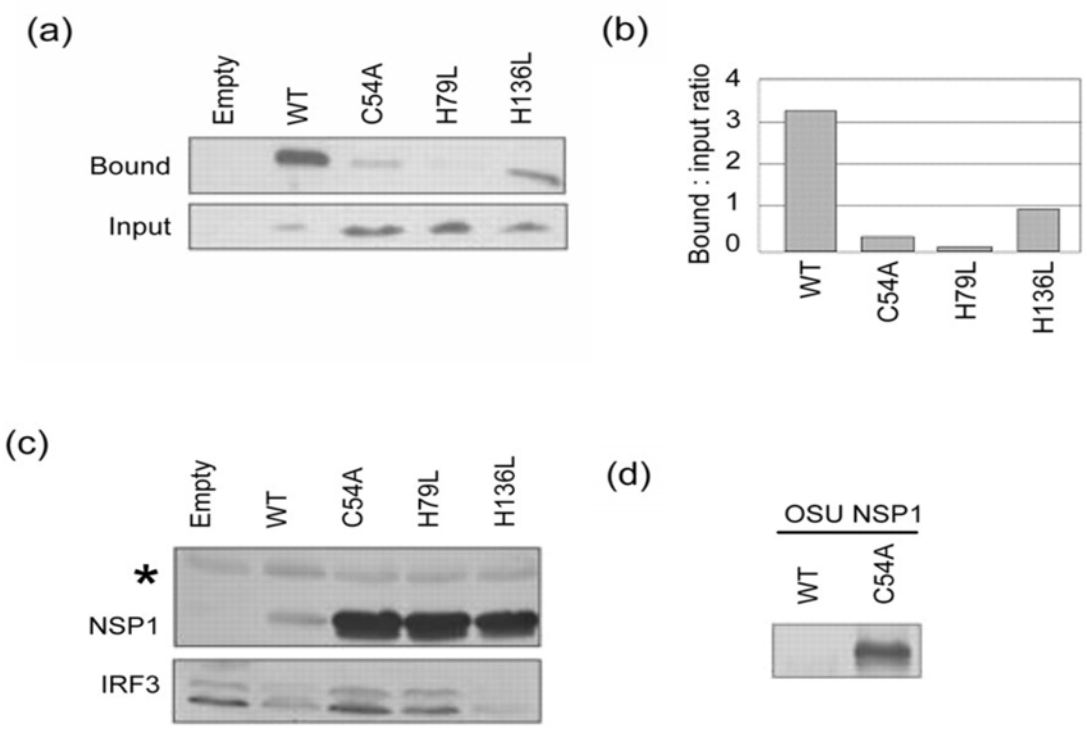

Figure 3.4: Integrity of the zinc-binding domain is required for IRF3 binding and degradation, and for NSP1 stability. (a) 293 cells were transfected with the indicated wild-type or mutant plasmids and cell lysates were subjected to GST pulldown assay. Top panel: immunoblots of pull-down eluates probed with anti-myc mAb to detect myc-tagged NSP1. Bottom panel: immunoblot of lysate not subjected to pull-down assay, probed with anti-myc mAb. Input is 10 % of the amount of lysate used in the pull-down reaction. (b) Binding was determined with densitometry by calculating the ratio of GST-IRF3-bound NSP1 to input NSP1 and expressed in arbitrary units. (c) 293 cells were transfected with pEYFP-IRES (Empty), wild-type pB-NSP1 (WT) or pB-NSP1 mutants containing the indicated substitution. The asterisk indicates a protein cross-reactive with the myc antibody. Top panel: accumulation of NSP1 in transfected 293 cells detected in immunoblots probed with anti-myc mAb. Bottom panel: transfected cell lysates probed with anti-IRF3 mAb. (d) OSU wild-type and C54A mutant NSP1 were translated in cell-free extracts in the presence of Trans ^{35}S label. Bands were visualized by autoradiography.

compared to wild-type protein suggests that NSP1 may regulate its own stability via a functional zinc-binding domain, in addition to regulating the stability of IRF3. Pulse-chase analysis of wild-type and mutant NSP1 confirmed that the mutations resulted in increased stability (Figure 3.5). The H136L mutation is outside the zinc-binding domain. This mutant retained the ability to direct IRF3 degradation

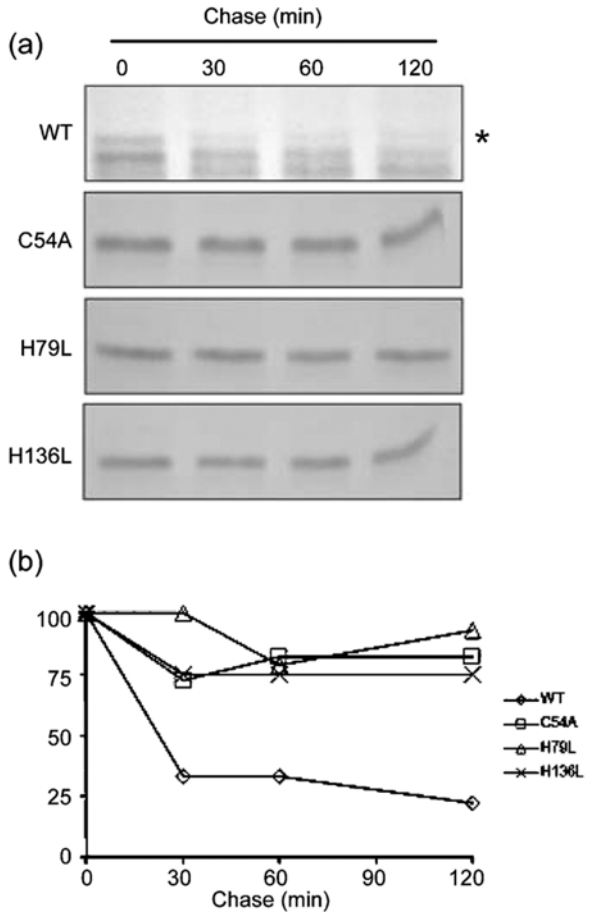

Figure 3.5: Increase in B641 NSP1 stability is due to C54A, H79L and H136L mutations. (a) Wild-type (WT) B641 NSP1 and indicated B641 NSP1 mutants were expressed in the presence of Trans ^{35}S label in a transcription-translation coupled reaction. The radiolabeling was quenched using a mixture of unlabelled methionine and cysteine at 0 min. Samples were collected at indicated times during the chase. Expression levels were visualized by autoradiography. The asterisk indicates migration of NSP1. (b) Densitometric analysis of autoradiography shown in (a) was used to quantify the level of indicated B641 NSP1 at each time point. Results are displayed as the level of NSP1 relative to the 0 min time point.

but, interestingly, was more stable than wild-type NSP1. The explanation for this result is not entirely clear, but the data suggest that IRF3 degradation and intrinsic NSP1 stability are functionally separable.

OSU NSP1 has an intact zinc-binding domain as determined by sequence analysis, but was unable to bind or degrade IRF3. We tested whether this domain played a role in stability of NSP1. A C54A mutation stabilized OSU

NSP1 in cell-free translation reactions, suggesting that the zinc-binding domain was important in stability of OSU NSP1, similar to what was observed for B641 NSP1 (Figure 3.4(d)).

B641 NSP1 and OSU NSP1 Are Susceptible to Proteasome Degradation in Transfected Cells

Higher levels of OSU NSP1 compared to B641 NSP1 were consistently observed in transfected cells. We confirmed by sequencing that the OSU NSP1- and B641 NSP1-expressing constructs were exactly the same, with the only difference being in the protein-coding regions. One explanation for the level of OSU NSP1 was that, in contrast to B641 NSP1, OSU NSP1 may not be susceptible to rapid proteasome degradation. We tested this possibility by measuring NSP1 levels in cells transfected in the presence of the proteasome inhibitor, MG132. The data shown in Figure 3.6 indicate an approximately 2.5-fold increase in the amount of both OSU and B641 NSP1 in the presence of

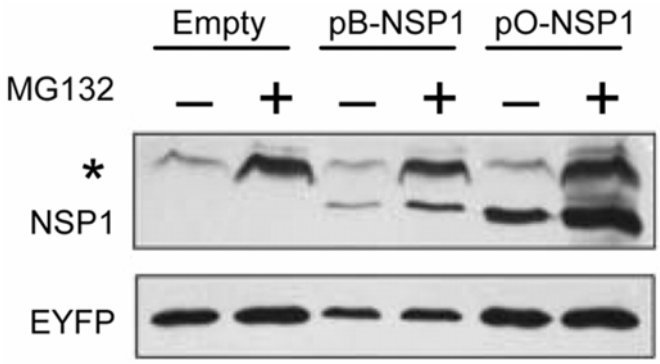

Figure 3.6: B641 NSP1 and OSU NSP1 are stabilized by inhibition of proteasome activity. 293 cells were transfected with pEYFP-IRES (Empty), pB-NSP1 or pONSP1. The cells were treated with the proteasome inhibitor MG132 or an equivalent volume of DMSO during the final 8 h of incubation. Lysates were prepared 48 h post-transfection. Immunoblots were probed with anti-myc mAb to detect myc-tagged NSP1 (top panel) or anti-EYFP (bottom panel) to measure transfection efficiency. The asterisk indicates a protein cross-reactive with the myc antibody.

MG132. These data demonstrate an inherent sensitivity of NSP1 to proteasome degradation and show that the high level of OSU NSP1 in transfected cells is not due to insensitivity to proteasome degradation.

Discussion

We have demonstrated the importance of the conserved zinc-binding domain of NSP1 in IRF3 binding, degradation and intrinsic NSP1 stability. By extension, several lines of evidence in this report support the hypothesis that rotavirus NSP1 has E3 ubiquitin ligase activity. First, an E3 ubiquitin ligase gives the ubiquitin-proteasome system its specificity, as substrates that are targeted for degradation must interact with an E3 (366). B641 NSP1 bound IRF3 strongly and IRF3 was degraded in a proteasome-dependent manner, whereas the OSU NSP1-IRF3 interaction was weak and IRF3 was stable. Second, the RING domain is important for the activity of an E3. There is clearly strong evolutionary pressure to maintain the cysteine and histidine residues that form the zinc-binding domain in NSP1, because these residues are completely conserved in all published NSP1 sequences. Mutation of two conserved cysteine and histidine residues of the B641 NSP1 zinc-binding domain significantly weakened the NSP1-IRF3 interaction, and IRF3 was not degraded in the presence of these mutants. A mutation to a highly conserved histidine residue downstream of the zinc-binding domain was less detrimental to the strength of the NSP1-IRF3 interaction and did not abrogate the ability of B641 NSP1 to cause IRF3

degradation. The spacing of the conserved cysteine and histidine residues in NSP1 does not correspond to the RING consensus found in cellular E3 ligases. Thus the NSP1 zinc-binding domain probably represents a viral protein with a variant E3 signature, as noted previously for KSHV RTA and paramyxovirus V proteins (431, 450). Finally, E3 proteins are commonly capable of autoregulation through self-ubiquitination (388). Mutations within the RING or RING-like domains, or inhibition of proteasome activity, cause accumulation of E3 proteins in cells (431, 500). Inhibition of proteasome activity resulted in accumulation of both B641 NSP1 and OSU NSP1 in transfected cells, and mutations within the zinc-binding motif of either strain caused NSP1 to accumulate in transfected cells or cell-free extracts. Collectively, the observations described above are consistent with the hypothesis that NSP1 is an E3 ubiquitin ligase.

NSP1-IRF3 binding experiments showed that OSU NSP1 could bind IRF3, but at levels lower than 10% of those observed with B641 NSP1. These data were not a result of insufficient protein because OSU NSP1 accumulated to higher levels than B641 NSP1 in transfected cells. A weak interaction suggests that variations in OSU NSP1 sequence or structure variations result in assembly of an unstable proteasome-targeting complex. It should be noted, however, that experiments were performed in cells of monkey or human origin. Thus the possibility exists that there is species specificity or co-factors involved in OSU NSP1 interactions that are not required for the bovine NSP1 interactions with human or monkey IRF3. Sequence comparisons between B641 NSP1 and OSU

NSP1 did not reveal obvious differences in the N-terminal domain of the protein that would suggest a basis for distinct IRF3-binding patterns. The region with the highest sequence variation within NSP1 of all rotavirus strains is in the C-terminal half of the protein (155). Previous data showed that the C terminus of NSP1 played a role in IRF3 binding and IRF3 degradation in infected cells (459, 490). Consistent with this, a C-terminal fragment of OSU NSP1 did not interact with IRF3 in a yeast two-hybrid assay (data not shown). These data suggest that the C terminus is critical for interactions with IRF3, and that variation in the C termini of NSP1 of B641 and OSU may direct potentially different target specificities.

IRF3 targeting by B641 NSP1, but not by OSU NSP1, leads to the prediction that OSU NSP1 may target a unique set of substrates. Precedent for this prediction comes from studies of the paramyxovirus V proteins. V proteins from different paramyxoviruses target distinct proteins involved in JAK/STAT signal transduction. For example, Simian virus *5* targets STAT1 for proteasome degradation (453), while human parainfluenza virus *2* targets STAT2 (454) and mumps virus V protein can target both STAT1 and STAT3 (455). Additional support for the prediction that B641 NSP1 and OSU NSP1 have unique substrates is the dichotomy in the stability of each of these proteins when comparing protein levels in cells. In 293 cells, OSU NSP1 is more stable than B641 NSP1. KSHV RTA accumulates in cells until its IRF7 substrate is no longer detectable, at which point RTA also becomes undetectable, presumably through autoregulation (431). Based on this, we predict that 293 cells have a higher

cumulative level of OSU NSP1-specific substrate than B641 NSP1 substrate, resulting in higher levels of OSU NSP1 accumulation. Alternatively, as an example, HSV ICP0 is protected from self-ubiquitination in cells through interactions with ubiquitin-specific protease USP7 (501), and such an inhibitory interaction also may exist for OSU NSP1. The variations in reported NSP1 levels of different rotavirus strains could be a function of the cumulative specific substrate levels or interacting proteins in different cell lines for each unique NSP1, in addition to levels regulated by their individual translation efficiencies (502). Expression of OSU NSP1 fails to cause IRF3 degradation in 293 cells, and it will be worthwhile to investigate whether OSU NSP1 targets other protein(s) involved in the induction of an IFN response. OSU NSP1 targeting of other signaling molecules involved in IFN induction or amplification could have a similar biological effect to B641 NSP1 targeting IFN induction by degrading IRF3.

Generation of rotavirus strains deficient in the ability of NSP1 to interfere with IFN signal transduction would be an attractive feature in an attenuated rotavirus vaccine. The effects of IFN production in stimulating innate immune responses have been well documented, but only recently have the effects of IFN production on adaptive immune responses been appreciated (229). Biochemical analysis of the phenotype of rotavirus NSP1 mutants such as those provided here will help provide a framework for rational attenuated vaccine development.

NOTE: The experiments described in Figure 3.2(b) and Figure 3.2(c) were perfomed by Julie Ewen.

PORCINE ROTAVIRUS OSU ANTAGONIZES IFNβ INDUCTION BY BLOCKING NFκB SIGNALING

Abstract

Mechanisms by which viruses counter innate host defense responses generally involve interference with one or more components of the interferon (IFN) system. Multiple steps in the induction and amplification of IFN signaling are targeted for inhibition, and many viral IFN antagonists have direct or indirect effects on activation of latent cytoplasmic transcription factors. Rotavirus nonstructural protein NSP1 blocks transcription of type I IFNα/β by inducing proteasome-dependent degradation of IFN-regulatory factors 3 (IRF3), IRF5, and IRF7. In this study, we show that rotavirus NSP1 also inhibits activation of NFκB, and does so by a novel mechanism. Proteasome-mediated degradation of inhibitor of κB (IκBα) is required for NFκB activation. Phosphorylated IκBα is a substrate for polyubiquitination by a multisubunit E3 ubiquitin ligase Skp1/Cul1/F-box complex, in which the F-box substrate recognition protein is β-transducin repeat containing protein (β-TrCP). The data presented show that IκBα is phosphorylated and stable in rotavirus infected cells, because infection induces proteasome-mediated degradation of β-TrCP. NSP1 expressed in isolation in transiently transfected cells is sufficient to induce this effect. Targeted degradation of an F-box protein of an E3 ligase complex that plays a prominent role in modulation of innate immune signaling pathways is a unique mechanism

of IFN antagonism, and defines a second strategy of immune evasion by rotaviruses.

Introduction

Research into mechanisms by which viruses evade host defense has received increased attention in the past several years because of the potential to develop attenuated vaccines based on viruses with weakened evasion strategies, or antivirals that target specific immune system antagonists. Most, if not all, viruses encode proteins that interfere with signal transduction pathways involved in induction or amplification of the immune response, particularly the innate response driven by type I interferon (IFNα/β) (321). IFNα/β are antiviral cytokines that stimulate expression of genes that interfere directly with steps in the virus replication cycle, and genes whose protein products modulate and recruit the adaptive immune response. The antiviral state that is established by the IFN signaling network serves to restrict virus replication and spread while effectors of the slower adaptive immune response are recruited to the site of infection.

Each of the steps in the IFN signaling pathway has been reported as targets for viral IFN antagonists. A recent summary of mechanisms of interference with the IFN response clearly illustrates that some viral proteins target more than one step in the pathway (e.g. influenza virus NS1) and some viruses encode more than one IFN antagonist (e.g. paramyxovirus V, C, and N

proteins), exemplifying the importance of IFN signaling to host defense (177, 321).

Signal transduction pathways that activate IRF3 and NFκB have been well studied in the context of the virus-induced IFN response. IRF3 is one of a family of nine transcription factors that share a conserved N-terminal DNA binding domain containing five tryptophan repeats (231). Upon virus detection, IRF3 is phosphorylated at its C terminus by TBK1 or IKKε (196), dimerizes and then translocates to the nucleus to assemble at the IFNβ promoter and select ISRE-containing promoters in cooperation with transcription co-activators CBP/p300 (171). IRF3 activation is required for IFNβ transcription, and the number of reports of viruses that interfere directly with the function of IRF3, or the steps preceding its activation has grown significantly in recent years (321). For example, nonstructural protein NS1 of influenza virus interacts with dsRNA binding protein RIG-I, and blocks activation of IRF3 (349, 350, 353, 360). The hepatitis C virus NS3-4A protease complex cleaves TLR3 adaptor protein TRIF, blocks RIG-I signaling and cleaves adaptor protein IPS/MAVS/Cardif/VISA to release it from the mitochondrial membrane, thus blocking activation of IRF3 (191, 330). NS1/NS2 proteins of respiratory syncytial virus both play roles in inhibiting antiviral signaling, as deletion of these proteins results in increased phosphorylation of IRF3 (503). One of the more recently defined viral IFN antagonists is rotavirus nonstructural protein NSP1. NSP1 targets IRF3, IRF5,

and IRF7 for proteasome-dependent degradation early post-infection, resulting in inhibition of IFNβ transcription (490, 504).

Similar to IRF3, NFκB is required for induction of IFNβ transcription. NFκB is activated by multiple stimuli, and in addition to regulating innate and adaptive immune response gene expression, functions in signaling pathways associated with cell division and apoptosis (253). NFκB subunits are held inactive in the cytoplasm by association with inhibitors of kappa B (IκB), and phosphorylation of IκB by IκB kinases (IKKα/β) results in its rapid ubiquitination and degradation by the 26S proteasome (259, 505). IκB degradation releases the p50/relA (p65) heterodimer, which is phosphorylated and translocates to the nucleus for promoter binding and transcription of NFκB target genes (253). Similar to viral antagonism seen with IRF3 signaling, multiple steps in the NFκB pathway have been reported as targets for viral IFN antagonists, some of which are common to the IRF3 activation pathway (506).

Rotaviruses cause severe gastroenteritis in infants and young children, and in newborns of most mammalian species. Results from our laboratory and others have shown that NSP1 from several different rotavirus strains targets IRF3 for proteasome degradation early post-infection, resulting in inhibition of IFNβ transcription (490, 504). Expression of NSP1 in the absence of infection directs IRF3 degradation, indicating it is the sole viral protein that mediates this effect (Chapter 3). NSP1 of simian rotavirus strains also directs degradation of

IRF5 and IRF7, both critical participants in induction and amplification of IFN response (504).

We recently reported that IRF3 was activated and stable in cells infected with porcine rotavirus strain OSU (Chapter 3). Therefore, we sought to determine if an alternative mechanism to block induction of IFNβ was encoded in the rotavirus genome. The studies reported herein revealed that NFκB activation was blocked in OSU infected cells due to stabilization of phosphorylated IκBα. Dissection of the steps involved in IκBα degradation revealed that the substrate recognition protein, β transducin repeat containing protein (β-TrCP), of the cellular E3 ubiquitin ligase complex Skp1/Cul1/F-box (SCF), is targeted for proteasome degradation by NSP1. This $SCF^{\beta\text{-}TrCP}$ E3 ligase complex is responsible for ubiquitination of IκB (395, 507), thus providing an explanation for IκBα stabilization and the lack of NFκB activation in infected cells. Targeted degradation by a viral protein of a cellular F-box protein required for E3 ligase substrate recognition is a novel IFN evasion strategy, and defines a second mechanism of interference with the innate immune response encoded in the rotavirus genome.

Materials and Methods

Cells and Viruses

MA104 cells (ATCC) were grown in M199 media (Mediatech) supplemented with 5% FBS (Atlanta Biologicals). 293 (also known as HEK293)

cells (ATCC) were grown in RPMI 1640 media (Mediatech) supplemented with 10% FBS, 10 mM HEPES, 1X nonessential amino acids, 2 mM L-glutamine, and 1 mM sodium pyruvate. 293-TLR3 cells (also known as Wt-11; kindly provided by Dr. G. Sen Cleveland Clinic, Cleveland, OH (508)), were grown in the same conditions as 293 cells except that the media was supplemented with 400 μg/mL of G418 (Mediatech). All cell lines were incubated at 37°C with 5% CO_2.

The rotavirus strains A5-16 (bovine), NCDV (bovine), and OSU (porcine) were propagated in MA104 cells. After complete lysis of the infected MA104 monolayer was observed, the medium was clarified of cell debris at 2000 x *g* for 10 minutes, and the virus was concentrated by centrifugation at 26K rpm in an SW-28 rotor (Sorvall) for 2 hours at 4°C. Virus pellets were suspended in M199 lacking FBS and stored at -80°C. Virus titers were determined by plaque assay.

RT-PCR

MA104 cells were infected with 3 pfu/cell using rotavirus stocks that were activated with 10 μg/mL Worthington trypsin at 37°C for 30 minutes. Infections were carried out at 37°C in M199 lacking FBS. At 8 hours post-infection (hpi) total cell RNA was extracted using TRIzol (Invitrogen). After DNase treatment (Ambion) and phenol/chloroform extraction, reverse transcription reactions primed with random hexamers (Promega) were carried out using Superscript II (Invitrogen). PCR reactions were performed with Taq polymerase (Promega) to detect cDNA encoding IFNβ (forward 5' - CTC CTC CAA ATT GCT CTC CTG – 3'; reverse 5' – GCA AAC TGC TCA CGA ATT TTC C – 3') , ISG56 (forward 5' –

AAC ACC TGA AAG GCC AGA ATG AGG-3'; reverse 5' – AAG ACA GAA GTG GGT GTT TCC TGC-3'), IP-10 (forward 5' – CTG CGA TTC TGA TTT GCT GCC – 3'; reverse 5' – GGA GAT CTT TTA GAC ATT TCC TTG CTA ACT GC – 3'), c-Jun (forward 5' – AAC GAC CTT CTA TGA CGA TGC CCT C – 3'; reverse 5' – GCG AAC CCC TCC TGC TCA TCT GTC – 3') (the c-Jun primers were previously described (509)) and β-actin (forward 5' – CAT GTT TGA GAC CTT CAA CAC – 3'; reverse 5' – CAT CTC CTG CTC GAA GTC TAG – 3').

Dual Luciferase Assays

293-TLR3 cells were transfected with three plasmids using TransIT-293 Transfection Reagent (Mirus): 1) either an NSP1 expression vector or empty expression vector (described in Chapter 3), 2) phRL-CMV (Promega) renilla luciferase control, and 3) either IFNβ-Luc (kindly provided by Dr. J. Hiscott McGill University, Montreal, Quebec (510)) or pNF-κB-Luc *Cis* Reporter (Stratagene) firefly luciferase reporter. At 40 hours post-transfection, the cells were treated by adding polyI:C (GE Healthcare) to a working concentration of 100 μg/mL directly to the medium. Cell lysates were harvested 8 hours later and analyzed using the Dual Luciferase Assay (Promega). Luciferase activity was measured using a Lumat LB 9507 luminometer (EG&G Berthold) and each transfection combination was performed in triplicate in two independent experiments.

ELISA

MA104 infections were performed as described in the RT-PCR section. Whole cell extracts (WCE) were harvested at 6 hpi in Lysis Buffer AM1 (Active Motif). Protein concentration was determined using the RC DC Protein Assay (Bio-Rad Laboratories) and 20 μg of WCE were used in a TransAM p50 Activation Assay (Active Motif) to compare the level of NFκB subunit p50 capable of binding the oligonucleotides containing NFκB binding sites. Three independent experiments were performed and p-values were determined using the Student's unpaired t-test.

Time Course Analysis

MA104 infections were performed as described in the RT-PCR section. WCE were harvested at the indicated times post-infection in RIPA buffer (150 mM NaCl, 1% sodium deoxycholate, 1% Triton X-100, 0.1% SDS, 10 mM Tris-HCl pH 7.2). Immunoblots were performed as previously described (Chapter 3). Antibodies were used to detect the following proteins: p65 (Rockland), IκBα (Cell Signaling), IκBα with phosphorylated serine 32 (Cell Signaling), JNK1/JNK2 with phosphorylated threonine 183 and tyrosine 185 (Abcam), p38 with phosphorylated threonine 180 and tyrosine 182 (Cell Signaling), c-Jun with phosphorylated serine 63 (Cell Signaling), and GAPDH (Ambion). Immunoblots were performed using WCE from at least two independent infection time courses.

TNFα Challenge

MA104 infections were performed as described in the RT-PCR section. At 8 hpi, TNFα (PeproTech) was added directly to the media to a working concentration of 50 ng/mL and the cells were returned to 37°C for incubation. WCE were harvested in RIPA buffer after 15 minutes of TNFα treatment. The WCE were used in immunoblot analysis of total IκBα and phosphorylated IκBα.

Immunoprecipitation

MA104 cells were grown to 90% confluency in M199 supplemented with 5% FBS. After a 16 hour incubation in M199 supplemented with 2% FBS and 5 μg/mL actinomycin D, infections were performed at an MOI = 10 pfu/cell in M199 lacking FBS. Following a 1.5 h adsorption, the inoculum was replaced with DMEM lacking L-cysteine and L-methionine (Mediatech), but supplemented with 5 μg/mL actinomycin D and 30 μCi/mL ^{35}S trans label (MP Biomedicals, Inc.) and incubated 6 hours at 37°C. WCE were harvested in PBS by cell scraping. After centrifugation at 750 x g for 30 s, the cell pellets were lysed in ECB buffer (120 mM NaCl, 1 mM EDTA, 0.5% Igepal CA-630, 50 mM Tris-Cl pH 8.0) supplemented with protease inhibitor cocktail (Roche Diagnostics). As an input control, 10% of each sample was set aside and the remaining WCE of each sample was divided evenly and probed with either anti-p65 (Rockland) or normal rabbit serum. Immunoprecipitations were performed using GammaBind Plus Sepharose (GE Healthcare) according to the manufacturer's recommendations. The input controls and eluted samples were separated on a 12% acrylamide gel.

Autoradiography was performed to detect rotavirus proteins that co-immunoprecipitated with p65.

293 cells were transfected in 60 mm dishes with pCMV-Flag-β-TrCP2 plasmid (kindly provided by Dr. W. Harper, Department of Pathology, Harvard Medical School, Boston, MA), or mock transfected. At 20 hours post-transfection, the medium was changed to RPMI 1640 lacking FBS (2.5 mL per dish) and the cells were infected with 3 pfu/cell of OSU. At 1 hpi, 2.5 mL RPMI 1640 supplemented with 10% FBS was added. At 8 hpi, WCE were harvested in 500 µL FLAG immunoprecipitation lysis buffer (50 mM Tris-HCl, pH 7.5, 150 mM NaCl, 1% Triton X-100, 1 mM EDTA) supplemented with a protease inhibitor cocktail tablet (Roche Diagnostics). WCE were passed through a 30 gauge needle 5 times and subsequently precleared by 10 min centrifugation at 10,000 x g at 4°C. As an input control, 10% of each sample was set aside and the FLAG-tagged βTrCP2 was immunoprecipitated from the remaining WCE using ANTI-FLAG M2-agarose Affinity Gel (Sigma) according to the manufacturer's recommendations. The input controls and eluted samples were used in immunoblot analysis using antibodies for FLAG (Sigma) and a custom rabbit polyclonal antibody raised against the C terminal region of OSU NSP1 (Open Bioscience). At least two independent experiments were performed for each type of immunoprecipitation.

Sample Preparation for Microscopy

MA104 cells were grown in 4-well chamber slides (BD Falcon) and infected with 3 pfu/cell using rotavirus stocks that were activated with 10 μg/mL Worthington trypsin at 37°C for 30 minutes. Infections were carried out at 37°C in M199 lacking FBS. At 6 hpi, the cells were fixed with paraformaldehyde (2% w/v in PBS) for 10 minutes at room temperature and permeabilized with methanol for 10 minutes at -20°C. The samples were incubated in blocking solution (PBS supplemented with 5% v/v horse serum and 5% v/v goat serum) overnight at 4°C. The samples were incubated in primary antibody diluted in blocking serum for 1 hour at room temperature followed by 3 rinses with PBS. The primary antibodies used were mouse anti-IRF3 (Santa Cruz Biotechnology), rabbit anti-p65 (Rockland), mouse anti-VP6 (511), and guinea pig anti-NSP2 (kindly provided by Dr. M. Estes, Baylor College of Medicine, Houston, TX). The cells were then stained with the appropriate Alexa Fluor 488-, 594-, and 633-conjugated goat secondary antibodies (Invitrogen) and mounted in ProLong Gold (Invitrogen) under a glass cover slip.

Immunofluorescence Microscopy

IRF3 stained cells were viewed on an AxioImager.A1 microscope (Zeiss) using a 40X (0.75 NA) objective lens. The images were obtained using an AxioCam MRc5 camera (Zeiss) and analyzed with the Axiovision version 4.6.3 (Zeiss) software package. Exposure parameters were equal for images of each sample.

Cells stained for p65 were viewed on an LSM 510 Meta confocal microscope (Zeiss) using a 63X (1.40 NA) objective lens. Excitation of Alexa Fluor 488 was achieved using a 488 nm argon laser. The pinhole was set to 1 Airy unit. Images were obtained with each line being scanned 8 times to increase the signal-to-noise ratio. The images were analyzed with the LSM Image Browser (Zeiss).

VP6, NSP2, and p65 triple stained cells were viewed on an LSM 510 Meta confocal microscope (Zeiss) using a 63X (1.40 NA) objective lens. The zoom function was used to image single cells. Excitation of Alexa Fluor 488, Alexa Fluor 594, and Alexa Fluor 633 was achieved using a 488 nm argon laser, a helium-neon 543 nm laser, and a helium-neon 633 nm laser, respectively. The pinhole was set to 1 Airy unit for each channel. Images were obtained using the multitrack scanning mode to minimize crosstalk between channels and with each line being scanned 8 times to increase the signal-to-noise ratio. The images were analyzed with the LSM Image Browser (Zeiss).

β-Catenin Stabilization

293 cells were infected with 3 pfu/cell using rotavirus stocks that were activated with 10 μg/mL Worthington trypsin at 37°C for 30 minutes. Infected cells were incubated at 37°C in RPMI lacking FBS for one hour at which time FBS was added to 5% (v/v). At 10 hours post-infection (hpi), WCE were harvested in RIPA buffer and subsequently used in immunoblot analysis using

antibodies for β-Catenin (Santa Cruz Biotechnology) and GAPDH. β-Catenin stabilization was assayed in three independent experiments.

Results

IRF3 Accumulates in the Nucleus of OSU Infected Cells

IRF3 is phosphorylated in OSU infected MA104 cells, indicating that the virus is detected and signaling pathways leading to IRF3 phosphorylation are intact (Chapter 3). Once phosphorylated, IRF3 dimerizes and translocates to the nucleus to assemble with transcription co-activators on the IFNβ promoter and ISRE-containing sites. To test whether these latter steps in the activation pathway were affected by OSU infection, the cellular distribution of IRF3 was analysed by immunofluorescence (IF) microscopy (Figure 4.1(a)). Bovine rotavirus strains A5-16 and NCDV were also analyzed in these experiments for comparisons with OSU because the behavior of these strains, with respect to IRF3, has been described. A5-16 encodes a truncated NSP1, and IFNβ transcription is induced in A5-16 infected cells (Chapter 2). NCDV encodes an NSP1 that binds to and targets IRF3 to the proteasome, resulting in inhibition of IFNβ expression (Chapter 2). IF microscopy revealed that in mock-infected cells, IRF3 was diffusely distributed in the cytoplasm. As expected, IRF3 accumulated in the nucleus of A5-16 infected cells, and was not detected in NCDV infected cells. IRF3 also accumulated in the nucleus of OSU infected cells, indicating

IRF3 nuclear translocation is not inhibited in MA104 cells infected with this rotavirus strain.

IFNβ Promoter-Regulated Gene Induction Is Inhibited in OSU Infected Cells and the Block is Mediated by NSP1

IFNβ mRNA levels were measured to test the activity of nuclear IRF3 in cells infected with the three strains (Figure 4.1(b)). IFNβ was strongly induced in A5-16 infected cells as expected, but not in NCDV or OSU infected cells. The lack of IFNβ induction in NCDV infected cells can be explained by degradation of IRF3. However, activation of IRF3 in OSU infected cells, observed in previous experiments, suggested that an alternative mechanism was used by this virus to block IFNβ transcription.

To determine whether NSP1 encoded by OSU played a role in inhibiting IFNβ transcription, 293-TLR3 cells were transfected with a reporter plasmid encoding firefly luciferase under the control of the IFNβ promoter, and then treated with polyI:C to induce reporter gene expression. Expression of OSU NSP1 reduced polyI:C-induced luciferase expression by approximately 20-fold compared to cells transfected with empty vector (Figure 4.1(c)). Reporter expression in cells transfected with NCDV NSP1 was reduced approximately 30-fold; a substantial portion of this reduction can be attributed to IRF3 degradation. These results demonstrate that OSU NSP1 inhibits IFNβ promoter-driven gene expression in the absence of infection, and without an obvious mechanism to interfere with the function of IRF3.

IRF3-regulated genes IP-10 and ISG56 have different transcription factor requirements for expression. While IFNβ and IP-10 require both IRF3 and NFκB, IRF3 is sufficient to induce ISG56 transcription (512). Since IFNβ was not induced in OSU infected cells, and IRF3 was stable, we analyzed IP-10 and ISG56 mRNA by RT-PCR to further dissect the activity of transcription factors

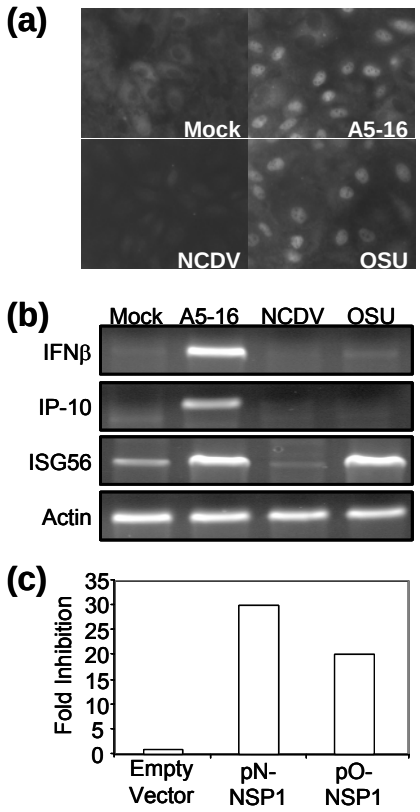

Figure 4.1: IFNβ induction is blocked during OSU infection and this block is mediated by expression of NSP1. (a) The cellular localization of IRF3 was examined by immunofluorescence microscopy (40X, NA 0.75) in MA104 cells infected with 3 pfu/cell of the indicated virus strain at 6 hours post-infection (hpi). (b) RT-PCR analysis of IRF3 regulated genes using RNA collected at 8 hpi from MA104 cells infected with 3 pfu/cell of the indicated virus strain. RT-PCR of actin was used as a template loading control. (c) 293-TLR3 cells were cotransfected with a control renilla luciferase reporter, a firefly luciferase reporter driven from the IFNβ promoter, and the indicated NSP1 expression vector or empty vector control. At 40 hours post-transfection, the cells were treated by adding polyI:C to 100 μg/mL in the media and whole cell extracts (WCE) were collected 8 hours later for use in a dual luciferase assay. Data are represented as fold inhibition of IFNβ reporter induction normalized to cells transfected with empty expression vector. Bars indicate the mean from samples in triplicate wells. (pN-NSP1 encodes NCDV NSP1; pO-NSP1 encodes OSU NSP1).

required for expression of these genes. A5-16 induced transcription of both IP-10 and ISG56 transcription in infected cells, but neither were induced in NCDV infected cells (Figure 4.1(b)). OSU infection induced ISG56, but not IP-10. ISG56 induction in OSU infected cells confirmed that IRF3 signaling is intact, and inhibition of IFNβ expression may be due to a block in NFκB signaling.

NFκB Promoter-Regulated Gene Induction Is Inhibited in OSU Infected Cells and the Block is Mediated by NSP1

NFκB activation in OSU infected cells was evaluated with the TransAM ELISA, which measures the ability of the p50 subunit of NFκB to bind DNA (Figure 4.2(a)). MA104 cells were infected with A5-16, NCDV, or OSU, and whole cell lysates were harvested 6 hpi. The amount of activated p50 was significantly higher in A5-16 and NCDV infected cell lysates compared to mock infected cells ($P < 0.01$). By contrast, the amount of activated p50 in OSU infected cell lysates was not different from mock infected lysates. The NFκB p50 subunit most commonly forms a p65-p50 heterodimer with transactivation activity (513). However, p50 also forms homodimers that act as repressors when bound to promoters because the p50 subunit lacks a transactivation domain (514). The ELISA did not detect elevated levels of p50 capable of binding DNA in OSU infected cells, indicating that infection did not induce formation of the activated p65-p50 heterodimer or the inhibitory p50 homodimer.

Next, we asked whether OSU NSP1 played a role in modulation of NFκB signaling in the absence of viral infection. 293-TLR3 cells were co-transfected with a plasmid encoding OSU NSP1 and a luciferase reporter plasmid containing tandem repeats of NFκB binding sites. The cells were then treated with polyI:C, and reporter expression in cell lysates was analyzed by luciferase assay (Figure

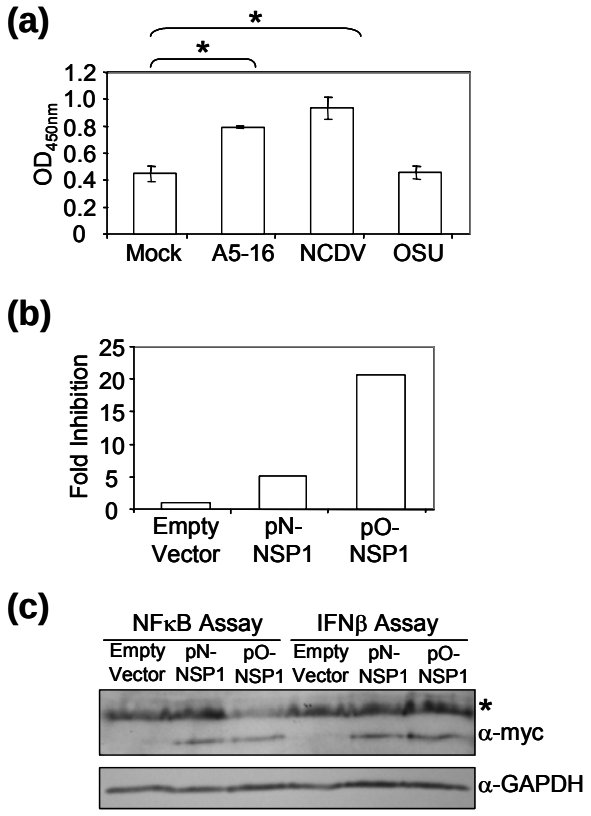

Figure 4.2: NFκB signaling block in OSU infected cells is mediated by expression of NSP1. (a) WCE were collected at 6 hpi from MA104 cells infected with 10 pfu/cell of the indicated virus strain. The ability of NFκB subunit p50 within the WCE to bind κB sites was determined using a TransAM p50 ELISA. Data are represented as the mean OD_{450nm} value from three independent experiments with error bars indicating the SEM. P-values were determined by unpaired Student's t-test (asterisk = $P < 0.01$). (b) 293-TLR3 cells were co-transfected and treated with polyI:C as described in Figure 4.1(c), except the firefly luciferase reporter used in this experiment was driven by κB sites within the promoter. Data are represented as fold inhibition of NFκB reporter induction normalized to cells transfected with the empty expression vector. Bars indicate the mean from samples in triplicate wells. (c) Lysates used in the NFκB and IFNβ reporter luciferase assays (Figures 4.2(b) and 4.1(c), respectively) were analyzed by immunoblot with anti-myc antibody to detect myc-tagged NSP1 expression (asterisk = cross-reactive band). The blots were probed again to detect GAPDH as a loading control.

4.2(b)). Expression of OSU NSP1 resulted in approximately 20-fold reduction of NFκB promoter-driven reporter gene expression relative to cells transfected with the empty vector. A five-fold reduction of luciferase expression was observed in cells expressing NCDV NSP1. Previously, we showed that OSU NSP1 accumulates to higher levels than NCDV NSP1 in transfected 293 cells (Chapter 3). Immunoblot analysis of cell lysates from the 293-TLR3 cells used for these luciferase reporter experiments showed that NCDV NSP1 and OSU NSP1 were expressed at equal levels in these experiments (Figure 4.2(c)), indicating the difference in fold-inhibition between NSP1 of these two strains is not due to differences in expression levels. Taken together, these data suggest a predominant mechanism of IFNβ antagonism in OSU infected cells was interference with NFκB activation and that NSP1 alone could mediate this effect. Likewise, inhibition of NFκB activation in NCDV infected cells also occurred, but to a lesser degree.

Cellular Distribution of NFκB Subunit p65

The fact that IRF3 is targeted for proteasome degradation early post-infection by some rotavirus strains led us to test whether targeted degradation of NFκB subunits in OSU infected cells was responsible for inhibition of NFκB activation. Cell lysates from mock infected and infected cells were collected every two hours for ten hours, and the abundance of NFκB subunits p65 (Figure 4.3(a)) and p50 (data not shown) was analyzed by immunoblot. Both p65 and

p50 in cells infected with all three viruses were equal to the levels detected in mock infected cells, indicating these subunits are not targeted for proteasome degradation by any of these strains.

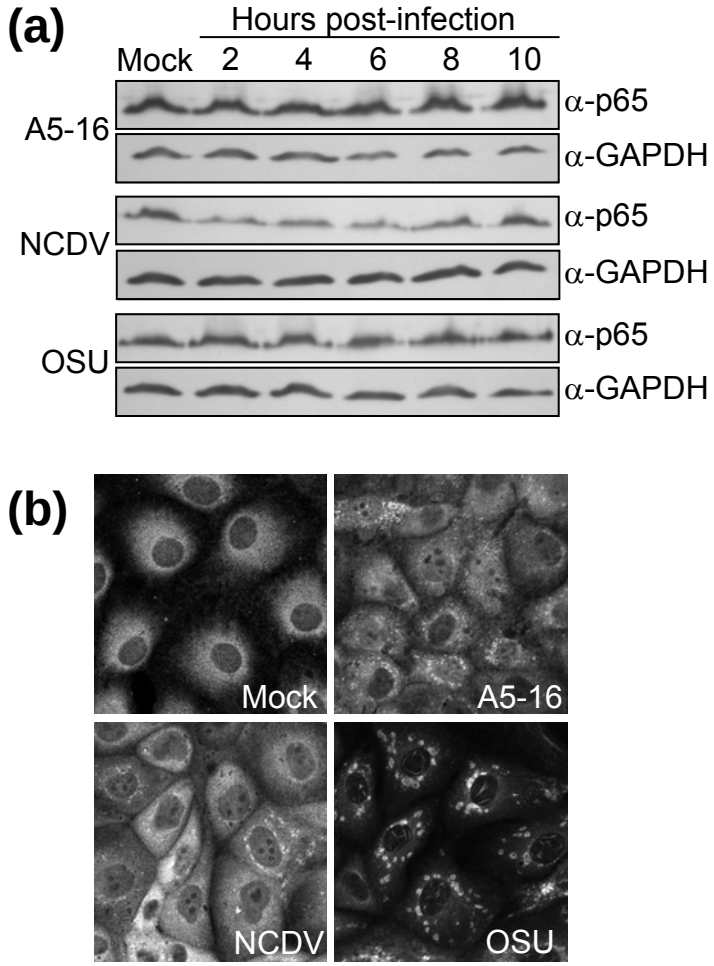

Figure 4.3: The NFκB subunit p65 abundance is stable but cellular localization of p65 is altered in rotavirus infected cells. (a) WCE were collected at 2, 4, 6, 8, and 10 hpi from MA104 cells infected with 3 pfu/cell of the indicated virus strain. The WCE were used in immunoblots to detect the abundance of p65 throughout the course of infection. The blots were probed again to detect GAPDH as a loading control. (b) The cellular localization of total p65 was determined by confocal microscopy (63X, NA 1.40) in MA104 cells infected with 3 pfu/cell of the indicated virus strain at 6 hpi.

The localization of p65 was analyzed by immunofluorescence microscopy in A5-16, NCDV, or OSU infected MA104 cells to determine if a block to nuclear translocation could explain the lack of IFNβ expression (Figure 4.3(b)). Nuclear accumulation of p65 was greatly reduced in OSU infected cells when compared to either A5-16 or NCDV infected cells. Nuclear p65 in A5-16 and NCDV infected cells resembled the pattern of p65 in cells treated with a nuclear export inhibitor (266). However, the pattern of p65 localization within the nucleus of OSU infected cells had a distinct fibrous appearance. Punctate cytoplasmic p65 staining was noted in cells infected with each of the three strains. The foci were the most prominent in OSU infected cells.

Cytoplasmic p65 Interacts with VP6 in Infected Cells

To our knowledge, punctate cytoplasmic p65 staining, as shown here, has not been reported. Also, the differences in appearance of cytoplasmic p65 in the cells infected with the rotavirus strains tested were reminiscent of the appearance of VP6 staining in each of these strains (unpublished observation). We therefore tested whether p65 was associated with VP6.

VP6, p65, and NSP2 triple stained cells analyzed by confocal microscopy indicated co-localization of p65 and VP6 (Figure 4.4(a)). The points of p65-VP6 colocalization were often adjacent to viroplasms, as defined by NSP2 staining. To test whether p65 interacts with VP6, rotavirus proteins were radiolabeled in MA104 cells infected with the three strains and extracts from these cells were used in an immunoprecipitation with anti-p65. Autoradiography indicated that

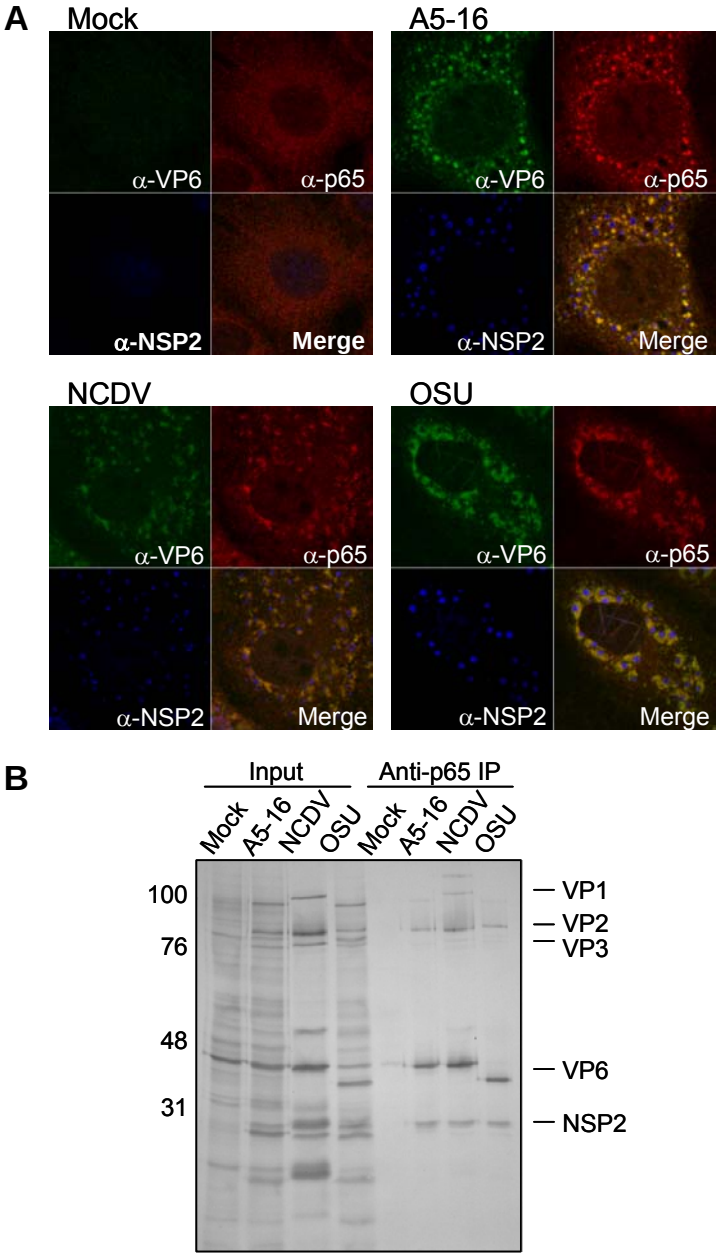

Figure 4.4: The NFκB subunit, p65, interacts with VP6. (a) The cellular localization of p65, VP6, and NSP2 in MA104 cells infected with 3 pfu/cell of the indicated virus strain was determined by confocal microscopy (63X, NA 1.40) at 6 hpi. The zoom function was used to allow for analysis of individual cells. (b) Rotavirus proteins were radiolabeled for 6 hours in MA104 cells infected with 10 pfu/cell of the indicated virus strain. WCE were harvested and 10% of each sample set aside as an input control, while the remaining WCE was divided equally for immunoprecipitation with anti-p65 or normal rabbit serum (data not shown). Input controls and immunoprecipitated samples were separated by SDS-PAGE and autoradiography was used to detect radiolabeled proteins.

several rotavirus proteins, including VP6, specifically co-immunoprecipitated with p65 (Figure 4.4(b)). No rotavirus proteins co-immunoprecipitated with normal rabbit serum (data not shown). These results suggest that the p65 that does not translocate to the nucleus is associated with rotavirus proteins. The biological significance of this observation is unknown. It is also unknown whether the p65-VP6 interaction is direct or indirect.

IκBα is Stable in OSU and NCDV Infected Cells

Phosphorylation of IκBα, subsequent ubiquitination, and proteasome degradation is required for NFκB activation. To determine whether OSU infection affected the activation status of IκBα, cells were infected with each of the three strains, cell lysates were harvested every two hours for ten hours, and IκBα was analyzed by immunoblot (Figure 4(a)). IκBα was completely degraded by eight hpi in A5-16 infected cells. By contrast, IκBα was detected in lysates from NCDV and OSU infected cells through the ten hour time point. Although IκBα was present at each point through the conclusion of the time course, analysis of band intensities by densitometry from three independent experiments indicated that IκBα was present in NCDV and OSU infected lysates at levels approximately 50% of the mock infected controls (data not shown), suggesting some degradation does occur.

IκBα is phosphorylated by the IKK complex on serine residues 32 and 36, resulting in recognition and ubiquitination by the $SCF^{\beta\text{-}TrCP}$ E3 ubiquitin ligase

complex (515). To distinguish between a block of phosphorylation of IκBα and a block of subsequent proteasome degradation in NCDV and OSU infected cells, immunoblots were probed with an antibody that recognizes the phosphorylated

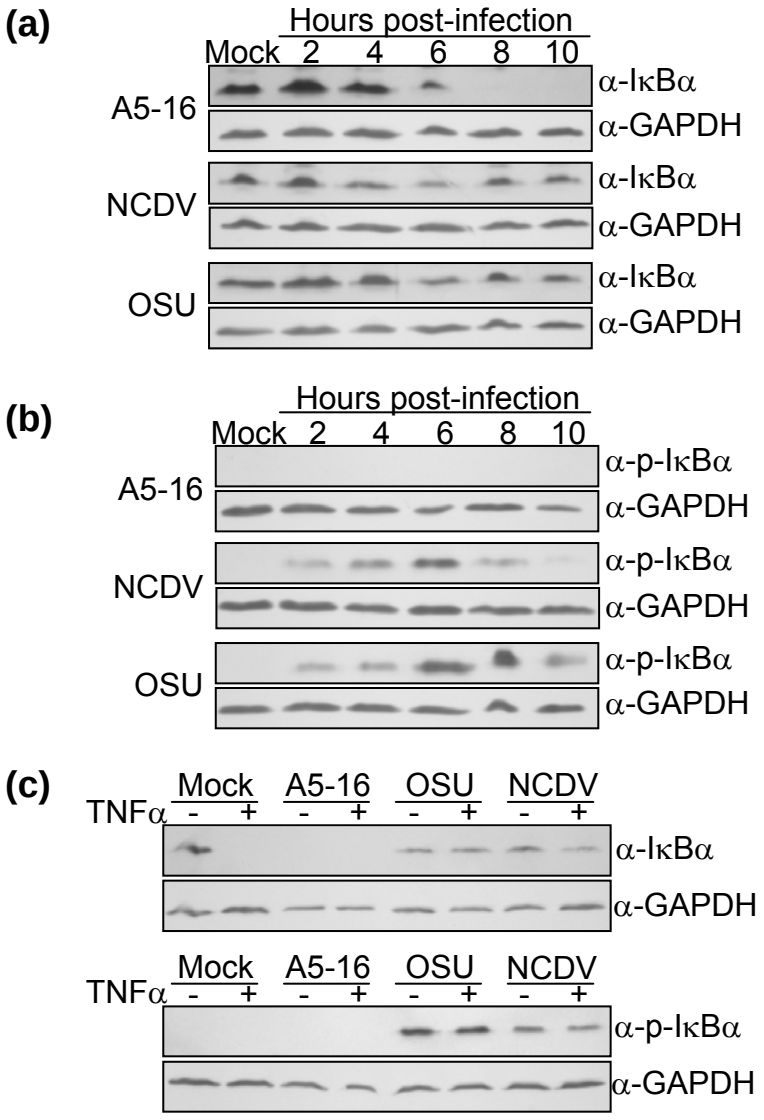

Figure 4.5: Degradation of phosphorylated IκBα was attenuated in wild-type, but not NSP1 null, rotavirus infected cells. The time course WCE samples were used in immunoblots to detect the abundance of (a) IκBα, and (b) phosphorylated IκBα (S32). The blots were reprobed to detect GAPDH as a loading control. (c) After 8 hours of infection with 3 pfu/cell of the indicated virus strain, MA104 cells were treated with TNFα (50 ng/mL) for 15 minutes. WCE were harvested and used in immunoblot analyses of total IκBα and phosphorylated IκBα (S32) and were reprobed to detect GAPDH as a loading control.

form of IκBα (p-IκBα). p-IκBα was not detected at any time during the infection with A5-16 because this form is rapidly degraded (Figure 4(b). Phosphorylated IκBα was detected in both NCDV and OSU infected cells, with accumulations peaking at 6-8 hpi. The presence of p-IκBα indicated that signaling activity of the IKK complex was not disrupted by either of these viruses, and that rapid proteasome-mediated degradation of IκBα is inhibited by both.

Next, we tested whether IκBα degradation could be induced in OSU or NCDV infected cells treated with a potent NFκB agonist. MA104 cells were mock infected or infected for eight hours, and then treated with TNFα for 15 minutes. Cell lysates were probed with anti-IκBα or anti-p-IκBα. The results revealed that upon treatment with TNFα, IκBα was stable in infected cells, but not in TNFα-treated mock infected cells (Figure 4.5(c)). These data show that treatment with a strong inducer of NFκB activation does not overcome the virus infection-associated block in this signaling pathway, and further support the conclusion that IκBα degradation is inhibited in OSU and NCDV infected cells.

β-TrCP is Degraded in OSU and NCDV Infected Cells

The $SCF^{\beta\text{-}TrCP}$ complex targets several cellular proteins with roles in regulating cell proliferation for degradation , including IκBα, the NFκB subunits p100 and p105, cyclin dependent kinases, and β-catenin (447). We reasoned that if $SCF^{\beta\text{-}TrCP}$ was nonfunctional in infected cells, β-catenin, in addition to IκBα,

would accumulate to levels higher than that of mock infected cells. The amount of β-catenin in OSU infected cells was higher than mock infected cells or in cells infected with the NSP1 null rotavirus A5-16 (Figure 4.6), providing additional evidence that the activity of $SCF^{\beta\text{-}TrCP}$ was impaired in OSU infected cells.

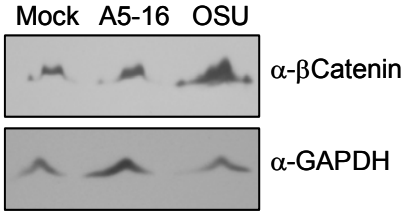

Figure 4.6: β-Catenin is stabilized in OSU infected cells. WCE were collected at 10 hpi from 293 cells infected with 3 pfu/cell of the indicated virus strain. The WCE were used in immunoblots to detect the abundance of β-Catenin. The blots were probed again to detect GAPDH as a loading control.

To test the theory that $SCF^{\beta\text{-}TrCP}$ may not be functional in OSU and NCDV infected cells, 293 cells were transfected with a plasmid encoding a Flag-tagged β-TrCP, and then infected with the three strains as in prior experiments. Immunoblots were probed with anti-Flag antibody to detect β-TrCP, or an NSP1 polyclonal antibody. In A5-16 infected cells, β-TrCP was present in approximately the same amounts as the transfected, but uninfected control cells (Figure 4.7(a)). By contrast, β-TrCP was not detected in either OSU or NCDV infected cells (Figure 4.7(a)). This data led us to suspect that β-TrCP may be targeted to the proteasome in cells infected with NCDV or OSU. To address this question, extracts from 293 cells that were transfected with Flag-tagged β-TrCP and then infected in the presence of the proteasome inhibitor MG132 were used in immunoblots to detect β-TrCP and NSP1. The results show that when

proteasome activity was inhibited, β-TrCP was stable in infected cells (Figure 4.7(b)). Together, these data demonstrate that β-TrCP was targeted for proteasome degradation in NCDV and OSU infections. The fact that β-TrCP was stable in cells infected with A5-16, suggests that NSP1 may play a role in this process.

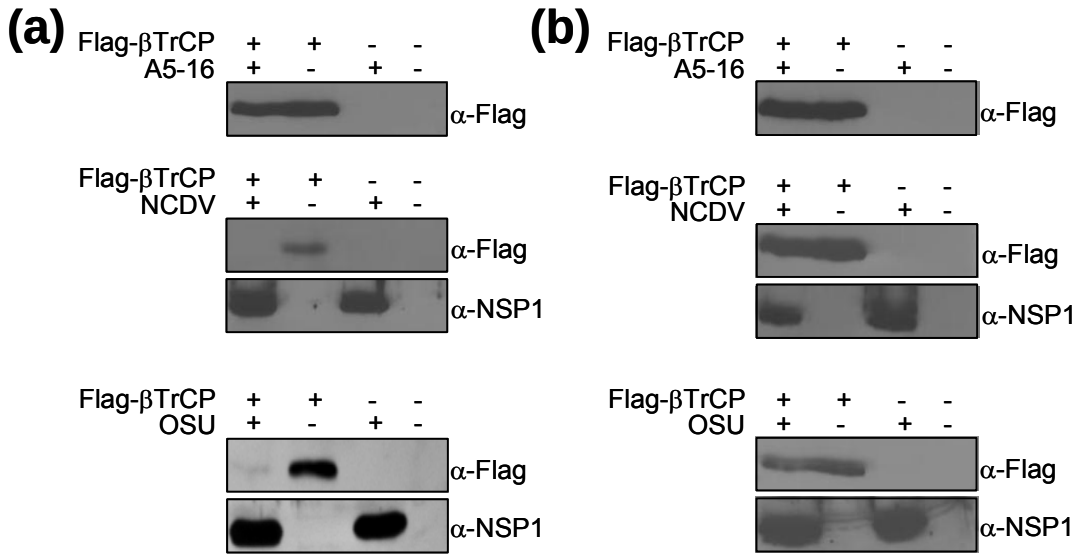

Figure 4.7: Wild-type, but not NPS1 null, rotavirus infections cause proteasome-mediated degradation of β-TrCP. (A) WCE were collected at 8 hpi from 293 cells expressing Flag-tagged β-TrCP infected with 3 pfu/cell of the indicated virus strain. The WCE were used in immunoblots with anti-Flag (all three panels) and anti-NCDV NSP1 (middle panel) or anti-OSU NSP1 (lower panel). Excess WCE from the OSU infected cells were immunoprecipitated with anti-Flag resin. Eluted samples were probed with anti-Flag and anti-OSU NSP1 (lower panel). (B) WCE were collected from 293 cells treated as described in 5A, except the proteasome inhibitor MG132 was added to a concentration of 10 μM at the time of infection. Immunoblots were also performed as described in panel A.

NSP1 Targets βTrCP for Proteasome Degradation in the Absence of Infection

To determine whether NSP1 was responsible for degradation of β-TrCP, 293 cells were co-transfected with plasmids encoding OSU NSP1 or NCDV NSP1 and Flag-tagged β-TrCP. Immunoblots were probed with anti-Flag or anti-NSP1.

The results shown in Figure 4.8 demonstrate that β-TrCP was degraded in cells expressing NSP1, supporting that NSP1 is responsible for proteasome-mediated degradation of β-TrCP.

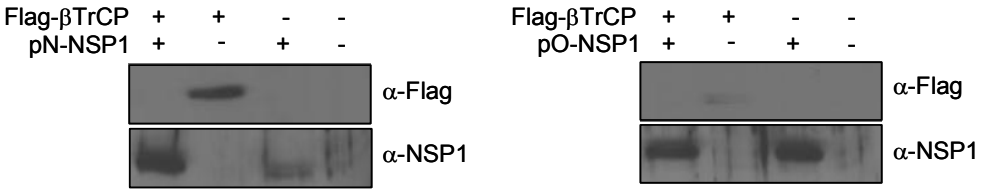

Figure 4.8: Expression of NCDV NSP1 or OSU NSP1 causes degradation of β-TrCP. WCE were collected from 293 cells co-transfected with expression plasmids encoding Flag-tagged β-TrCP and/or the indicated NSP1. WCE were used in immunoblots with anti-Flag (both panels) and anti-NCDV NSP1 (top panel) or anti-OSU NSP1 (lower panel). (pN-NSP1 encodes NCDV NSP1; pO-NSP1 encodes OSU NSP1).

NSP1-directed degradation of IRF3 required an interaction between the two proteins, since NCDV NSP1 can bind to and target the degradation of IRF3 but OSU NSP1 does not bind to or target the degradation of IRF3 (Chapter 3). We tested whether OSU NSP1 interacted with β-TrCP. 293 cells again were co-transfected with plasmids encoding NSP1 and Flag tagged β-TrCP in the presence of MG132, and co-immunoprecipitations were performed with anti-Flag, followed by immunoblot. Both NCDV NSP1 and OSU NSP1 co-immunoprecipitated with β-TrCP (Figure 4.9).

ATF-2 and c-Jun Are Activated in Rotavirus Infected Cells

Since IFNβ induction involves activation of IRF3, NFκB, and AP-1, the signaling leading to ATF2 and c-Jun activation was analyzed in an effort to determine whether NFκB pathway antagonism at the processes of IκBα

degradation and nuclear translocation, were the only points of modulation by OSU leading to a blockade in IFNβ induction. JNK and p38 are kinases known to activate the AP-1 transcription factors, ATF2 and c-Jun, via phosphorylation (275-277). Samples harvested from infection time course experiments, as described in Figure 4.5, were used in immunoblot analysis to determine whether the active, phosphorylated forms of JNK (Figure 4.10(a)) and p38 (Figure

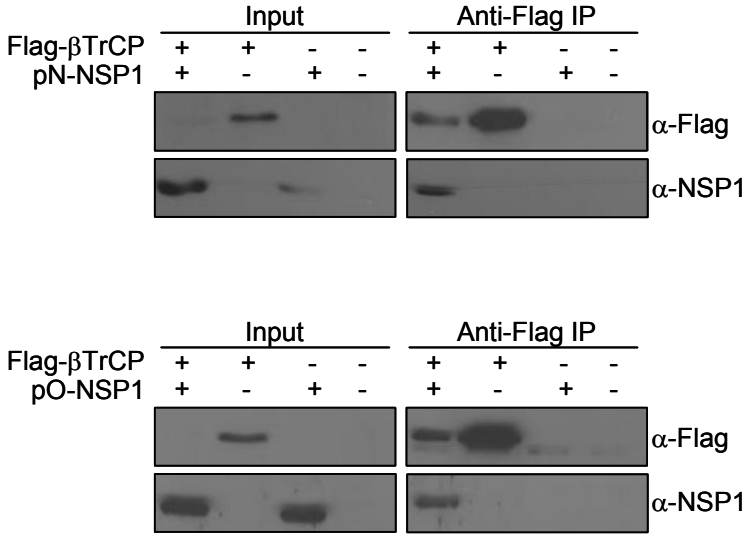

Figure 4.9: NCDV NSP1 and OSU NSP1 interact with β-TrCP. WCE were collected from 293 cells co-transfected as described in Figure 4.8. MG132 was added to 10 μM during the final 8 hours of incubation to allow for Flag-tagged β-TrCP to accumulate. An equal portion of each WCE was set aside as an input control while the remaining WCE was used in immunoprecipitations with anti-Flag resin. The input controls and eluted samples were used in immunoblots with anti-Flag to detect Flag-tagged β-TrCP (both panels) and anti-NCDV NSP1 (top panel) or anti-OSU NSP1 (lower panel).

4.10(b)) were detectable in cells infected with either A5-16, NCDV, or OSU. As was previously reported by Holloway *et al*, these kinases were activated in rotavirus infected cells around 6 hpi (516). Phosphorylated c-Jun was also detected in infections with all three strains (Figure 4.10(c)). The heterodimer of

ATF2 and c-Jun not only cooperate in the induction of IFNβ, these TFs also bind to the c-jun promoter and induce the expression of c-Jun as a positive feedback loop (517). As a readout for transcriptionally active ATF2 and c-Jun, we performed RT-PCR analysis of c-Jun transcript levels and found the expression

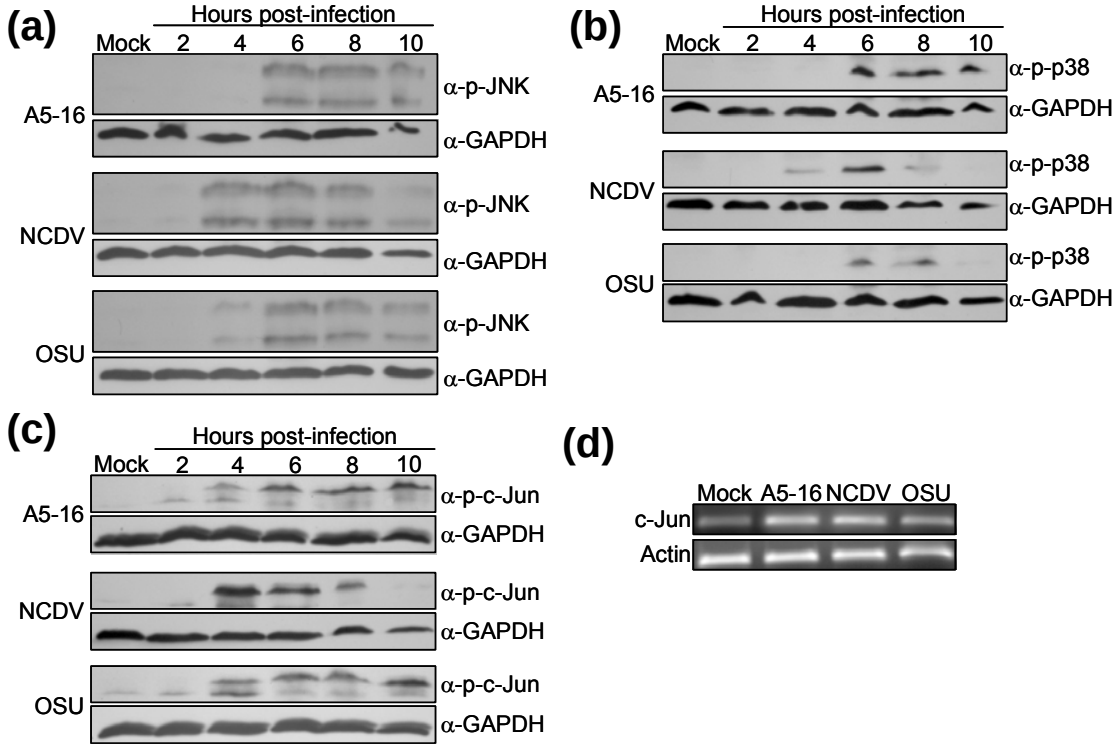

Figure 4.10: MAPK signaling is intact in rotavirus infected cells. The time course WCE samples were used in immunoblots to detect the abundance of (a) phosphorylated JNK (T183/Y185), (b) phosphorylated p38 (T180/Y182), and (c) phosphorylated c-Jun (S63) throughout the infection time course. The blots were reprobed to detect GAPDH as a loading control. (d) RT-PCR analysis of c-Jun using RNA collected at 8 hpi from MA104 cells infected with 3 pfu/cell of the indicated virus strain. RT-PCR of actin was used as a template loading control.

of this gene was higher in all three infected samples relative to the basal level seen in mock infected cells (Figure 4.10(d)). The serum-free conditions used for MA104 infections in this report could favor signaling leading to AP-1 activation, which may account for the higher than expected basal levels of c-Jun expression.

Regardless of the factor(s) leading to AP-1 activation, no antagonism of this pathway was detected in A5-16, NCDV, or OSU infected cells.

Discussion

Targeted degradation of IRF family members by rotavirus NSP1 was first described in cells infected with simian rotavirus strains (490). We found this same mechanism was used by bovine rotavirus strains (Chapter 2). In this report, we characterized a porcine rotavirus strain, OSU, which was unable to target IRF3 for degradation, even though it encodes a full-length NSP1. Thorough analysis of signaling pathways revealed that OSU antagonizes several steps of NFκB signaling rather than antagonizing IRF signaling to block the induction of IFNβ.

Activation of NFκB leading to the induction of genes regulated by this well-studied TF family was originally thought to be primarily dependent on whether or not the IκB family of NFκB inhibitors was degraded in response to various stimuli. However, in addition to the degradation of the IκB proteins, NFκB subunit posttranslational modifications are required for efficient DNA-binding and transactivation activity (515, 518). A critical modification of the p65 subunit is the phosphorylation of serine residue 276 (S276), which is required for high affinity DNA-binding by the p65-p50 heterodimer (267, 268). The ELISA analysis (Figure 4.2(a)) using WCE from OSU infected cells indicated a lack of DNA-binding by NFκB heterodimers containing p50, which by extension implies that

p65 (S276) is not phosphorylated. Furthermore, immunoblot analysis suggested that this residue is poorly phosphorylated in OSU infected cells compared to cells infected with either A5-16 or NCDV (data not shown). The reduced level of p65 nuclear staining in OSU infected cells (Figure 4.3(b)) likely reflects the inability of the p65-p50 to bind DNA and aid in the induction of IFNβ. OSU may do this either by targeting the kinases, MSK1 or PKAc, responsible for this modification or by antagonizing the signaling pathways upstream of these kinases.

While the absence of DNA-binding activity by NFκB was unique to cells infected with OSU, the colocalization of VP6 and p65 was detected in cells infected with each of the three strains. These results indicate that this modulation of NFκB signaling is independent of the expression of NSP1. It remains unknown if rotaviruses sequester p65 as an alternative means of antagonizing NFκB signaling. The p65-VP6 structures are most prominent in OSU infected cells and could indicate accelerated kinetics of viroplasm formation relative to the kinetics in NCDV and A5-16 infected cells. Complete sequestration of p65 by the action of rotavirus proteins, prior to IκBα degradation and/or p65 phosphorylation, is a potential mechanism rotaviruses could use to block NFκB-regulated gene induction.

The final NFκB modulatory activity we detected in OSU infected cells was the targeted degradation of β-TrCP, the F box protein of the SCF E3 uqituitin ligase responsible for recognition and ubiquitination of phosphorylated IκBα. This finding explained the stabilization of IκBα and accumulation of

phosphorylated IκBα in OSU infected cells. Since these observations were also seen in NCDV, but not A5-16, infected cells, we speculated that β-TrCP degradation was dependent on the expression of NSP1. Indeed, expression of NCDV NSP1 or OSU NSP1 alone destabilized β-TrCP. Furthermore, NCDV NSP1 or OSU NSP1 was found to co-immunoprecipitate with β-TrCP when MG132 was used to stabilize β-TrCP. These findings help explain why the expression of NSP1 from both viruses was able to inhibit NFκB reporter gene expression. Since stabilization of phosphorylated IκBα peaks at 6-8 hpi, this mechanism of NFκB signaling blockade may act to limit NFκB signaling in NCDV infected cells and work in synergy with the lack of nuclear NFκB accumulation in OSU infected cells. This model is supported by the luciferase reporter assay which shows OSU NSP1 is more efficient than NCDV NSP1 at inhibiting the expression of NFκB-regulated genes.

The implications of NSP1-targeted degradation of β-TrCP beyond the effect on NFκB signaling are unclear. Additional β-TrCP substrates are known to act in cell cycle regulation or development (447). However, the primary site of rotavirus replication is in mature, non-replicating enterocytes. Perhaps rotavirus infections release the enterocytes from cell-cycle arrest and the resulting proliferative state of a cell is beneficial to rotavirus replication. The type I IFN receptor, as well as pro-apoptotic proteins, are targeted for ubiquitination by $SCF^{\beta TrCP}$ (519-521), but it is difficult to envision a scenario in which stabilization of these substrates would be beneficial to rotavirus replication. Inhibitors of β-

TrCP have been hypothesized to be potential anti-cancer therapies (447), lending credence to investigating the use of NSP1 in gene therapy in cancerous cells that overexpress β-TrCP.

An interesting aspect of this study is that unique mechanisms are used by different rotavirus strains to block the induction of IFNβ. OSU achieves the blockade of IFNβ induction by primarily targeting NFκB signaling, while the modulation of IRF3 is likely nonexistent due to the relatively weak OSU NSP1-IRF3 interaction (Chapter 3). Conversely, NCDV targets IRF3 for degradation (Chapter 2), yet allows for NFκB nuclear accumulation and DNA-binding. Additional experiments are needed to further define the shared and unique properties of NCDV NSP1 and OSU NSP1.

NOTE: The experiment described in Figure 4.5(c) was performed by Dana Kreitel and the experiments described in Figure 4.7, Figure 4.8, and Figure 4.9 were performed by Dr. Khalil Ettayebi.

SUMMARY AND CONCLUSIONS

Since our initial report describing the interaction between IRF3 and bovine NSP1 (459) several reports have defined properties of NSP1 (117, 118, 490, 504, 522, 523), although there are certainly more questions about NSP1 now than there were just a few years ago.

The data collected in Chapter 2 were obtained prior to my graduate school training but were included in this dissertation because these observations laid the groundwork for the subsequent chapters. Using a bovine NSP1 as the bait protein in a yeast-two hybrid interaction trap, it was determined that NSP1 binds the cellular protein IRF3, a key transcription factor involved in the induction of type I IFN. We hypothesized that rotavirus NSP1 may function as an IFN system antagonist. RT-PCR analysis of IFNβ transcripts in samples collected from infected cells proved this hypothesis to be correct which led to a series of experiments to describe the point of IRF3 signaling blocked by rotavirus infection. We quickly learned that IRF3 is degraded in cells infected with wild-type bovine rotavirus strains, but not in a bovine rotavirus strain encoding a null NSP1. Furthermore, the degradation of IRF3 was prevented by treating the cells with a proteasome inhibitor. While most of our efforts were aimed at understanding the bovine NSP1-IRF3 interaction, we also showed that murine NSP1 interacts with IRF3. This hinted that the degradation of IRF3 in rotavirus-infected cells is a property of rotaviruses that is not limited to a few bovine-specific strains.

Based on the major observations that NSP1 interacts with IRF3 and that IRF3 is degraded in a proteasome-mediated manner in cells infected with wild-type rotavirus strains, we then formed the hypothesis that rotavirus NSP1 is an E3 ubiquitin ligase. These enzymes are known to have either HECT domains or RING domains. Although the spacing of the cysteine and histidine residues of the zinc-binding domain found in all NSP1 sequences does not fit the consensus pattern found in a typical RING domain, we sought to determine whether NSP1 is an E3 ubiquitin ligase with an atypical RING domain. Direct evidence to define a protein as a RING E3 enzyme is displayed by detecting the ability of the putative RING E3 to catalyze the formation of polyubiquitin chains in an *in vitro* ubiquitin conjugating assay. Repeated attempts to identify this activity in a GST-NSP1 fusion protein failed (data not shown), so we took a different approach. Chapter 3 describes an alternative method to test whether NSP1 has RING E3 properties. Mutation of RING domain cysteine and histidines has been shown to abolish the ability of these enzymes to target their substrates and themselves for ubiquitination (381, 386-389). Therefore we carried out a mutational analysis study to determine if mutations to the zinc-binding residues of NSP1 had similar effects on the stability of IRF3 and NSP1. A major advance that allowed us to perform these experiments was the development of a bicistronic expression construct that drives NSP1 translation from an internal ribosomal entry site. All previous attempts to express NSP1 in transfected mammalian cells did not lead to detectable levels of NSP1 expression. The C54A and H79L mutations within

the zinc-binding domain of NSP1 resulted in stabilization of both IRF3 and NSP1. Unfortunately, data showing that IRF3 is stabilized by these mutations is inconclusive because these mutations weakened the strength of the NSP1-IRF3 interaction. The stabilization of NSP1 upon mutation of the zinc-binding domain is consistent with the hypothesis that NSP1 contains an atypical RING domain.

Another important observation from Chapter 3 came from an experiment characterizing OSU NSP1. The porcine strain OSU was intriguing since it encodes a full-length NSP1 with an intact zinc-binding domain, yet IRF3 was stable in cells expressing OSU NSP1. Using OSU NSP1 in a GST pull-down assay side-by-side with a bovine NSP1 showed that the OSU NSP1-IRF3 interaction was comparatively weak. Initial experiments in Chapter 4 demonstrated that even though IRF3 signaling was intact, IFNβ induction was blocked. Subsequent analysis of ATF2 and c-Jun activation indicated that this pathway was also intact in OSU infected cells. These observations indicate that OSU modulates NFκB signaling to block IFNβ induction. Indeed, the steps of i) IκBα degradation, ii) NFκB nuclear accumulation, and iii) NFκB DNA binding were shown to be antagonized in OSU infected cells. The block in NFκB signaling in OSU infected cells is partially or completely dependent on the OSU encoded NSP1, as shown by the potent inhibition of expression in NFκB-regulated genes in cells expressing OSU NSP1 in the absence of infection.

Chapter 4 also describes an exciting discovery whereby NCDV NSP1 and OSU NSP1 are each capable of interacting with and targeting the degradation of

βTrCP, an F box subunit of the SCF E3 ubiquitin ligase complex. Preliminary sequence comparisons between βTrCP and IRF3 indicate that these proteins share little sequence similarity. However, mapping the NSP1 interacting domain of βTrCP and further mapping the NSP1 interacting domain of IRF3 could reveal a shared motif that could be insightful for identifying additional NSP1 substrates.

Some basic properties of rotavirus NSP1 were known prior to the studies described here, but the function was unknown. We have defined rotavirus NSP1 as an IFN system antagonist. These studies revealed unique mechanisms of IFN antagonism are mediated by NSP1 proteins encoded by different strains of rotavirus. Importantly, we found that the basis for the two mechanisms of IFN system antagonism is NSP1-dependent targeting of proteins essential to IFNβ induction for proteasome-mediated degradation.

FUTURE DIRECTIONS

Three Important Questions

The results described in the previous chapters have opened the door for many interesting avenues of rotavirus research. The following three questions represent valuable areas that now need to be addressed.

Is NSP1 an E3 Ubiquitin Ligase or Does It Reprogram a Cellular E3 Enzyme?

It is possible that NSP1 acts either as a single-subunit RING E3 or as a regulator of a cellular E3. The mutational analysis of the cysteine-rich region of NSP1 described in Chapter 3 is consistent with NSP1 being a single-subunit E3 ligase with an atypical RING domain. However, the cysteine-rich region within V proteins of paramyxoviruses does not result in the V proteins acting as RING E3 enzymes. Rather than being single-subunit E3 enzymes, the V proteins reprogram a cellular multi-subunit E3 (450). So it is possible that NSP1 could do the same. Furthermore, if NSP1 acts as an atypical single-subunit RING E3, the findings would advance our understanding of cysteine-rich regions that are capable of ubiquitin ligase activity.

What Is the Mechanism of NSP1-Mediated IFN Resistance?

Viruses have been shown to antagonize the IFN system in many ways. The research efforts described here have focused on antagonism of signaling pathways leading to IFNβ induction. We obtained data suggesting that OSU and

NCDV are moderately resistant to the action of type I IFN, relative to A5-16. The discrepancy in type I IFN resistance between strains increased in cells pretreated with even higher levels of type I IFN. We hypothesized that NSP1 expression is directly correlated with resistance to type I IFN.

The resistance to IFN pretreatment suggests that NSP1 counteracts the activity of one or more of the IFN-induced antiviral proteins. Hundreds of genes are upregulated in response to IFN pretreatment, yet relatively few of these encode proteins with known antiviral activity. It would be important to determine the antiviral gene or genes that have antagonistic activity toward rotavirus replication and how NSP1 provides this activity.

Could the Characterization of NSP1 Lead to Rational Vaccine Development?

The characterization of NSP1 to this point has been confined to tissue culture settings. It would be of interest to determine whether the NSP1 encoded by a given rotavirus affects the replication of that virus in an animal model. This is especially relevant for rotaviruses since rotavirus vaccine candidates are often attenuated strains of rotavirus (77). An attenuated rotavirus vaccine is currently being used in humans, which contains a genome with segments from both human and bovine rotavirus strains (524). However, the genetic basis for the observed attenuation is not well defined (77). A common property of rotaviruses is host range restriction, the ability to replicate efficiently in the species from which the strain was originally isolated, but inoculation into another species

results in attenuated replication (70, 525, 526). Since the NSP1 of porcine and bovine rotavirus strains had different properties in human (293) cells, it is conceivable that human rotavirus vaccines would be attenuated to different degrees based on the NSP1 encoded by the vaccine strain. Thus, the type of immune response would likely be different between vaccine candidates encoding the IRF3-targeting bovine NSP1, the NFκB-targeting porcine NSP1, or an A5-16-like null NSP1.

REFERENCE LIST

1. Murphy, F. A. (1996) in *Fundamental Virology*, eds. Fields, B. N., Knipe, D. M., & Howley, P. M. (Lippincott, Williams, & Wilkins, Philadelphia, PA), pp. 15-57.

2. Ramig, R. F. (2004) *J Virol* 78, 10213-10220.

3. Estes, M. K. (1996) in *Fundamental Virology*, eds. Fields, B. N., Knipe, D. M., & Howley, P. M. (Lippincott Williams & Wilkins, Philiadelphia), pp. 731-761.

4. Prasad, B. V., Wang, G. J., Clerx, J. P., & Chiu, W. (1988) *J Mol. Biol.* 199, 269-275.

5. Imai, M., Akatani, K., Ikegami, N., & Furuichi, Y. (1983) *J Virol* 47, 125-136.

6. McCrae, M. A. & McCorquodale, J. G. (1983) *Virology* 126, 204-212.

7. Poncet, D., Laurent, S., & Cohen, J. (1994) *EMBO J* 13, 4165-4173.

8. Broome, R. L., Vo, P. T., Ward, R. L., Clark, H. F., & Greenberg, H. B. (1993) *J. Virol.* 67, 2448-2455.

9. Greenberg, H. B., Flores, J., Kalica, A. R., Wyatt, R. G., & Jones, R. (1983) *J. Gen. Virol.* 64 (Pt 2), 313-320.

10. Hoshino, Y., Sereno, M. M., Midthun, K., Flores, J., Kapikian, A. Z., & Chanock, R. M. (1985) *Proc. Natl. Acad. Sci. U. S. A* 82, 8701-8704.

11. Hoshino, Y., Saif, L. J., Kang, S. Y., Sereno, M. M., Chen, W. K., & Kapikian, A. Z. (1995) *Virology* 209, 274-280.

12. Kalica, A. R., Sereno, M. M., Wyatt, R. G., Mebus, C. A., Chanock, R. M., & Kapikian, A. Z. (1978) *Virology* 87, 247-255.

13. Liu, M., Offit, P. A., & Estes, M. K. (1988) *Virology* 163, 26-32.

14. Offit, P. A., Blavat, G., Greenberg, H. B., & Clark, H. F. (1986) *J. Virol.* 57, 46-49.

15. Offit, P. A., Clark, H. F., Blavat, G., & Greenberg, H. B. (1986) *J. Virol.* 60, 491-496.

16. Ramig, R. F. & Galle, K. L. (1990) *J. Virol.* 64, 1044-1049.

17. Zheng, S. L., Woode, G. N., Melendy, D. R., & Ramig, R. F. (1989) *J. Clin. Microbiol.* 27, 1939-1945.

18. Arias, C. F., Dector, M. A., Segovia, L., Lopez, T., Camacho, M., Isa, P., Espinosa, R., & Lopez, S. (2004) *Virus Res.* 102, 43-51.

19. Campagna, M., Eichwald, C., Vascotto, F., & Burrone, O. R. (2005) *J Gen Virol* 86, 1481-1487.

20. Cuadras, M. A., Bordier, B. B., Zambrano, J. L., Ludert, J. E., & Greenberg, H. B. (2006) *J. Virol.* 80, 3935-3946.

21. Lopez, T., Rojas, M., yala-Breton, C., Lopez, S., & Arias, C. F. (2005) *J Gen Virol* 86, 1609-1617.

22. Lopez, T., Camacho, M., Zayas, M., Najera, R., Sanchez, R., Arias, C. F., & Lopez, S. (2005) *J. Virol.* 79, 184-192.

23. Montero, H., Arias, C. F., & Lopez, S. (2006) *J Virol* 80, 9031-9038.

24. Montero, H., Rojas, M., Arias, C. F., & Lopez, S. (2008) *J Virol* 82, 1496-1504.

25. Rainsford, E. W. & McCrae, M. A. (2007) *Virus Res.* 130, 193-201.

26. Silvestri, L. S., Taraporewala, Z. F., & Patton, J. T. (2004) *J Virol* 78, 7763-7774.

27. Silvestri, L. S., Tortorici, M. A., Vasquez-Del, C. R., & Patton, J. T. (2005) *J Virol* 79, 15165-15174.

28. Shaw, A. L., Rothnagel, R., Chen, D., Ramig, R. F., Chiu, W., & Prasad, B. V. (1993) *Cell* 74, 693-701.

29. Yeager, M., Berriman, J. A., Baker, T. S., & Bellamy, A. R. (1994) *EMBO J* 13, 1011-1018.

30. Lawton, J. A., Zeng, C. Q., Mukherjee, S. K., Cohen, J., Estes, M. K., & Prasad, B. V. (1997) *J Virol* 71, 7353-7360.

31. Flewitt, T. H., Bryden, A. S., Davies, H., Woode, G. N., Bridger, J. C., & Derrick, J. M. (1974) *Lancet* 2, 61-63.

32. Yolken, R., rango-Jaramillo, S., Eiden, J., & Vonderfecht, S. (1988) *J Infect. Dis.* 158, 1120-1123.

33. Saif, L. J., Terrett, L. A., Miller, K. L., & Cross, R. F. (1988) *J Clin. Microbiol.* 26, 1277-1282.

34. Welter, M. W., Welter, C. J., Chambers, D. M., & Svensson, L. (1991) *Arch. Virol* 120, 297-304.

35. Graham, D. Y. & Estes, M. K. (1985) *Ann Inst Pasteur* 136, 5-12.

36. Hoshino, Y., Wyatt, R. G., Greenberg, H. B., Flores, J., & Kapikian, A. Z. (1984) *J Infect. Dis.* 149, 694-702.

37. Rodger, S. M. & Holmes, I. H. (1979) *J Virol* 30, 839-846.

38. Matthijnssens, J., Ciarlet, M., Heiman, E., Arijs, I., Delbeke, T., McDonald, S. M., Palombo, E. A., Iturriza-Gomara, M., Maes, P., Patton, J. T. *et al.* (2008) *J Virol*.

39. Del Castillo, Jr., Ludert, J. E., Sanchez, A., Ruiz, M. C., Michelangeli, F., & Liprandi, F. (1991) *J. Gen. Virol.* 72 (Pt 3), 541-547.

40. Michelangeli, F., Ruiz, M. C., Del Castillo, Jr., Ludert, J. E., & Liprandi, F. (1991) *Virology* 181, 520-527.

41. Brunet, J. P., Jourdan, N., Cotte-Laffitte, J., Linxe, C., Geniteau-Legendre, M., Servin, A., & Quero, A. M. (2000) *J. Virol.* 74, 10801-10806.

42. Brunet, J. P., Cotte-Laffitte, J., Linxe, C., Quero, A. M., Geniteau-Legendre, M., & Servin, A. (2000) *J. Virol.* 74, 2323-2332.

43. Graham, D. Y. & Estes, M. K. (1988) in *Gastroenterology*, ed. Gitnick, G. (Medical Examination Publishing Company, New Hyde Park, N.Y.), pp. 566-578.

44. Boshuizen, J. A., Reimerink, J. H., Korteland-van Male, A. M., van, H., V, Koopmans, M. P., Buller, H. A., Dekker, J., & Einerhand, A. W. (2003) *J Virol* 77, 13005-13016.

45. Ciarlet, M., Gilger, M. A., Barone, C., McArthur, M., Estes, M. K., & Conner, M. E. (1998) *Virology* 251, 343-360.

46. Shaw, D. P., Morehouse, L. G., & Solorzano, R. F. (1989) *Am. J. Vet. Res.* 50, 1961-1965.

47. Varshney, K. C., Bridger, J. C., Parsons, K. R., Cook, R., Teucher, J., & Hall, G. A. (1995) *Vet. Pathol.* 32, 619-627.

48. Yason, C. V., Summers, B. A., & Schat, K. A. (1987) *Am. J. Vet. Res.* 48, 927-938.

49. Ball, J. M., Tian, P., Zeng, C. Q., Morris, A. P., & Estes, M. K. (1996) *Science* 272, 101-104.

50. Lundgren, O., Peregrin, A. T., Persson, K., Kordasti, S., Uhnoo, I., & Svensson, L. (2000) *Science* 287, 491-495.

51. Lundgren, O. & Svensson, L. (2001) *Microbes. Infect.* 3, 1145-1156.

52. Osborne, M. P., Haddon, S. J., Spencer, A. J., Collins, J., Starkey, W. G., Wallis, T. S., Clarke, G. J., Worton, K. J., Candy, D. C., & Stephen, J. (1988) *J Pediatr. Gastroenterol. Nutr.* 7, 236-248.

53. Zhang, M., Zeng, C. Q., Morris, A. P., & Estes, M. K. (2000) *J Virol* 74, 11663-11670.

54. Tian, P., Hu, Y., Schilling, W. P., Lindsay, D. A., Eiden, J., & Estes, M. K. (1994) *J. Virol.* 68, 251-257.

55. Halaihel, N., Lievin, V., Ball, J. M., Estes, M. K., Alvarado, F., & Vasseur, M. (2000) *J. Virol.* 74, 9464-9470.

56. Shaw, R. D., Hempson, S. J., & Mackow, E. R. (1995) *J. Virol.* 69, 5946-5950.

57. Kraft, L. M. (1958) *Yale J. Biol. Med.* 31, 121-137.

58. Mossel, E. C. & Ramig, R. F. (2002) *J Virol* 76, 6502-6509.

59. Mossel, E. C. & Ramig, R. F. (2003) *J Virol* 77, 12352-12356.

60. Blutt, S. E., Kirkwood, C. D., Parreno, V., Warfield, K. L., Ciarlet, M., Estes, M. K., Bok, K., Bishop, R. F., & Conner, M. E. (2003) *Lancet* 362, 1445-1449.

61. Blutt, S. E., Matson, D. O., Crawford, S. E., Staat, M. A., Azimi, P., Bennett, B. L., Piedra, P. A., & Conner, M. E. (2007) *PLoS. Med.* 4, e121.

62. Parashar, U. D., Hummelman, E. G., Bresee, J. S., Miller, M. A., & Glass, R. I. (2003) *Emerg. Infect. Dis.* 9, 565-572.

63. Parashar, U. D., Gibson, C. J., Bresse, J. S., & Glass, R. I. (2006) *Emerg. Infect. Dis.* 12, 304-306.

64. McNulty, M. S., Allan, G. M., Pearson, G. R., McFerran, J. B., Curran, W. L., & McCracken, R. M. (1976) *Infect. Immun.* 14, 1332-1338.

65. Saif, L. J., Bohl, E. H., Kohler, E. M., & Hughes, J. H. (1977) *Am. J Vet. Res.* 38, 13-20.

66. Woode, G. N., Bridger, J. C., Hall, G., & Dennis, M. J. (1974) *Res. Vet. Sci.* 16, 102-105.

67. Woode, G. N., Bridger, J., Hall, G. A., Jones, J. M., & Jackson, G. (1976) *J Med. Microbiol.* 9, 203-209.

68. Burns, J. W., Krishnaney, A. A., Vo, P. T., Rouse, R. V., Anderson, L. J., & Greenberg, H. B. (1995) *Virology* 207, 143-153.

69. Ciarlet, M., Estes, M. K., Barone, C., Ramig, R. F., & Conner, M. E. (1998) *J. Virol.* 72, 2341-2351.

70. Conner, M. E., Estes, M. K., & Graham, D. Y. (1988) *J. Virol.* 62, 1625-1633.

71. Conner, M. E., Gilger, M. A., Estes, M. K., & Graham, D. Y. (1991) *J. Virol.* 65, 2562-2571.

72. Feng, N., Burns, J. W., Bracy, L., & Greenberg, H. B. (1994) *J. Virol.* 68, 7766-7773.

73. Franco, M. A., Feng, N., & Greenberg, H. B. (1996) *J. Infect. Dis.* 174 Suppl 1, S47-S50.

74. Greenberg, H. B., Vo, P. T., & Jones, R. (1986) *J. Virol.* 57, 585-590.

75. McNeal, M. M., Broome, R. L., & Ward, R. L. (1994) *Virology* 204, 642-650.

76. Offit, P. A., Clark, H. F., Kornstein, M. J., & Plotkin, S. A. (1984) *J. Virol.* 51, 233-236.

77. Angel, J., Franco, M. A., & Greenberg, H. B. (2007) *Nat. Rev. Microbiol.* 5, 529-539.

78. Santos, N. & Hoshino, Y. (2005) *Rev. Med. Virol* 15, 29-56.

79. Lopez, S. & Arias, C. F. (2004) *Trends Microbiol.* 12, 271-278.

80. Espejo, R. T., Lopez, S., & Arias, C. (1981) *J Virol* 37, 156-160.

81. Estes, M. K., Graham, D. Y., & Mason, B. B. (1981) *J Virol* 39, 879-888.

82. Fiore, L., Greenberg, H. B., & Mackow, E. R. (1991) *Virology* 181, 553-563.

83. Fuentes-Panana, E. M., Lopez, S., Gorziglia, M., & Arias, C. F. (1995) *J Virol* 69, 2629-2632.

84. Ciarlet, M. & Estes, M. K. (1999) *J Gen Virol* 80 (Pt 4), 943-948.

85. Delorme, C., Brussow, H., Sidoti, J., Roche, N., Karlsson, K. A., Neeser, J. R., & Teneberg, S. (2001) *J Virol* 75, 2276-2287.

86. Coulson, B. S., Londrigan, S. L., & Lee, D. J. (1997) *Proc. Natl. Acad. Sci. U. S. A* 94, 5389-5394.

87. Hewish, M. J., Takada, Y., & Coulson, B. S. (2000) *J Virol* 74, 228-236.

88. Graham, K. L., Halasz, P., Tan, Y., Hewish, M. J., Takada, Y., Mackow, E. R., Robinson, M. K., & Coulson, B. S. (2003) *J Virol* 77, 9969-9978.

89. Guerrero, C. A., Mendez, E., Zarate, S., Isa, P., Lopez, S., & Arias, C. F. (2000) *Proc. Natl. Acad. Sci. U. S. A* 97, 14644-14649.

90. Guerrero, C. A., Bouyssounade, D., Zarate, S., Isa, P., Lopez, T., Espinosa, R., Romero, P., Mendez, E., Lopez, S., & Arias, C. F. (2002) *J Virol* 76, 4096-4102.

91. Jolly, C. L., Huang, J. A., & Holmes, I. H. (2001) *J Virol Methods* 98, 41-51.

92. Zarate, S., Cuadras, M. A., Espinosa, R., Romero, P., Juarez, K. O., Camacho-Nuez, M., Arias, C. F., & Lopez, S. (2003) *J Virol* 77, 7254-7260.

93. Zarate, S., Espinosa, R., Romero, P., Guerrero, C. A., Arias, C. F., & Lopez, S. (2000) *Virology* 278, 50-54.

94. Denisova, E., Dowling, W., LaMonica, R., Shaw, R., Scarlata, S., Ruggeri, F., & Mackow, E. R. (1999) *J Virol* 73, 3147-3153.

95. Dowling, W., Denisova, E., LaMonica, R., & Mackow, E. R. (2000) *J Virol* 74, 6368-6376.

96. Charpilienne, A., Abad, M. J., Michelangeli, F., Alvarado, F., Vasseur, M., Cohen, J., & Ruiz, M. C. (1997) *J Gen Virol* 78 (Pt 6), 1367-1371.

97. Chemello, M. E., Aristimuno, O. C., Michelangeli, F., & Ruiz, M. C. (2002) *J Virol* 76, 13083-13087.

98. Isa, P., Realpe, M., Romero, P., Lopez, S., & Arias, C. F. (2004) *Virology* 322, 370-381.

99. Guerrero, C. A., Zarate, S., Corkidi, G., Lopez, S., & Arias, C. F. (2000) *J Virol* 74, 9362-9371.

100. Lawton, J. A., Estes, M. K., & Prasad, B. V. (1997) *Nat. Struct. Biol.* 4, 118-121.

101. Dormitzer, P. R. & Greenberg, H. B. (1992) *Virology* 189, 828-832.

102. Dormitzer, P. R., Ho, D. Y., Mackow, E. R., Mocarski, E. S., & Greenberg, H. B. (1992) *Virology* 187, 18-32.

103. Clapham, D. E. (2007) *Cell* 131, 1047-1058.

104. Cohen, J., Laporte, J., Charpilienne, A., & Scherrer, R. (1979) *Arch. Virol* 60, 177-186.

105. Valenzuela, S., Pizarro, J., Sandino, A. M., Vasquez, M., Fernandez, J., Hernandez, O., Patton, J., & Spencer, E. (1991) *J Virol* 65, 3964-3967.

106. Chen, D., Luongo, C. L., Nibert, M. L., & Patton, J. T. (1999) *Virology* 265, 120-130.

107. Liu, M., Mattion, N. M., & Estes, M. K. (1992) *Virology* 188, 77-84.

108. Prasad, B. V., Rothnagel, R., Zeng, C. Q., Jakana, J., Lawton, J. A., Chiu, W., & Estes, M. K. (1996) *Nature* 382, 471-473.

109. Jayaram, H., Estes, M. K., & Prasad, B. V. (2004) *Virus Res.* 101, 67-81.

110. Imataka, H., Gradi, A., & Sonenberg, N. (1998) *EMBO J* 17, 7480-7489.

111. Preiss, T. & Hentze, M. W. (1998) *Nature* 392, 516-520.

112. Tarun, S. Z., Jr. & Sachs, A. B. (1995) *Genes Dev.* 9, 2997-3007.

113. Piron, M., Vende, P., Cohen, J., & Poncet, D. (1998) *EMBO J* 17, 5811-5821.

114. Vende, P., Piron, M., Castagne, N., & Poncet, D. (2000) *J Virol* 74, 7064-7071.

115. Johnson, M. A. & McCrae, M. A. (1989) *J Virol* 63, 2048-2055.

116. Mitzel, D. N., Weisend, C. M., White, M. W., & Hardy, M. E. (2003) *J Gen Virol* 84, 383-391.

117. Graff, J. W., Ewen, J., Ettayebi, K., & Hardy, M. E. (2007) *J Gen Virol* 88, 613-620.

118. Pina-Vazquez, C., De Nova-Ocampo, M., Guzman-Leon, S., & Padilla-Noriega, L. (2007) *Arch. Virol* 152, 345-368.

119. Broquet, A. H., Lenoir, C., Gardet, A., Sapin, C., Chwetzoff, S., Jouniaux, A. M., Lopez, S., Trugnan, G., Bachelet, M., & Thomas, G. (2007) *J Virol* 81, 1297-1304.

120. Altenburg, B. C., Graham, D. Y., & Estes, M. K. (1980) *J Gen Virol* 46, 75-85.

121. Esparza, J., Gorziglia, M., Gil, F., & Romer, H. (1980) *J Gen Virol* 47, 461-472.

122. Petrie, B. L., Greenberg, H. B., Graham, D. Y., & Estes, M. K. (1984) *Virus Res.* 1, 133-152.

123. Eichwald, C., Rodriguez, J. F., & Burrone, O. R. (2004) *J Gen Virol* 85, 625-634.

124. Fabbretti, E., Afrikanova, I., Vascotto, F., & Burrone, O. R. (1999) *J Gen Virol* 80 (Pt 2), 333-339.

125. Berkova, Z., Crawford, S. E., Trugnan, G., Yoshimori, T., Morris, A. P., & Estes, M. K. (2006) *J Virol* 80, 6061-6071.

126. Wileman, T. (2006) *Science* 312, 875-878.

127. Taraporewala, Z. F. & Patton, J. T. (2004) *Virus Res.* 101, 57-66.

128. Patton, J. T. (1986) *Virus Res.* 6, 217-233.

129. Patton, J. T. & Gallegos, C. O. (1990) *J Gen Virol* 71 (Pt 5), 1087-1094.

130. Patton, J. T., Jones, M. T., Kalbach, A. N., He, Y. W., & Xiaobo, J. (1997) *J Virol* 71, 9618-9626.

131. Chen, D., Zeng, C. Q., Wentz, M. J., Gorziglia, M., Estes, M. K., & Ramig, R. F. (1994) *J Virol* 68, 7030-7039.

132. Zeng, C. Q., Wentz, M. J., Cohen, J., Estes, M. K., & Ramig, R. F. (1996) *J Virol* 70, 2736-2742.

133. Gonzalez, R. A., Torres-Vega, M. A., Lopez, S., & Arias, C. F. (1998) *Arch. Virol* 143, 981-996.

134. Mattion, N. M., Mitchell, D. B., Both, G. W., & Estes, M. K. (1991) *Virology* 181, 295-304.

135. Torres-Vega, M. A., Gonzalez, R. A., Duarte, M., Poncet, D., Lopez, S., & Arias, C. F. (2000) *J Gen Virol* 81, 821-830.

136. Bergmann, C. C., Maass, D., Poruchynsky, M. S., Atkinson, P. H., & Bellamy, A. R. (1989) *EMBO J* 8, 1695-1703.

137. Chan, W. K., Au, K. S., & Estes, M. K. (1988) *Virology* 164, 435-442.

138. Gonzalez, R. A., Espinosa, R., Romero, P., Lopez, S., & Arias, C. F. (2000) *Arch. Virol* 145, 1963-1973.

139. Maass, D. R. & Atkinson, P. H. (1994) *J Virol* 68, 366-378.

140. Au, K. S., Chan, W. K., Burns, J. W., & Estes, M. K. (1989) *J Virol* 63, 4553-4562.

141. Taylor, J. A., O'Brien, J. A., & Yeager, M. (1996) *EMBO J* 15, 4469-4476.

142. Estes, M. K., Palmer, E. L., & Obijeski, J. F. (1983) *Curr. Top. Microbiol. Immunol.* 105, 123-184.

143. Maass, D. R. & Atkinson, P. H. (1990) *J Virol* 64, 2632-2641.

144. Dector, M. A., Romero, P., Lopez, S., & Arias, C. F. (2002) *EMBO Rep.* 3, 1175-1180.

145. Poruchynsky, M. S., Maass, D. R., & Atkinson, P. H. (1991) *J Cell Biol.* 114, 651-656.

146. Tian, P., Ball, J. M., Zeng, C. Q., & Estes, M. K. (1996) *J Virol* 70, 6973-6981.

147. Cuadras, M. A. & Greenberg, H. B. (2003) *Virology* 313, 308-321.

148. Delmas, O., Breton, M., Sapin, C., Le, B. A., Colard, O., & Trugnan, G. (2007) *J Virol* 81, 1610-1618.

149. Jourdan, N., Maurice, M., Delautier, D., Quero, A. M., Servin, A. L., & Trugnan, G. (1997) *J Virol* 71, 8268-8278.

150. Nickel, W. (2003) *Eur. J Biochem.* 270, 2109-2119.

151. Sapin, C., Colard, O., Delmas, O., Tessier, C., Breton, M., Enouf, V., Chwetzoff, S., Ouanich, J., Cohen, J., Wolf, C. *et al.* (2002) *J Virol* 76, 4591-4602.

152. Dunn, S. J., Cross, T. L., & Greenberg, H. B. (1994) *Virology* 203, 178-183.

153. Hua, J., Mansell, E. A., & Patton, J. T. (1993) *Virology* 196, 372-378.

154. Bremont, M., Chabanne-Vautherot, D., & Cohen, J. (1993) *Arch. Virol.* 130, 85-92.

155. Mitchell, D. B. & Both, G. W. (1990) *Virology* 174, 618-621.

156. Eiden, J. J. (1994) *Virology* 199, 212-218.

157. Berg, J. M. (1990) *J. Biol. Chem.* 265, 6513-6516.

158. Freemont, P. S., Hanson, I. M., & Trowsdale, J. (1991) *Cell* 64, 483-484.

159. Brottier, P., Nandi, P., Bremont, M., & Cohen, J. (1992) *J. Gen. Virol.* 73 (Pt 8), 1931-1938.

160. Hua, J., Chen, X., & Patton, J. T. (1994) *J. Virol.* 68, 3990-4000.

161. Taniguchi, K., Kojima, K., Kobayashi, N., Urasawa, T., & Urasawa, S. (1996) *Arch. Virol. Suppl* 12, 53-58.

162. Hundley, F., Biryahwaho, B., Gow, M., & Desselberger, U. (1985) *Virology* 143, 88-103.

163. Hua, J. & Patton, J. T. (1994) *Virology* 198, 567-576.

164. Taniguchi, K., Kojima, K., & Urasawa, S. (1996) *J Virol* 70, 4125-4130.

165. Isaacs, A. & Lindenmann, J. (1957) *Proc. R. Soc. Lond B Biol. Sci.* 147, 258-267.

166. Pestka, S., Krause, C. D., & Walter, M. R. (2004) *Immunol Rev.* 202, 8-32.

167. Farrar, M. A. & Schreiber, R. D. (1993) *Annu. Rev. Immunol* 11, 571-611.

168. Ank, N., West, H., & Paludan, S. R. (2006) *J Interferon Cytokine Res.* 26, 373-379.

169. Marie, I., Durbin, J. E., & Levy, D. E. (1998) *EMBO J.* 17, 6660-6669.

170. Sato, M., Tanaka, N., Hata, N., Oda, E., & Taniguchi, T. (1998) *FEBS Lett.* 425, 112-116.

171. Wathelet, M. G., Lin, C. H., Parekh, B. S., Ronco, L. V., Howley, P. M., & Maniatis, T. (1998) *Mol. Cell* 1, 507-518.

172. Prakash, A., Smith, E., Lee, C. K., & Levy, D. E. (2005) *J. Biol. Chem.* 280, 18651-18657.

173. Sato, M., Suemori, H., Hata, N., Asagiri, M., Ogasawara, K., Nakao, K., Nakaya, T., Katsuki, M., Noguchi, S., Tanaka, N. *et al.* (2000) *Immunity.* 13, 539-548.

174. Der, S. D., Zhou, A., Williams, B. R., & Silverman, R. H. (1998) *Proc. Natl. Acad. Sci. U. S. A* 95, 15623-15628.

175. Pedersen, I. M., Cheng, G., Wieland, S., Volinia, S., Croce, C. M., Chisari, F. V., & David, M. (2007) *Nature* 449, 919-922.

176. Samuel, C. E. (2001) *Clin. Microbiol. Rev.* 14, 778-809, table.

177. Haller, O., Kochs, G., & Weber, F. (2006) *Virology* 344, 119-130.

178. Yoneyama, M., Kikuchi, M., Natsukawa, T., Shinobu, N., Imaizumi, T., Miyagishi, M., Taira, K., Akira, S., & Fujita, T. (2004) *Nat. Immunol* 5, 730-737.

179. Rothenfusser, S., Goutagny, N., DiPerna, G., Gong, M., Monks, B. G., Schoenemeyer, A., Yamamoto, M., Akira, S., & Fitzgerald, K. A. (2005) *J Immunol* 175, 5260-5268.

180. Yoneyama, M., Kikuchi, M., Matsumoto, K., Imaizumi, T., Miyagishi, M., Taira, K., Foy, E., Loo, Y. M., Gale, M., Jr., Akira, S. *et al.* (2005) *J Immunol* 175, 2851-2858.

181. Venkataraman, T., Valdes, M., Elsby, R., Kakuta, S., Caceres, G., Saijo, S., Iwakura, Y., & Barber, G. N. (2007) *J Immunol* 178, 6444-6455.

182. Kato, H., Sato, S., Yoneyama, M., Yamamoto, M., Uematsu, S., Matsui, K., Tsujimura, T., Takeda, K., Fujita, T., Takeuchi, O. *et al.* (2005) *Immunity.* 23, 19-28.

183. Kato, H., Takeuchi, O., Sato, S., Yoneyama, M., Yamamoto, M., Matsui, K., Uematsu, S., Jung, A., Kawai, T., Ishii, K. J. *et al.* (2006) *Nature* 441, 101-105.

184. Gitlin, L., Barchet, W., Gilfillan, S., Cella, M., Beutler, B., Flavell, R. A., Diamond, M. S., & Colonna, M. (2006) *Proc. Natl. Acad. Sci. U. S. A* 103, 8459-8464.

185. Saito, T., Hirai, R., Loo, Y. M., Owen, D., Johnson, C. L., Sinha, S. C., Akira, S., Fujita, T., & Gale, M., Jr. (2007) *Proc. Natl. Acad. Sci. U. S. A* 104, 582-587.

186. Hornung, V., Ellegast, J., Kim, S., Brzozka, K., Jung, A., Kato, H., Poeck, H., Akira, S., Conzelmann, K. K., Schlee, M. *et al.* (2006) *Science* 314, 994-997.

187. Pichlmair, A., Schulz, O., Tan, C. P., Naslund, T. I., Liljestrom, P., Weber, F., & Reis e Sousa (2006) *Science* 314, 997-1001.

188. Gack, M. U., Shin, Y. C., Joo, C. H., Urano, T., Liang, C., Sun, L., Takeuchi, O., Akira, S., Chen, Z., Inoue, S. *et al.* (2007) *Nature* 446, 916-920.

189. Diao, F., Li, S., Tian, Y., Zhang, M., Xu, L. G., Zhang, Y., Wang, R. P., Chen, D., Zhai, Z., Zhong, B. *et al.* (2007) *Proc. Natl. Acad. Sci. U. S. A* 104, 11706-11711.

190. Kawai, T., Takahashi, K., Sato, S., Coban, C., Kumar, H., Kato, H., Ishii, K. J., Takeuchi, O., & Akira, S. (2005) *Nat. Immunol* 6, 981-988.

191. Meylan, E., Curran, J., Hofmann, K., Moradpour, D., Binder, M., Bartenschlager, R., & Tschopp, J. (2005) *Nature* 437, 1167-1172.

192. Seth, R. B., Sun, L., Ea, C. K., & Chen, Z. J. (2005) *Cell* 122, 669-682.

193. Xu, L. G., Wang, Y. Y., Han, K. J., Li, L. Y., Zhai, Z., & Shu, H. B. (2005) *Mol. Cell* 19, 727-740.

194. Kumar, H., Kawai, T., Kato, H., Sato, S., Takahashi, K., Coban, C., Yamamoto, M., Uematsu, S., Ishii, K. J., Takeuchi, O. *et al.* (2006) *J Exp. Med.* 203, 1795-1803.

195. Sun, Q., Sun, L., Liu, H. H., Chen, X., Seth, R. B., Forman, J., & Chen, Z. J. (2006) *Immunity.* 24, 633-642.

196. Fitzgerald, K. A., McWhirter, S. M., Faia, K. L., Rowe, D. C., Latz, E., Golenbock, D. T., Coyle, A. J., Liao, S. M., & Maniatis, T. (2003) *Nat. Immunol* 4, 491-496.

197. Hemmi, H., Takeuchi, O., Sato, S., Yamamoto, M., Kaisho, T., Sanjo, H., Kawai, T., Hoshino, K., Takeda, K., & Akira, S. (2004) *J Exp. Med.* 199, 1641-1650.

198. Sharma, S., tenOever, B. R., Grandvaux, N., Zhou, G. P., Lin, R., & Hiscott, J. (2003) *Science* 300, 1148-1151.

199. Oganesyan, G., Saha, S. K., Guo, B., He, J. Q., Shahangian, A., Zarnegar, B., Perry, A., & Cheng, G. (2006) *Nature* 439, 208-211.

200. Saha, S. K., Pietras, E. M., He, J. Q., Kang, J. R., Liu, S. Y., Oganesyan, G., Shahangian, A., Zarnegar, B., Shiba, T. L., Wang, Y. *et al.* (2006) *EMBO J* 25, 3257-3263.

201. Balachandran, S., Thomas, E., & Barber, G. N. (2004) *Nature* 432, 401-405.

202. Takahashi, K., Kawai, T., Kumar, H., Sato, S., Yonehara, S., & Akira, S. (2006) *J Immunol* 176, 4520-4524.

203. Alexopoulou, L., Holt, A. C., Medzhitov, R., & Flavell, R. A. (2001) *Nature* 413, 732-738.

204. Aliprantis, A. O., Yang, R. B., Mark, M. R., Suggett, S., Devaux, B., Radolf, J. D., Klimpel, G. R., Godowski, P., & Zychlinsky, A. (1999) *Science* 285, 736-739.

205. Hayashi, F., Smith, K. D., Ozinsky, A., Hawn, T. R., Yi, E. C., Goodlett, D. R., Eng, J. K., Akira, S., Underhill, D. M., & Aderem, A. (2001) *Nature* 410, 1099-1103.

206. Heil, F., Hemmi, H., Hochrein, H., Ampenberger, F., Kirschning, C., Akira, S., Lipford, G., Wagner, H., & Bauer, S. (2004) *Science* 303, 1526-1529.

207. Hemmi, H., Takeuchi, O., Kawai, T., Kaisho, T., Sato, S., Sanjo, H., Matsumoto, M., Hoshino, K., Wagner, H., Takeda, K. *et al.* (2000) *Nature* 408, 740-745.

208. Poltorak, A., He, X., Smirnova, I., Liu, M. Y., Van, H. C., Du, X., Birdwell, D., Alejos, E., Silva, M., Galanos, C. *et al.* (1998) *Science* 282, 2085-2088.

209. Underhill, D. M., Ozinsky, A., Hajjar, A. M., Stevens, A., Wilson, C. B., Bassetti, M., & Aderem, A. (1999) *Nature* 401, 811-815.

210. Akira, S., Uematsu, S., & Takeuchi, O. (2006) *Cell* 124, 783-801.

211. Brinkmann, M. M., Spooner, E., Hoebe, K., Beutler, B., Ploegh, H. L., & Kim, Y. M. (2007) *J Cell Biol.* 177, 265-275.

212. Tabeta, K., Hoebe, K., Janssen, E. M., Du, X., Georgel, P., Crozat, K., Mudd, S., Mann, N., Sovath, S., Goode, J. *et al.* (2006) *Nat. Immunol* 7, 156-164.

213. Matsumoto, M., Kikkawa, S., Kohase, M., Miyake, K., & Seya, T. (2002) *Biochem. Biophys. Res. Commun.* 293, 1364-1369.

214. Matsumoto, M., Funami, K., Tanabe, M., Oshiumi, H., Shingai, M., Seto, Y., Yamamoto, A., & Seya, T. (2003) *J Immunol* 171, 3154-3162.

215. Zhou, R., Wei, H., Sun, R., & Tian, Z. (2007) *J Immunol* 178, 4548-4556.

216. Takeda, K., Kaisho, T., & Akira, S. (2003) *Annu. Rev. Immunol.* 21, 335-376.

217. Saito, T. & Gale, M., Jr. (2007) *Curr. Opin. Immunol.* 19, 17-23.

218. Pichlmair, A. & Reis e Sousa (2007) *Immunity.* 27, 370-383.

219. Johnsen, I. B., Nguyen, T. T., Ringdal, M., Tryggestad, A. M., Bakke, O., Lien, E., Espevik, T., & Anthonsen, M. W. (2006) *EMBO J* 25, 3335-3346.

220. Lee, H. K., Dunzendorfer, S., Soldau, K., & Tobias, P. S. (2006) *Immunity.* 24, 153-163.

221. Hacker, H., Redecke, V., Blagoev, B., Kratchmarova, I., Hsu, L. C., Wang, G. G., Kamps, M. P., Raz, E., Wagner, H., Hacker, G. *et al.* (2006) *Nature* 439, 204-207.

222. Sasai, M., Oshiumi, H., Matsumoto, M., Inoue, N., Fujita, F., Nakanishi, M., & Seya, T. (2005) *J Immunol* 174, 27-30.

223. Meylan, E., Burns, K., Hofmann, K., Blancheteau, V., Martinon, F., Kelliher, M., & Tschopp, J. (2004) *Nat. Immunol* 5, 503-507.

224. Sato, S., Sugiyama, M., Yamamoto, M., Watanabe, Y., Kawai, T., Takeda, K., & Akira, S. (2003) *J Immunol* 171, 4304-4310.

225. Sarkar, S. N., Peters, K. L., Elco, C. P., Sakamoto, S., Pal, S., & Sen, G. C. (2004) *Nat. Struct. Mol. Biol.* 11, 1060-1067.

226. Hirata, Y., Broquet, A. H., Menchen, L., & Kagnoff, M. F. (2007) *J Immunol* 179, 5425-5432.

227. Schulz, O., Diebold, S. S., Chen, M., Naslund, T. I., Nolte, M. A., Alexopoulou, L., Azuma, Y. T., Flavell, R. A., Liljestrom, P., & Reis e Sousa (2005) *Nature* 433, 887-892.

228. Narvaez, C. F., Angel, J., & Franco, M. A. (2005) *J Virol* 79, 14526-14535.

229. Pulendran, B. & Ahmed, R. (2006) *Cell* 124, 849-863.

230. Mamane, Y., Heylbroeck, C., Genin, P., Algarte, M., Servant, M. J., LePage, C., DeLuca, C., Kwon, H., Lin, R., & Hiscott, J. (1999) *Gene* 237, 1-14.

231. Taniguchi, T., Ogasawara, K., Takaoka, A., & Tanaka, N. (2001) *Annu. Rev. Immunol* 19, 623-655.

232. Matsuyama, T., Kimura, T., Kitagawa, M., Pfeffer, K., Kawakami, T., Watanabe, N., Kundig, T. M., Amakawa, R., Kishihara, K., Wakeham, A. *et al.* (1993) *Cell* 75, 83-97.

233. Takaoka, A., Yanai, H., Kondo, S., Duncan, G., Negishi, H., Mizutani, T., Kano, S., Honda, K., Ohba, Y., Mak, T. W. *et al.* (2005) *Nature* 434, 243-249.

234. Servant, M. J., tenOever, B., & Lin, R. (2002) *J. Interferon Cytokine Res.* 22, 49-58.

235. Lin, R., Heylbroeck, C., Pitha, P. M., & Hiscott, J. (1998) *Mol. Cell Biol.* 18, 2986-2996.

236. Yoneyama, M., Suhara, W., Fukuhara, Y., Fukuda, M., Nishida, E., & Fujita, T. (1998) *EMBO J* 17, 1087-1095.

237. Mori, M., Yoneyama, M., Ito, T., Takahashi, K., Inagaki, F., & Fujita, T. (2004) *J Biol. Chem.* 279, 9698-9702.

238. Servant, M. J., Grandvaux, N., tenOever, B. R., Duguay, D., Lin, R., & Hiscott, J. (2003) *J Biol. Chem.* 278, 9441-9447.

239. Qin, B. Y., Liu, C., Lam, S. S., Srinath, H., Delston, R., Correia, J. J., Derynck, R., & Lin, K. (2003) *Nat. Struct. Biol.* 10, 913-921.

240. Takahasi, K., Suzuki, N. N., Horiuchi, M., Mori, M., Suhara, W., Okabe, Y., Fukuhara, Y., Terasawa, H., Akira, S., Fujita, T. *et al.* (2003) *Nat. Struct. Biol.* 10, 922-927.

241. Kumar, K. P., McBride, K. M., Weaver, B. K., Dingwall, C., & Reich, N. C. (2000) *Mol. Cell Biol.* 20, 4159-4168.

242. Suhara, W., Yoneyama, M., Kitabayashi, I., & Fujita, T. (2002) *J Biol. Chem.* 277, 22304-22313.

243. Saitoh, T., Tun-Kyi, A., Ryo, A., Yamamoto, M., Finn, G., Fujita, T., Akira, S., Yamamoto, N., Lu, K. P., & Yamaoka, S. (2006) *Nat. Immunol* 7, 598-605.

244. Bibeau-Poirier, A., Gravel, S. P., Clement, J. F., Rolland, S., Rodier, G., Coulombe, P., Hiscott, J., Grandvaux, N., Meloche, S., & Servant, M. J. (2006) *J Immunol* 177, 5059-5067.

245. Honda, K., Yanai, H., Negishi, H., Asagiri, M., Sato, M., Mizutani, T., Shimada, N., Ohba, Y., Takaoka, A., Yoshida, N. *et al.* (2005) *Nature* 434, 772-777.

246. Cusson-Hermance, N., Khurana, S., Lee, T. H., Fitzgerald, K. A., & Kelliher, M. A. (2005) *J. Biol. Chem.* 280, 36560-36566.

247. Chen, Z. J., Bhoj, V., & Seth, R. B. (2006) *Cell Death. Differ.* 13, 687-692.

248. Deng, L., Wang, C., Spencer, E., Yang, L., Braun, A., You, J., Slaughter, C., Pickart, C., & Chen, Z. J. (2000) *Cell* 103, 351-361.

249. Opipari, A. W., Jr., Hu, H. M., Yabkowitz, R., & Dixit, V. M. (1992) *J. Biol. Chem.* 267, 12424-12427.

250. Kobayashi, N., Kadono, Y., Naito, A., Matsumoto, K., Yamamoto, T., Tanaka, S., & Inoue, J. (2001) *EMBO J.* 20, 1271-1280.

251. Lamothe, B., Besse, A., Campos, A. D., Webster, W. K., Wu, H., & Darnay, B. G. (2007) *J. Biol. Chem.* 282, 4102-4112.

252. Lee, T. H., Shank, J., Cusson, N., & Kelliher, M. A. (2004) *J. Biol. Chem.* 279, 33185-33191.

253. Hayden, M. S. & Ghosh, S. (2008) *Cell* 132, 344-362.

254. Hacker, H. & Karin, M. (2006) *Sci. STKE.* 2006, re13.

255. Kray, A. E., Carter, R. S., Pennington, K. N., Gomez, R. J., Sanders, L. E., Llanes, J. M., Khan, W. N., Ballard, D. W., & Wadzinski, B. E. (2005) *J. Biol. Chem.* 280, 35974-35982.

256. Palkowitsch, L., Leidner, J., Ghosh, S., & Marienfeld, R. B. (2008) *J. Biol. Chem.* 283, 76-86.

257. Prajapati, S., Verma, U., Yamamoto, Y., Kwak, Y. T., & Gaynor, R. B. (2004) *J. Biol. Chem.* 279, 1739-1746.

258. DiDonato, J. A., Hayakawa, M., Rothwarf, D. M., Zandi, E., & Karin, M. (1997) *Nature* 388, 548-554.

259. Kroll, M., Margottin, F., Kohl, A., Renard, P., Durand, H., Concordet, J. P., Bachelerie, F., renzana-Seisdedos, F., & Benarous, R. (1999) *J. Biol. Chem.* 274, 7941-7945.

260. Hoffmann, A., Levchenko, A., Scott, M. L., & Baltimore, D. (2002) *Science* 298, 1241-1245.

261. Wu, C. & Ghosh, S. (2003) *J. Biol. Chem.* 278, 31980-31987.

262. Ghosh, S. & Karin, M. (2002) *Cell* 109 Suppl, S81-S96.

263. Baeuerle, P. A. & Baltimore, D. (1988) *Cell* 53, 211-217.

264. Reimer, T., Schweizer, M., & Jungi, T. W. (2007) *J. Interferon Cytokine Res.* 27, 751-755.

265. Arenzana-Seisdedos, F., Turpin, P., Rodriguez, M., Thomas, D., Hay, R. T., Virelizier, J. L., & Dargemont, C. (1997) *J. Cell Sci.* 110 (Pt 3), 369-378.

266. Tergaonkar, V., Correa, R. G., Ikawa, M., & Verma, I. M. (2005) *Nat. Cell Biol.* 7, 921-923.

267. Vermeulen, L., De, W. G., Van, D. P., Vanden, B. W., & Haegeman, G. (2003) *EMBO J.* 22, 1313-1324.

268. Zhong, H., Voll, R. E., & Ghosh, S. (1998) *Mol. Cell* 1, 661-671.

269. Chen, L. F., Williams, S. A., Mu, Y., Nakano, H., Duerr, J. M., Buckbinder, L., & Greene, W. C. (2005) *Mol. Cell Biol.* 25, 7966-7975.

270. Chen, L. F., Mu, Y., & Greene, W. C. (2002) *EMBO J.* 21, 6539-6548.

271. Du, W. & Maniatis, T. (1992) *Proc. Natl. Acad. Sci. U. S. A* 89, 2150-2154.

272. Falvo, J. V., Parekh, B. S., Lin, C. H., Fraenkel, E., & Maniatis, T. (2000) *Mol. Cell Biol.* 20, 4814-4825.

273. Deng, T. & Karin, M. (1994) *Nature* 371, 171-175.

274. Smeal, T., Binetruy, B., Mercola, D., Grover-Bardwick, A., Heidecker, G., Rapp, U. R., & Karin, M. (1992) *Mol. Cell Biol.* 12, 3507-3513.

275. Devary, Y., Gottlieb, R. A., Smeal, T., & Karin, M. (1992) *Cell* 71, 1081-1091.

276. Gupta, S., Campbell, D., Derijard, B., & Davis, R. J. (1995) *Science* 267, 389-393.

277. Sano, Y., Harada, J., Tashiro, S., Gotoh-Mandeville, R., Maekawa, T., & Ishii, S. (1999) *J. Biol. Chem.* 274, 8949-8957.

278. Fukushima, T., Matsuzawa, S., Kress, C. L., Bruey, J. M., Krajewska, M., Lefebvre, S., Zapata, J. M., Ronai, Z., & Reed, J. C. (2007) *Proc. Natl. Acad. Sci. U. S. A* 104, 6371-6376.

279. Yamamoto, M., Sato, S., Saitoh, T., Sakurai, H., Uematsu, S., Kawai, T., Ishii, K. J., Takeuchi, O., & Akira, S. (2006) *J. Immunol.* 177, 7520-7524.

280. Agalioti, T., Lomvardas, S., Parekh, B., Yie, J., Maniatis, T., & Thanos, D. (2000) *Cell* 103, 667-678.

281. Maniatis, T., Falvo, J. V., Kim, T. H., Kim, T. K., Lin, C. H., Parekh, B. S., & Wathelet, M. G. (1998) *Cold Spring Harb. Symp. Quant. Biol.* 63, 609-620.

282. Munshi, N., Yie, Y., Merika, M., Senger, K., Lomvardas, S., Agalioti, T., & Thanos, D. (1999) *Cold Spring Harb. Symp. Quant. Biol.* 64, 149-159.

283. Kim, T. K. & Maniatis, T. (1997) *Mol. Cell* 1, 119-129.

284. Cohen, B., Novick, D., Barak, S., & Rubinstein, M. (1995) *Mol. Cell Biol.* 15, 4208-4214.

285. Russell-Harde, D., Pu, H., Betts, M., Harkins, R. N., Perez, H. D., & Croze, E. (1995) *J. Biol. Chem.* 270, 26033-26036.

286. Fu, X. Y. (1992) *Cell* 70, 323-335.

287. Schindler, C., Shuai, K., Prezioso, V. R., & Darnell, J. E., Jr. (1992) *Science* 257, 809-813.

288. Veals, S. A., Schindler, C., Leonard, D., Fu, X. Y., Aebersold, R., Darnell, J. E., Jr., & Levy, D. E. (1992) *Mol. Cell Biol.* 12, 3315-3324.

289. Colamonici, O., Yan, H., Domanski, P., Handa, R., Smalley, D., Mullersman, J., Witte, M., Krishnan, K., & Krolewski, J. (1994) *Mol. Cell Biol.* 14, 8133-8142.

290. Colamonici, O. R., Uyttendaele, H., Domanski, P., Yan, H., & Krolewski, J. J. (1994) *J. Biol. Chem.* 269, 3518-3522.

291. Gauzzi, M. C., Velazquez, L., McKendry, R., Mogensen, K. E., Fellous, M., & Pellegrini, S. (1996) *J. Biol. Chem.* 271, 20494-20500.

292. Krishnan, K., Yan, H., Lim, J. T., & Krolewski, J. J. (1996) *Oncogene* 13, 125-133.

293. Yan, H., Krishnan, K., Greenlund, A. C., Gupta, S., Lim, J. T., Schreiber, R. D., Schindler, C. W., & Krolewski, J. J. (1996) *EMBO J.* 15, 1064-1074.

294. Lau, J. F., Parisien, J. P., & Horvath, C. M. (2000) *Proc. Natl. Acad. Sci. U. S. A* 97, 7278-7283.

295. Martinez-Moczygemba, M., Gutch, M. J., French, D. L., & Reich, N. C. (1997) *J. Biol. Chem.* 272, 20070-20076.

296. Gutch, M. J., Daly, C., & Reich, N. C. (1992) *Proc. Natl. Acad. Sci. U. S. A* 89, 11411-11415.

297. Shuai, K., Horvath, C. M., Huang, L. H., Qureshi, S. A., Cowburn, D., & Darnell, J. E., Jr. (1994) *Cell* 76, 821-828.

298. van Boxel-Dezaire, A. H., Rani, M. R., & Stark, G. R. (2006) *Immunity.* 25, 361-372.

299. Bhattacharya, S., Eckner, R., Grossman, S., Oldread, E., Arany, Z., D'Andrea, A., & Livingston, D. M. (1996) *Nature* 383, 344-347.

300. Platanias, L. C. (2005) *Nat. Rev. Immunol.* 5, 375-386.

301. Hwang, S. Y., Hertzog, P. J., Holland, K. A., Sumarsono, S. H., Tymms, M. J., Hamilton, J. A., Whitty, G., Bertoncello, I., & Kola, I. (1995) *Proc. Natl. Acad. Sci. U. S. A* 92, 11284-11288.

302. de Veer, M. J., Holko, M., Frevel, M., Walker, E., Der, S., Paranjape, J. M., Silverman, R. H., & Williams, B. R. (2001) *J. Leukoc. Biol.* 69, 912-920.

303. Deonarain, R., Chan, D. C., Platanias, L. C., & Fish, E. N. (2002) *Curr. Pharm. Des* 8, 2131-2137.

304. Guo, J., Hui, D. J., Merrick, W. C., & Sen, G. C. (2000) *EMBO J.* 19, 6891-6899.

305. Hui, D. J., Bhasker, C. R., Merrick, W. C., & Sen, G. C. (2003) *J. Biol. Chem.* 278, 39477-39482.

306. Meurs, E., Chong, K., Galabru, J., Thomas, N. S., Kerr, I. M., Williams, B. R., & Hovanessian, A. G. (1990) *Cell* 62, 379-390.

307. Carroll, S. S., Chen, E., Viscount, T., Geib, J., Sardana, M. K., Gehman, J., & Kuo, L. C. (1996) *J. Biol. Chem.* 271, 4988-4992.

308. Ghosh, S. K., Kusari, J., Bandyopadhyay, S. K., Samanta, H., Kumar, R., & Sen, G. C. (1991) *J. Biol. Chem.* 266, 15293-15299.

309. Kerr, I. M. & Brown, R. E. (1978) *Proc. Natl. Acad. Sci. U. S. A* 75, 256-260.

310. Malathi, K., Dong, B., Gale, M., Jr., & Silverman, R. H. (2007) *Nature* 448, 816-819.

311. Cooper, M. D. & Alder, M. N. (2006) *Cell* 124, 815-822.

312. Krause, C. D. & Pestka, S. (2005) *Pharmacol. Ther.* 106, 299-346.

313. Le Bon, A. & Tough, D. F. (2002) *Curr. Opin. Immunol.* 14, 432-436.

314. Stetson, D. B. & Medzhitov, R. (2006) *Immunity.* 25, 373-381.

315. van den Broek, M. F., Muller, U., Huang, S., Zinkernagel, R. M., & Aguet, M. (1995) *Immunol. Rev.* 148, 5-18.

316. Kolumam, G. A., Thomas, S., Thompson, L. J., Sprent, J., & Murali-Krishna, K. (2005) *J. Exp. Med.* 202, 637-650.

317. Le Bon, A., Durand, V., Kamphuis, E., Thompson, C., Bulfone-Paus, S., Rossmann, C., Kalinke, U., & Tough, D. F. (2006) *J. Immunol.* 176, 4682-4689.

318. Marrack, P., Kappler, J., & Mitchell, T. (1999) *J. Exp. Med.* 189, 521-530.

319. Petricoin, E. F., III, Ito, S., Williams, B. L., Audet, S., Stancato, L. F., Gamero, A., Clouse, K., Grimley, P., Weiss, A., Beeler, J. *et al.* (1997) *Nature* 390, 629-632.

320. Le Bon, A., Etchart, N., Rossmann, C., Ashton, M., Hou, S., Gewert, D., Borrow, P., & Tough, D. F. (2003) *Nat. Immunol.* 4, 1009-1015.

321. Randall, R. E. & Goodbourn, S. (2008) *J. Gen. Virol.* 89, 1-47.

322. Gale, M., Jr. & Foy, E. M. (2005) *Nature* 436, 939-945.

323. De Francesco R., Neddermann, P., Tomei, L., Steinkuhler, C., Gallinari, P., & Folgori, A. (2000) *Semin. Liver Dis.* 20, 69-83.

324. Sumpter, R., Jr., Loo, Y. M., Foy, E., Li, K., Yoneyama, M., Fujita, T., Lemon, S. M., & Gale, M., Jr. (2005) *J. Virol.* 79, 2689-2699.

325. Cheng, G., Zhong, J., & Chisari, F. V. (2006) *Proc. Natl. Acad. Sci. U. S. A* 103, 8499-8504.

326. Kaukinen, P., Sillanpaa, M., Kotenko, S., Lin, R., Hiscott, J., Melen, K., & Julkunen, I. (2006) *Virol. J.* 3, 66.

327. Li, X. D., Sun, L., Seth, R. B., Pineda, G., & Chen, Z. J. (2005) *Proc. Natl. Acad. Sci. U. S. A* 102, 17717-17722.

328. Lin, R., Lacoste, J., Nakhaei, P., Sun, Q., Yang, L., Paz, S., Wilkinson, P., Julkunen, I., Vitour, D., Meurs, E. *et al.* (2006) *J. Virol.* 80, 6072-6083.

329. Loo, Y. M., Owen, D. M., Li, K., Erickson, A. K., Johnson, C. L., Fish, P. M., Carney, D. S., Wang, T., Ishida, H., Yoneyama, M. *et al.* (2006) *Proc. Natl. Acad. Sci. U. S. A* 103, 6001-6006.

330. Li, K., Foy, E., Ferreon, J. C., Nakamura, M., Ferreon, A. C., Ikeda, M., Ray, S. C., Gale, M., Jr., & Lemon, S. M. (2005) *Proc. Natl. Acad. Sci. U. S. A* 102, 2992-2997.

331. Foy, E., Li, K., Wang, C., Sumpter, R., Jr., Ikeda, M., Lemon, S. M., & Gale, M., Jr. (2003) *Science* 300, 1145-1148.

332. Foy, E., Li, K., Sumpter, R., Jr., Loo, Y. M., Johnson, C. L., Wang, C., Fish, P. M., Yoneyama, M., Fujita, T., Lemon, S. M. *et al.* (2005) *Proc. Natl. Acad. Sci. U. S. A* 102, 2986-2991.

333. Frese, M., Pietschmann, T., Moradpour, D., Haller, O., & Bartenschlager, R. (2001) *J. Gen. Virol.* 82, 723-733.

334. Kim, C. S., Jung, J. H., Wakita, T., Yoon, S. K., & Jang, S. K. (2007) *J. Virol.* 81, 8814-8820.

335. Windisch, M. P., Frese, M., Kaul, A., Trippler, M., Lohmann, V., & Bartenschlager, R. (2005) *J. Virol.* 79, 13778-13793.

336. McHutchison, J. G., Poynard, T., Esteban-Mur, R., Davis, G. L., Goodman, Z. D., Harvey, J., Ling, M. H., Garaud, J. J., Albrecht, J. K., Patel, K. *et al.* (2002) *Hepatology* 35, 688-693.

337. Lin, W., Kim, S. S., Yeung, E., Kamegaya, Y., Blackard, J. T., Kim, K. A., Holtzman, M. J., & Chung, R. T. (2006) *J. Virol.* 80, 9226-9235.

338. Bode, J. G., Ludwig, S., Ehrhardt, C., Albrecht, U., Erhardt, A., Schaper, F., Heinrich, P. C., & Haussinger, D. (2003) *FASEB J.* 17, 488-490.

339. Duong, F. H., Filipowicz, M., Tripodi, M., La, M. N., & Heim, M. H. (2004) *Gastroenterology* 126, 263-277.

340. Ciccaglione, A. R., Stellacci, E., Marcantonio, C., Muto, V., Equestre, M., Marsili, G., Rapicetta, M., & Battistini, A. (2007) *J. Virol.* 81, 202-214.

341. Chen, Z., Li, Y., & Krug, R. M. (1999) *EMBO J.* 18, 2273-2283.

342. Fortes, P., Beloso, A., & Ortin, J. (1994) *EMBO J.* 13, 704-712.

343. Kim, M. J., Latham, A. G., & Krug, R. M. (2002) *Proc. Natl. Acad. Sci. U. S. A* 99, 10096-10101.

344. Li, Y., Chen, Z. Y., Wang, W., Baker, C. C., & Krug, R. M. (2001) *RNA.* 7, 920-931.

345. Noah, D. L., Twu, K. Y., & Krug, R. M. (2003) *Virology* 307, 386-395.

346. Satterly, N., Tsai, P. L., van, D. J., Nussenzveig, D. R., Wang, Y., Faria, P. A., Levay, A., Levy, D. E., & Fontoura, B. M. (2007) *Proc. Natl. Acad. Sci. U. S. A* 104, 1853-1858.

347. Kochs, G., Garcia-Sastre, A., & Martinez-Sobrido, L. (2007) *J. Virol.* 81, 7011-7021.

348. Guo, Z., Chen, L. M., Zeng, H., Gomez, J. A., Plowden, J., Fujita, T., Katz, J. M., Donis, R. O., & Sambhara, S. (2007) *Am. J. Respir. Cell Mol. Biol.* 36, 263-269.

349. Mibayashi, M., Martinez-Sobrido, L., Loo, Y. M., Cardenas, W. B., Gale, M., Jr., & Garcia-Sastre, A. (2007) *J. Virol.* 81, 514-524.

350. Opitz, B., Rejaibi, A., Dauber, B., Eckhard, J., Vinzing, M., Schmeck, B., Hippenstiel, S., Suttorp, N., & Wolff, T. (2007) *Cell Microbiol.* 9, 930-938.

351. Li, S., Min, J. Y., Krug, R. M., & Sen, G. C. (2006) *Virology* 349, 13-21.

352. Talon, J., Horvath, C. M., Polley, R., Basler, C. F., Muster, T., Palese, P., & Garcia-Sastre, A. (2000) *J. Virol.* 74, 7989-7996.

353. Wang, X., Li, M., Zheng, H., Muster, T., Palese, P., Beg, A. A., & Garcia-Sastre, A. (2000) *J. Virol.* 74, 11566-11573.

354. Hartmann, R., Justesen, J., Sarkar, S. N., Sen, G. C., & Yee, V. C. (2003) *Mol. Cell* 12, 1173-1185.

355. Min, J. Y. & Krug, R. M. (2006) *Proc. Natl. Acad. Sci. U. S. A* 103, 7100-7105.

356. Hayman, A., Comely, S., Lackenby, A., Hartgroves, L. C., Goodbourn, S., McCauley, J. W., & Barclay, W. S. (2007) *J. Virol.* 81, 2318-2327.

357. Baskin, C. R., Bielefeldt-Ohmann, H., Garcia-Sastre, A., Tumpey, T. M., Van, H. N., Carter, V. S., Thomas, M. J., Proll, S., Solorzano, A., Billharz, R. *et al.* (2007) *J. Virol.* 81, 11817-11827.

358. Fernandez-Sesma, A., Marukian, S., Ebersole, B. J., Kaminski, D., Park, M. S., Yuen, T., Sealfon, S. C., Garcia-Sastre, A., & Moran, T. M. (2006) *J. Virol.* 80, 6295-6304.

359. Richt, J. A., Lekcharoensuk, P., Lager, K. M., Vincent, A. L., Loiacono, C. M., Janke, B. H., Wu, W. H., Yoon, K. J., Webby, R. J., Solorzano, A. *et al.* (2006) *J. Virol.* 80, 11009-11018.

360. Talon, J., Salvatore, M., O'Neill, R. E., Nakaya, Y., Zheng, H., Muster, T., Garcia-Sastre, A., & Palese, P. (2000) *Proc. Natl. Acad. Sci. U. S. A* 97, 4309-4314.

361. Kobasa, D., Jones, S. M., Shinya, K., Kash, J. C., Copps, J., Ebihara, H., Hatta, Y., Kim, J. H., Halfmann, P., Hatta, M. *et al.* (2007) *Nature* 445, 319-323.

362. Ciechanover, A., Finley, D., & Varshavsky, A. (1984) *Cell* 37, 57-66.

363. Finley, D., Ciechanover, A., & Varshavsky, A. (1984) *Cell* 37, 43-55.

364. Hershko, A., Heller, H., Elias, S., & Ciechanover, A. (1983) *J. Biol. Chem.* 258, 8206-8214.

365. Chen, P., Johnson, P., Sommer, T., Jentsch, S., & Hochstrasser, M. (1993) *Cell* 74, 357-369.

366. Pickart, C. M. (2001) *Annu. Rev. Biochem.* 70, 503-533.

367. Kim, J. H., Park, K. C., Chung, S. S., Bang, O., & Chung, C. H. (2003) *J. Biochem.* 134, 9-18.

368. Weissman, A. M. (2001) *Nat. Rev. Mol. Cell Biol.* 2, 169-178.

369. Peng, J., Schwartz, D., Elias, J. E., Thoreen, C. C., Cheng, D., Marsischky, G., Roelofs, J., Finley, D., & Gygi, S. P. (2003) *Nat. Biotechnol.* 21, 921-926.

370. McGrath, J. P., Jentsch, S., & Varshavsky, A. (1991) *EMBO J.* 10, 227-236.

371. Zacksenhaus, E. & Sheinin, R. (1990) *EMBO J.* 9, 2923-2929.

372. Jin, J., Li, X., Gygi, S. P., & Harper, J. W. (2007) *Nature* 447, 1135-1138.

373. Hershko, A., Ciechanover, A., & Rose, I. A. (1981) *J. Biol. Chem.* 256, 1525-1528.

374. Haas, A. L., Warms, J. V., Hershko, A., & Rose, I. A. (1982) *J. Biol. Chem.* 257, 2543-2548.

375. Semple, C. A. (2003) *Genome Res.* 13, 1389-1394.

376. Cook, W. J., Jeffrey, L. C., Xu, Y., & Chau, V. (1993) *Biochemistry* 32, 13809-13817.

377. Jiang, F. & Basavappa, R. (1999) *Biochemistry* 38, 6471-6478.

378. Worthylake, D. K., Prakash, S., Prakash, L., & Hill, C. P. (1998) *J. Biol. Chem.* 273, 6271-6276.

379. Deshaies, R. J. (1999) *Annu. Rev. Cell Dev. Biol.* 15, 435-467.

380. Huibregtse, J. M., Scheffner, M., Beaudenon, S., & Howley, P. M. (1995) *Proc. Natl. Acad. Sci. U. S. A* 92, 5249.

381. Lorick, K. L., Jensen, J. P., Fang, S., Ong, A. M., Hatakeyama, S., & Weissman, A. M. (1999) *Proc. Natl. Acad. Sci. U. S. A* 96, 11364-11369.

382. Scheffner, M., Huibregtse, J. M., Vierstra, R. D., & Howley, P. M. (1993) *Cell* 75, 495-505.

383. Scheffner, M., Nuber, U., & Huibregtse, J. M. (1995) *Nature* 373, 81-83.

384. Borden, K. L. (2000) *J. Mol. Biol.* 295, 1103-1112.

385. Zheng, N., Wang, P., Jeffrey, P. D., & Pavletich, N. P. (2000) *Cell* 102, 533-539.

386. Fang, S., Jensen, J. P., Ludwig, R. L., Vousden, K. H., & Weissman, A. M. (2000) *J. Biol. Chem.* 275, 8945-8951.

387. Joazeiro, C. A., Wing, S. S., Huang, H., Leverson, J. D., Hunter, T., & Liu, Y. C. (1999) *Science* 286, 309-312.

388. Joazeiro, C. A. & Weissman, A. M. (2000) *Cell* 102, 549-552.

389. Waterman, H., Levkowitz, G., Alroy, I., & Yarden, Y. (1999) *J. Biol. Chem.* 274, 22151-22154.

390. Devin, A., Cook, A., Lin, Y., Rodriguez, Y., Kelliher, M., & Liu, Z. (2000) *Immunity.* 12, 419-429.

391. Kamura, T., Koepp, D. M., Conrad, M. N., Skowyra, D., Moreland, R. J., Iliopoulos, O., Lane, W. S., Kaelin, W. G., Jr., Elledge, S. J., Conaway, R. C. *et al.* (1999) *Science* 284, 657-661.

392. Ohta, T., Michel, J. J., Schottelius, A. J., & Xiong, Y. (1999) *Mol. Cell* 3, 535-541.

393. Seol, J. H., Feldman, R. M., Zachariae, W., Shevchenko, A., Correll, C. C., Lyapina, S., Chi, Y., Galova, M., Claypool, J., Sandmeyer, S. *et al.* (1999) *Genes Dev.* 13, 1614-1626.

394. Skowyra, D., Craig, K. L., Tyers, M., Elledge, S. J., & Harper, J. W. (1997) *Cell* 91, 209-219.

395. Tan, P., Fuchs, S. Y., Chen, A., Wu, K., Gomez, C., Ronai, Z., & Pan, Z. Q. (1999) *Mol. Cell* 3, 527-533.

396. Chen, A., Wu, K., Fuchs, S. Y., Tan, P., Gomez, C., & Pan, Z. Q. (2000) *J. Biol. Chem.* 275, 15432-15439.

397. Feldman, R. M., Correll, C. C., Kaplan, K. B., & Deshaies, R. J. (1997) *Cell* 91, 221-230.

398. Pickart, C. M. (2004) *Cell* 116, 181-190.

399. Hoffman, L., Pratt, G., & Rechsteiner, M. (1992) *J. Biol. Chem.* 267, 22362-22368.

400. Deveraux, Q., Ustrell, V., Pickart, C., & Rechsteiner, M. (1994) *J. Biol. Chem.* 269, 7059-7061.

401. Husnjak, K., Elsasser, S., Zhang, N., Chen, X., Randles, L., Shi, Y., Hofmann, K., Walters, K. J., Finley, D., & Dikic, I. (2008) *Nature* 453, 481-488.

402. Schreiner, P., Chen, X., Husnjak, K., Randles, L., Zhang, N., Elsasser, S., Finley, D., Dikic, I., Walters, K. J., & Groll, M. (2008) *Nature* 453, 548-552.

403. Glickman, M. H., Rubin, D. M., Fried, V. A., & Finley, D. (1998) *Mol. Cell Biol.* 18, 3149-3162.

404. Pickart, C. M. & Cohen, R. E. (2004) *Nat. Rev. Mol. Cell Biol.* 5, 177-187.

405. Voges, D., Zwickl, P., & Baumeister, W. (1999) *Annu. Rev. Biochem.* 68, 1015-1068.

406. Hershko, A., Ciechanover, A., Heller, H., Haas, A. L., & Rose, I. A. (1980) *Proc. Natl. Acad. Sci. U. S. A* 77, 1783-1786.

407. Nandi, D., Tahiliani, P., Kumar, A., & Chandu, D. (2006) *J. Biosci.* 31, 137-155.

408. Groll, M., Heinemeyer, W., Jager, S., Ullrich, T., Bochtler, M., Wolf, D. H., & Huber, R. (1999) *Proc. Natl. Acad. Sci. U. S. A* 96, 10976-10983.

409. Heinemeyer, W., Fischer, M., Krimmer, T., Stachon, U., & Wolf, D. H. (1997) *J. Biol. Chem.* 272, 25200-25209.

410. Frentzel, S., Pesold-Hurt, B., Seelig, A., & Kloetzel, P. M. (1994) *J. Mol. Biol.* 236, 975-981.

411. Griffin, T. A., Nandi, D., Cruz, M., Fehling, H. J., Kaer, L. V., Monaco, J. J., & Colbert, R. A. (1998) *J. Exp. Med.* 187, 97-104.

412. Nandi, D., Woodward, E., Ginsburg, D. B., & Monaco, J. J. (1997) *EMBO J.* 16, 5363-5375.

413. Niedermann, G., Grimm, R., Geier, E., Maurer, M., Realini, C., Gartmann, C., Soll, J., Omura, S., Rechsteiner, M. C., Baumeister, W. *et al.* (1997) *J. Exp. Med.* 186, 209-220.

414. Fehling, H. J., Swat, W., Laplace, C., Kuhn, R., Rajewsky, K., Muller, U., & von, B. H. (1994) *Science* 265, 1234-1237.

415. Van Kaer, L., shton-Rickardt, P. G., Eichelberger, M., Gaczynska, M., Nagashima, K., Rock, K. L., Goldberg, A. L., Doherty, P. C., & Tonegawa, S. (1994) *Immunity.* 1, 533-541.

416. Amerik, A. Y. & Hochstrasser, M. (2004) *Biochim. Biophys. Acta* 1695, 189-207.

417. Finley, D. & Chau, V. (1991) *Annu. Rev. Cell Biol.* 7, 25-69.

418. Turner, G. C. & Varshavsky, A. (2000) *Science* 289, 2117-2120.

419. Verma, R., Aravind, L., Oania, R., McDonald, W. H., Yates, J. R., III, Koonin, E. V., & Deshaies, R. J. (2002) *Science* 298, 611-615.

420. Yao, T. & Cohen, R. E. (2002) *Nature* 419, 403-407.

421. Amerik, A. Y., Swaminathan, S., Krantz, B. A., Wilkinson, K. D., & Hochstrasser, M. (1997) *EMBO J.* 16, 4826-4838.

422. Hadari, T., Warms, J. V., Rose, I. A., & Hershko, A. (1992) *J. Biol. Chem.* 267, 719-727.

423. Wilkinson, K. D., Tashayev, V. L., O'Connor, L. B., Larsen, C. N., Kasperek, E., & Pickart, C. M. (1995) *Biochemistry* 34, 14535-14546.

424. Lam, Y. A., Xu, W., DeMartino, G. N., & Cohen, R. E. (1997) *Nature* 385, 737-740.

425. Pickart, C. M. (2000) *Trends Biochem. Sci.* 25, 544-548.

426. Thrower, J. S., Hoffman, L., Rechsteiner, M., & Pickart, C. M. (2000) *EMBO J.* 19, 94-102.

427. Chen, M. & Gerlier, D. (2006) *Viral Immunol.* 19, 349-362.

428. Banks, L., Pim, D., & Thomas, M. (2003) *Trends Biochem. Sci.* 28, 452-459.

429. Liu, Y. C. (2004) *Annu. Rev. Immunol.* 22, 81-127.

430. Coscoy, L., Sanchez, D. J., & Ganem, D. (2001) *J. Cell Biol.* 155, 1265-1273.

431. Yu, Y., Wang, S. E., & Hayward, G. S. (2005) *Immunity.* 22, 59-70.

432. Aravind, L., Iyer, L. M., & Koonin, E. V. (2003) *Cell Cycle* 2, 123-126.

433. Coscoy, L. & Ganem, D. (2003) *Trends Cell Biol.* 13, 7-12.

434. Hagglund, R. & Roizman, B. (2004) *J. Virol.* 78, 2169-2178.

435. Van Sant C., Hagglund, R., Lopez, P., & Roizman, B. (2001) *Proc. Natl. Acad. Sci. U. S. A* 98, 8815-8820.

436. Boutell, C. & Everett, R. D. (2003) *J. Biol. Chem.* 278, 36596-36602.

437. Everett, R. D., Earnshaw, W. C., Findlay, J., & Lomonte, P. (1999) *EMBO J.* 18, 1526-1538.

438. Lomonte, P., Sullivan, K. F., & Everett, R. D. (2001) *J. Biol. Chem.* 276, 5829-5835.

439. Boutell, C., Orr, A., & Everett, R. D. (2003) *J. Virol.* 77, 8686-8694.

440. Chelbi-Alix, M. K. & de, T. H. (1999) *Oncogene* 18, 935-941.

441. Parkinson, J., Lees-Miller, S. P., & Everett, R. D. (1999) *J. Virol.* 73, 650-657.

442. Parkinson, J. & Everett, R. D. (2000) *J. Virol.* 74, 10006-10017.

443. Talis, A. L., Huibregtse, J. M., & Howley, P. M. (1998) *J. Biol. Chem.* 273, 6439-6445.

444. Ronco, L. V., Karpova, A. Y., Vidal, M., & Howley, P. M. (1998) *Genes Dev.* 12, 2061-2072.

445. Barry, M. & Fruh, K. (2006) *Sci. STKE.* 2006, e21.

446. Margottin, F., Bour, S. P., Durand, H., Selig, L., Benichou, S., Richard, V., Thomas, D., Strebel, K., & Benarous, R. (1998) *Mol. Cell* 1, 565-574.

447. Frescas, D. & Pagano, M. (2008) *Nat. Rev. Cancer* 8, 438-449.

448. Schubert, U. & Strebel, K. (1994) *J. Virol.* 68, 2260-2271.

449. Bour, S., Perrin, C., Akari, H., & Strebel, K. (2001) *J. Biol. Chem.* 276, 15920-15928.

450. Horvath, C. M. (2004) *Eur. J. Biochem.* 271, 4621-4628.

451. Liu, B., Sarkis, P. T., Luo, K., Yu, Y., & Yu, X. F. (2005) *J. Virol.* 79, 9579-9587.

452. Yu, X., Yu, Y., Liu, B., Luo, K., Kong, W., Mao, P., & Yu, X. F. (2003) *Science* 302, 1056-1060.

453. Didcock, L., Young, D. F., Goodbourn, S., & Randall, R. E. (1999) *J. Virol.* 73, 9928-9933.

454. Parisien, J. P., Lau, J. F., Rodriguez, J. J., Sullivan, B. M., Moscona, A., Parks, G. D., Lamb, R. A., & Horvath, C. M. (2001) *Virology* 283, 230-239.

455. Nishio, M., Garcin, D., Simonet, V., & Kolakofsky, D. (2002) *Virology* 300, 92-99.

456. Ulane, C. M., Rodriguez, J. J., Parisien, J. P., & Horvath, C. M. (2003) *J. Virol.* 77, 6385-6393.

457. Yu, Y., Xiao, Z., Ehrlich, E. S., Yu, X., & Yu, X. F. (2004) *Genes Dev.* 18, 2867-2872.

458. Malim, M. H. (2006) *C. R. Biol.* 329, 871-875.

459. Graff, J. W., Mitzel, D. N., Weisend, C. M., Flenniken, M. L., & Hardy, M. E. (2002) *J. Virol.* 76, 9545-9550.

460. Midthun, K. & Kapikian, A. Z. (1996) *Clin. Microbiol. Rev.* 9, 423-434.

461. Fernandez, F. M., Conner, M. E., Hodgins, D. C., Parwani, A. V., Nielsen, P. R., Crawford, S. E., Estes, M. K., & Saif, L. J. (1998) *Vaccine* 16, 507-516.

462. Saif, L. J. (1999) *Adv. Vet. Med.* 41, 429-446.

463. Estes, M. K. (2001) in *Fundamental Virology*, eds. Knipe, D. M. & Howley, P. M. (Lippincott Williams & Wilkins, Philadelphia), pp. 1747-1785.

464. Allen, A. M. & Desselberger, U. (1985) *J. Gen. Virol.* 66 (Pt 12), 2703-2714.

465. Biryahwaho, B., Hundley, F., & Desselberger, U. (1987) *Arch. Virol.* 96, 257-264.

466. Desselberger, U. (1996) *Adv. Virus Res.* 46, 69-95.

467. Pedley, S., Hundley, F., Chrystie, I., McCrae, M. A., & Desselberger, U. (1984) *J. Gen. Virol.* 65 (Pt 7), 1141-1150.

468. Tian, Y., Tarlow, O., Ballard, A., Desselberger, U., & McCrae, M. A. (1993) *J. Virol.* 67, 6625-6632.

469. Juang, Y. T., Lowther, W., Kellum, M., Au, W. C., Lin, R., Hiscott, J., & Pitha, P. M. (1998) *Proc. Natl. Acad. Sci. U. S. A* 95, 9837-9842.

470. Groene, W. S. & Shaw, R. D. (1992) *J. Virol. Methods* 38, 93-102.

471. Daughenbaugh, K. F., Fraser, C. S., Hershey, J. W., & Hardy, M. E. (2003) *EMBO J.* 22, 2852-2859.

472. Au, W. C., Moore, P. A., Lowther, W., Juang, Y. T., & Pitha, P. M. (1995) *Proc. Natl. Acad. Sci. U. S. A* 92, 11657-11661.

473. Hiscott, J., Pitha, P., Genin, P., Nguyen, H., Heylbroeck, C., Mamane, Y., Algarte, M., & Lin, R. (1999) *J. Interferon Cytokine Res.* 19, 1-13.

474. Lowther, W. J., Moore, P. A., Carter, K. C., & Pitha, P. M. (1999) *DNA Cell Biol.* 18, 685-692.

475. Lee, S. S., Weiss, R. S., & Javier, R. T. (1997) *Proc. Natl. Acad. Sci. U. S. A* 94, 6670-6675.

476. Weaver, B. K., Ando, O., Kumar, K. P., & Reich, N. C. (2001) *FASEB J.* 15, 501-515.

477. Braganca, J. & Civas, A. (1998) *Biochimie* 80, 673-687.

478. Schafer, S. L., Lin, R., Moore, P. A., Hiscott, J., & Pitha, P. M. (1998) *J. Biol. Chem.* 273, 2714-2720.

479. Heylbroeck, C., Balachandran, S., Servant, M. J., DeLuca, C., Barber, G. N., Lin, R., & Hiscott, J. (2000) *J. Virol.* 74, 3781-3792.

480. Nunez, G., Benedict, M. A., Hu, Y., & Inohara, N. (1998) *Oncogene* 17, 3237-3245.

481. Tang, X., Gao, J. S., Guan, Y. J., McLane, K. E., Yuan, Z. L., Ramratnam, B., & Chin, Y. E. (2007) *Cell* 131, 93-105.

482. Chaplin, P. J., Entrican, G., Gelder, K. I., & Collins, R. A. (1996) *J. Interferon Cytokine Res.* 16, 25-30.

483. De Boissieu, D., Lebon, P., Badoual, J., Bompard, Y., & Dupont, C. (1993) *J. Pediatr. Gastroenterol. Nutr.* 16, 29-32.

484. La Bonnardiere, C., Cohen, J., & Contrepois, M. (1981) *Ann. Rech. Vet.* 12, 85-91.

485. Schwers, A., Vanden, B. C., Maenhoudt, M., Beduin, J. M., Werenne, J., & Pastoret, P. P. (1985) *Ann. Rech. Vet.* 16, 213-218.

486. Lecce, J. G., Cummins, J. M., & Richards, A. B. (1990) *Mol. Biother.* 2, 211-216.

487. Rollo, E. E., Kumar, K. P., Reich, N. C., Cohen, J., Angel, J., Greenberg, H. B., Sheth, R., Anderson, J., Oh, B., Hempson, S. J. *et al.* (1999) *J. Immunol.* 163, 4442-4452.

488. Bass, D. M. (1997) *Gastroenterology* 113, 81-89.

489. Angel, J., Franco, M. A., Greenberg, H. B., & Bass, D. (1999) *J. Interferon Cytokine Res.* 19, 655-659.

490. Barro, M. & Patton, J. T. (2005) *Proc. Natl. Acad. Sci. U. S. A* 102, 4114-4119.

491. Hiscott, J., Grandvaux, N., Sharma, S., tenOever, B. R., Servant, M. J., & Lin, R. (2003) *Ann. N. Y. Acad. Sci.* 1010, 237-248.

492. Basler, C. F., Mikulasova, A., Martinez-Sobrido, L., Paragas, J., Muhlberger, E., Bray, M., Klenk, H. D., Palese, P., & Garcia-Sastre, A. (2003) *J. Virol.* 77, 7945-7956.

493. Brzozka, K., Finke, S., & Conzelmann, K. K. (2005) *J. Virol.* 79, 7673-7681.

494. Jennings, S., Martinez-Sobrido, L., Garcia-Sastre, A., Weber, F., & Kochs, G. (2005) *Virology* 331, 63-72.

495. Jackson, P. K., Eldridge, A. G., Freed, E., Furstenthal, L., Hsu, J. Y., Kaiser, B. K., & Reimann, J. D. (2000) *Trends Cell Biol.* 10, 429-439.

496. Barlow, P. N., Luisi, B., Milner, A., Elliott, M., & Everett, R. (1994) *J. Mol. Biol.* 237, 201-211.

497. Pereira, H. G., Azeredo, R. S., Fialho, A. M., & Vidal, M. N. (1984) *J. Gen. Virol.* 65 (Pt 4), 815-818.

498. Theil, K. W., Bohl, E. H., & Agnes, A. G. (1977) *Am. J. Vet. Res.* 38, 1765-1768.

499. Woode, G. N., Kelso, N. E., Simpson, T. F., Gaul, S. K., Evans, L. E., & Babiuk, L. (1983) *J. Clin. Microbiol.* 18, 358-364.

500. Yang, Y., Fang, S., Jensen, J. P., Weissman, A. M., & Ashwell, J. D. (2000) *Science* 288, 874-877.

501. Canning, M., Boutell, C., Parkinson, J., & Everett, R. D. (2004) *J. Biol. Chem.* 279, 38160-38168.

502. Patton, J. T., Taraporewala, Z., Chen, D., Chizhikov, V., Jones, M., Elhelu, A., Collins, M., Kearney, K., Wagner, M., Hoshino, Y. *et al.* (2001) *J. Virol.* 75, 2076-2086.

503. Spann, K. M., Tran, K. C., & Collins, P. L. (2005) *J. Virol.* 79, 5353-5362.

504. Barro, M. & Patton, J. T. (2007) *J. Virol.* 81, 4473-4481.

505. Brown, K., Gerstberger, S., Carlson, L., Franzoso, G., & Siebenlist, U. (1995) *Science* 267, 1485-1488.

506. Hiscott, J., Nguyen, T. L., Arguello, M., Nakhaei, P., & Paz, S. (2006) *Oncogene* 25, 6844-6867.

507. Shirane, M., Hatakeyama, S., Hattori, K., Nakayama, K., & Nakayama, K. (1999) *J. Biol. Chem.* 274, 28169-28174.

508. Sarkar, S. N., Smith, H. L., Rowe, T. M., & Sen, G. C. (2003) *J. Biol. Chem.* 278, 4393-4396.

509. Miao, Z. H. & Ding, J. (2003) *Cancer Res.* 63, 4527-4532.

510. Lin, R., Mamane, Y., & Hiscott, J. (2000) *J. Biol. Chem.* 275, 34320-34327.

511. Shaneyfelt, M. E., Burke, A. D., Graff, J. W., Jutila, M. A., & Hardy, M. E. (2006) *Virol. J.* 3, 68.

512. Grandvaux, N., Servant, M. J., tenOever, B., Sen, G. C., Balachandran, S., Barber, G. N., Lin, R., & Hiscott, J. (2002) *J. Virol.* 76, 5532-5539.

513. Li, Q. & Verma, I. M. (2002) *Nat. Rev. Immunol.* 2, 725-734.

514. Plaksin, D., Baeuerle, P. A., & Eisenbach, L. (1993) *J. Exp. Med.* 177, 1651-1662.

515. Perkins, N. D. (2006) *Oncogene* 25, 6717-6730.

516. Holloway, G. & Coulson, B. S. (2006) *J. Virol.* 80, 10624-10633.

517. Karin, M. (1995) *J. Biol. Chem.* 270, 16483-16486.

518. Chen, L. F. & Greene, W. C. (2004) *Nat. Rev. Mol. Cell Biol.* 5, 392-401.

519. Ding, Q., He, X., Hsu, J. M., Xia, W., Chen, C. T., Li, L. Y., Lee, D. F., Liu, J. C., Zhong, Q., Wang, X. *et al.* (2007) *Mol. Cell Biol.* 27, 4006-4017.

520. Gallegos, J. R., Litersky, J., Lee, H., Sun, Y., Nakayama, K., Nakayama, K., & Lu, H. (2008) *J. Biol. Chem.* 283, 66-75.

521. Kumar, K. G., Krolewski, J. J., & Fuchs, S. Y. (2004) *J. Biol. Chem.* 279, 46614-46620.

522. Douagi, I., McInerney, G. M., Hidmark, A. S., Miriallis, V., Johansen, K., Svensson, L., & Karlsson Hedestam, G. B. (2007) *J. Virol.* 81, 2758-2768.

523. Kearney, K., Chen, D., Taraporewala, Z. F., Vende, P., Hoshino, Y., Tortorici, M. A., Barro, M., & Patton, J. T. (2004) *EMBO J.* 23, 4072-4081.

524. Clark, H. F., Offit, P. A., Plotkin, S. A., & Heaton, P. M. (2006) *Pediatr. Infect. Dis. J.* 25, 577-583.

525. Ramig, R. F. (1988) *Microb. Pathog.* 4, 189-202.

526. Tzipori, S. R., Makin, T. J., & Smith, M. L. (1980) *Aust. J. Exp. Biol. Med. Sci.* 58, 309-318.